UNIVERSITÀ DEGLI STUDI DI NAPOLI FEDERICO II

SCUOLA DI DOTTORATO IN INGEGNERIA INDUSTRIALE

CORSO DI DOTTORATO IN
INGEGNERIA DEI MATERIALI E DELLE STRUTTURE
***Coordinatore: Prof. Ing. Domenico Acierno***

XXI CICLO

**SALVATORE SESSA**

**TESI DI DOTTORATO**

# *APPLICATION OF THE TAIL-EQUIVALENT LINEARIZATION METHOD FOR STOCHASTIC DYNAMIC ANALYSIS WITH ASYMMETRIC HYSTERESIS*

***TUTOR:***
***Prof. Ing. Luciano Rosati***

# Acknowledgements

The present research work would not have been possible without the hidden help of many people which I would like to warmly thank. First and foremost, my advisor Professor Luciano Rosati, who always trusted me since before my master graduation, for his always inspiring guidance, for his valuable advices and for his quizzical severity. Thanks, to the supervisor of my Berkeleian experience Professor Armen Der Kiureghian for his stimulating help that opened my mind to higher and higher challenges and for being shining example and model of work.

I would like to acknowledge the *Department of Civil and Environmental Engineering, University of California, Berkeley* and the *Pacific Earthquake*

*Engineering Research Center (PEER)* for the support and the resources that I recieved during my foreign visiting appointment.

I also received a precious support from the people of my two research groups. I express a deep gratitude to the Professor Nunziante Valoroso for sharing his valuable experiences with me, for encouraging me to quit smoking and for showing me that I don't know how to use LaTeX; to Dr. Roberto Serpieri and Dr. Francesco Marmo for their always useful advices.

Thanks also to Professor Filip C. Filippou for his help about constitutive models; to Frank McKenna which has helped me several times with implementation drawbacks and also to Proff. Michael H. Scott, Juhno Song and Terje Haukaas for their help about the software that have been used for this work.

My Berkeleian period would not have been profitable without the presence of Sanaz Razainean which has been co-working with me for a while, and without the useful discussions with Dr. Daniel Straub, Katerina Konakli, Michelle Bensi, Juthi Krishnan and Dr. Umberto Alibrandi. Of course, I cannot forget about Luca Garré whose friendship is even more important than the simple professional relationship.

Last, but not least, I have been fortunate to meet people in my life that contributed with their love and friendship to my growth and indirectly to my professional archievements. I would like to express my gratitude and my love to my parents and relatives which have been the first people to trust me without reserve, in particular to my father that has always been

the model for my life. Also, I am grateful to my friends which supported me both in Italy and in the United States.

Such a long period of work so far from home would have been very troublesome and sad without the presence of some people that have been walking with me on my path. Among fellows and mates, I would like to write a lot about everyone but I should restrict myself to a warm, collective *thank you*. However, I must lovingly express all my love and affection to Stefanie, whose daily presence has been irreplaceable, and to Emilia, whose love and sweetness made me to feel at home, for her invaluable support; after all, *"A friend is one who knows us, but loves us anyway"*.

Napoli, November 2008

Salvatore Sessa

# Contents

# List of Tables

# List of Figures

# Chapter 1

# Introduction

A new non-parametric method for random vibration analysis in presence of non-symmetric behavior of material is developed. The method is capable of capturing the non-Gaussian statistics of non-linear dynamic response of structures subjected to random excitations providing asymmetric probability distributions.

The conventional equivalent linearization method (ELM) (Lutes and Sarkani 2003) for nonlinear stochastic dynamic analysis requires the assumption of a distribution for the nonlinear response to allow computation of second moments. Although alternatives exist (Reccardi 2007), in the vast majority of cases ELM is applied under the assumption of Gaussian distribution (Atalik and Utku 1976, Wen 1976). As a result, the predicted distribution of the response is Gaussian, even when the assumed system hysteresis is asymmetric.

Recently, a new approach for nonlinear stochastic dynamic analysis by the tail-equivalent linearization method (TELM) has been developed (Fujimura and Der Kiureghian 2007). In this method, the tail-equivalent linear

system is defined by equating its tail probability for a specified threshold with the first-order approximation of the tail probability of the nonlinear response for the same threshold. This equality is imposed by matching the so-called design points of the linear and nonlinear responses in the space of a vector of standard normal random va-riables, which are obtained by discretizing the Gaussian input excitation. Here, the "design point" (also addressed as "performance point") refers to the point of linearization in the first-order reliability method (FORM) approximation of the tail probability problem. Fujimura and Der Kiureghian (2007) have shown that knowledge of the performance point provides complete information about the tail-equivalent linear system in terms of its unit impulse response function. This information is obtained in a numerical form and does not require the definition of a parameterized linear model. In this sense, TELM is a non-parametric equivalent linearization method.

The original TELM algorithm has been formulated and employed with classical Bouc-Wen costitutive models under the assumptions of symmetry of the hysteresis loop, non-degrading behavior and zero-mean response. In these conditions, TELM provides a linearized system with symmetric behavior, consequently, the response statistics is zero-mean and symmetric itself. In this work, the formulation of TELM is extended, under further hypothesys, to the non-symmetric hysteresis (chapter 4).

An important advantage of TELM is that it can accurately capture the non-Gaussian distribution of the nonlinear response in first-order approximation, particularly in the tail regions, *i.e.* small probabilities, which are the branches of interest for the usual applications of earthquake engineer-

ing. In particular, if the hysteretic law of the system is asymmetric, the predicted response distribution is not only non-Gaussian, but also asymmetric. Thus, TELM offers significant advantages over the conventional ELM in nonlinear stochastic dynamic analysis, particularly when the hysteresis law of the structure is asymmetric.

In this study, we also employ TELM to investigate the dynamic response of interconnected equipment items subjected to base acceleration, where the connecting element has inelastic behavior with an asymmetric hysteresis law (chapter 7). The problem is motivated by a study of dynamic interaction between interconnected electrical substation equipment conducted by Song et al. (2007), where it was shown that the interaction effect may have a detrimental influence on the high frequency equipment item. Tests by Stearns and Filiatrault (2004) have shown that the connecting element used in many substations in California has a distinctly asymmetric hysteresis loop. Song and Der Kiureghian (2006) developed a generalized Bouc-Wen model with asymmetric hysteresis, which closely matches the test results. It has been necessary to develop and calibrate a smoothed version of this generalized Bouc-Wen model (chapter 6) in order to to predict the non-Gaussian and asymmetric distribution of the system response by TELM.

The excitation is discretized in time steps and represented in terms of a finite set of standard normal variables. This convenction makes it possible to formulate and solve the FORM problem and to evaluate the tail probability of the non-linear system.

The response statistic provided by TELM leads to a more extended ran-

dom vibration analysis (chapter 5). A first-passage collapse mechanism is considered for the sample structures, thus, the knowledge og the step-in-time response statistics leads to the evaluation of the *First Passage Probability* of the system that consists in the extreme distribution of the response over an interval in time. Both a theoretical and a numerical solution are provided (*i.e.* the Vanmarcke's approach and the Series-System algorithm), the numerical one is also able to catch the extreme response distribution even in presence of non-stationary excitation.

Finally, the asymmetric TELM algorithm is implemented in softwares for scientific research purposes that already provide metodologies and algorithms used in structural reliability analysis, such as the FORM algorithm, the definition and managment of stochastic time-histories and the series-system analysis. In particular, the FORM algorithm is available in FERUM and OpenSees. FERUM (*http://www.ce.berkeley.edu/FERUM/*) is a MatLab framework developed for scientific research purposes by the University of California, Berkeley by Professor Armen Der Kiureghian; further objects have been implemented in FERUM in order to make it possible to run the TELM algorithm and are available for further research.

OpenSees (*http://opensees.berkeley.edu/index.php*) is a C++ framework for developing applications to simulate the performance of structural and geotechnical systems subjected to earthquakes, sponsored by the Pacific Earthquake Engineering Research Center (PEER). The TELM algorithm is available in OpenSees and the constitutive model of the material used in this work has been implemented and it is available for further applications and research.

Example applications of multi degrees of freedom asymmetric hysteretic systems illustrates various features of the method. Comparisons with results obtained by Monte Carlo simulation have been provided in order to validate the results of Asymmetric TELM. Also, basic guidelines about the implemented objects are available in appendix B and C.

# Chapter 2

# Representation of the dynamic excitation

An essential step in the non-linear dynamic analysis is the discrete representation of the ground motion by a finite set of random variables. An earthquake excitation is uncertain and we need stochastic methods to evaluate the response statistic and random variables to define the input process. In case of linear structures, the power spectral density is enough to get the response if used in conjunction with the modal analysis method. The other way round, for nonlinear structures, the modal shapes and frequencies of the structure do not exist, so, one cannot avoid to consider the ground motion like a displacement or acceleration input process, *i.e.* an array of base displacements or accelerations in time. However, the exact ground motion cannot be known and one can define an earthquake only by magnitude and power spectral characteristics. The structural responses of two ground motion processes can be very different even if the two ground motions have the some power spectral density, therefore, a probabilistic

analysis is required. The easiest but not best way to do it, is to consider several ground motions, then to perform a dynamic analysis for each one of them and finally to define the probabilistic distribution of the responses. Unfortunately, this kind of approach is not efficient for an intensive use in practice, in fact, to properly define a statistically efficient set of ground motions, we should consider an high number of process' realizations and they have to be consistent with the chosen power spectral density. These realizations can be easily defined by a Monte Carlo simulation, but, after that, it is necessary to perform a dynamic analysis for each one of them and the process is computationally demanding for practical applications. However, the Monte Carlo simulation is used in research to validate the results of experimented methods.

A more efficient representation of the stochastic excitation consists in defining the ground motion like the combination of two different array. Given a time-domain discretization in steps, the ground motion can be modeled like a train of random pulses. Each one of them is the combination of two entities: a random factor, which models only the uncertainties of the process, and a deterministic factor, which models the features of the seismic process, such as intensity, frequency content, cross-covariance in time and between different supports and even non-stationarities.

The advantages of this excitation philosophy are several. First of all, one does not have to deal with even one ground motion, because all the uncertainties are involved in only one pulse-vector; furthermore, one can deal with a fixed array of random variables and for this reason it is possible to improve the algorithm efficiency; finally, many efficient methods for

evaluating the response statistics are available.

## 2.1 Discrete representation of stochastic excitation

Several different kinds of stochastic discrete representation have been developed in years and are available for dynamic analysis purposes. In particular, the following formulation, developed by Der Kiureghian [16] is very efficient:

$$f(t) = \mu(t) + \sum_{i=1}^{n} s_i(t) u_i = \mu(t) + \mathbf{s}(t)\mathbf{u} \tag{2.1}$$

where $\mu(t)$ is the time-variant mean of the process, $\mathbf{u}$ is a time-invariant vector of standard normal variables, $\mathbf{s}(t)$ is a time-variant row vector of basis functions related to the covariance structure of the excitation process, and $n$ is a measure of the resolution of the representation. In case of zero-mean, second order Gaussian process all the representation have the form:

$$F(t) = \sum_{i=1}^{n} s_i(t) u_i = \mathbf{s}(t)\mathbf{u} \tag{2.2}$$

Each one of the available formulations differs in the definition of the basis functions $\mathbf{s}(t)$ and it makes this formulation very versatile because it is possible to define $\mathbf{s}(t)$ functions by several expansion methods, for example, the Karhunen-Loéve [40], trigonometric polynomials [31, 30], optimal linear estimation [37], and several others. The TELM method can be implemented in conjunction with each one of these formulations but, in this work, another formulation of particular interest in earthquake engineering will be used:

the filtered white-noise, in which the process is defined as the response of a linear filter subjected to a train of random pulses. The pulses can be considered as intermittent ruptures at the fault, whereas the filter may represent the medium through which the waves travel. This formulation has been proposed by Der Kiureghian [18] in order to make possible to perform FORM and SORM analysis. The same paper shows that if the pulses are Gaussian and the filter is linear, the process $F(t)$ itself is Gaussian.

Also, it appears clear from equation 2.2 that, even if the randomness is defined by the $\mathbf{u}$ vector, the moments of the process $F(t)$ are completely defined by the $\mathbf{s}(t)$ vector. The standard deviation of the process is the Euclideian norm $\sigma_f(t) = \|\mathbf{s}(t)\|$; the scalar product $\mathbf{k}_{ff}(t_1, t_2) = \mathbf{s}(t_1)^T\mathbf{s}(t_2)$ is the covariance of the process. Furthermore, because the $\mathbf{s}(t)$ vector is deterministic, each point in the space of $\mathbf{u}$ completely defines one realization of each one of the random variables $u_i$ that, consequently, also completely defines one realization of the global excitation in time $F(t)$. The likelyhood related to each realization is governed by the well-known standard normal joint probability density function $\varphi(\mathbf{u})$.

## 2.2 Unfiltered and filtered White-Noise excitation

Defined a white-noise process and a linear filter, the corresponding filtered white-noise process can be defined by the Duhamel's integral:

$$F(t) = \int_0^t h_f(t-\tau)W(\tau)\,d\tau \tag{2.3}$$

where $h_f$ is the IRF of the filter and $W(t)$ is the underlying white-noise process. If the filter is stable, after a transition time due to neglect the

influence of the initial conditions, the filtered process becomes stationary.

In order to implement the filtered white noise in computational random vibrations methods, it is necessary to get a discretized form of the equation 2.6. First, we define a discrete set of equally spaced time points $t_i = i\Delta t$ with constant interval $\Delta_t$, then we can approximate the white-noise $W(t)$ of the equation 2.6 with a train of rectangular pulses:

$$\hat{W}(t) = W_i = \frac{1}{\Delta t}\int_{t_{i-1}}^{t_i} W(\tau)\, d\tau \quad \text{with } t_{i-1} < t \leq t_i \tag{2.4}$$

.

Obviously, $W_i$ is the rectangular pulse amplitude in the interval $t_{i-1} < t \leq t_i$. Because the white-noise is a zero-mean uncorrelated process, the $W_i$ are statistically independent zero-mean random variables; furthermore, because the frequency content of the white-noise is constant, the variance of the $W_i$ should be infinite. Because of the time discretization, the white noise presents a upper frequency cutoff of the power spectral density at about $1/(2\Delta t)Hz$. The first consequence is the value of the standard deviation: because the excitation becomes a broad-banded white noise, it is $\sigma^2 = \frac{2\pi S}{\Delta t}$ with $S$ spectral density of $W(t)$ and it allows to define the discretized excitation as a set of standard normal random variables $u_i = W_i/\sigma$, so that the process can be written in the form 2.2 with:

$$\begin{aligned} &s_i(t) = \sigma \quad && t_{i-1} < t \leq t_i, i = 1, ..., n \\ &s_i(t) = 0 && \text{otherwise} \end{aligned} \tag{2.5}$$

However, the frequency cutoff *de facto* changes the frequency content of the excitation, the approximation does not affect its employment if the

time step $\Delta t$ is small enough and the upper frequency cutoff results far away from the physical frequencies of the system.

The stochastic process can be defined in the form:

$$\hat{F}(t) = \sum_{i=1}^{n} \frac{\sigma}{\Delta t} \int_{t_{i-1}}^{t_i} h_f(t-\tau)\, d\tau u_i, t_1 \leq t \leq t_n \tag{2.6}$$

where $\hat{F}(t)$ is the rectangular-pulse approximated form of $F(t)$. The white-noise process can be written in the form 2.2 with deterministic coefficients:

$$\begin{aligned} s_i(t) &= \tfrac{\sigma}{\Delta t} \textstyle\int_{t_{i-1}}^{t_i} h_f(t-\tau)\, d\tau \quad t_{i-1} < t \leq t_i, i = 1, ..., n \\ s_i(t) &= 0 \qquad\qquad\qquad\qquad \text{otherwise} \end{aligned} \tag{2.7}$$

Obviously, if one needs the unfiltered white-noise representation, the 2.2 form can be used with the $s_i(t)$ defined by 2.5.

Defining the filter parameters, it is possible to simulate many different kinds of earthquake motions. It is particularly useful the filter defined by Kanai (1957) and Tajimi (1960). The model considers the underlying white-noise as the earthquake excitation on the bedrock and the filter represents the medium behaviour of the surface ground; the filtered excitation is the acceleration response of the linear system. The IRF of the Kanai-Tajimi filter is [11]:

$$h_f(t) = -\exp\left(-\zeta_g \omega_g t\right) \left[ \frac{1-2\zeta_g^2}{\sqrt{1-\zeta_g^2}} \omega_g \sin\left(\omega_g \sqrt{1-\zeta_g^2 t}\right) + 2\zeta_g \omega_g \cos\left(\theta\right) \right] \tag{2.8}$$

where $\omega_g$ and $\zeta_g$ are respectively the natural frequency and the damping ratio of the linear oscillator and they are related to the predominant frequency and damping of the local soil layer. The Kanai-Tajimi filtered

excitation process, i.e. the filter response process, has the following power spectrum density (PSD):

$$S(\omega) = \frac{\omega_g^4 + 4\zeta_g^2\omega_g^2\omega^2}{\left(\omega_g^2 - \omega^2\right)^2 + 4\zeta_g^2\omega_g^2\omega^2} S \tag{2.9}$$

where $S$ is the underlying white-noise intensity. In the above formulation, it is important to select an appropriate time step $\Delta t$. Defined the upper bound of significant input frequencies for a structural system, $\omega_{MAX}$, then it has to be selected a small enough time step, specifically it should be $\Delta t \leq \pi/\omega_{MAX}$. The choose of the time step does not involve only the input process discretization. In the applications presented in [28] An adequate value for the time step was $\Delta t = 0.02sec$, in this work it could be not small enough, expecially when a degrading material is involved. If a different time step amplitude will be required, each application presented in chapter 5 will indicate the time step amplitude and the reason of its choice.

A sample representation of white-noise acceleration process is presented in Figure 2.1; a Kanai Tajimi power spectral density sample is reported in figure 2.2.

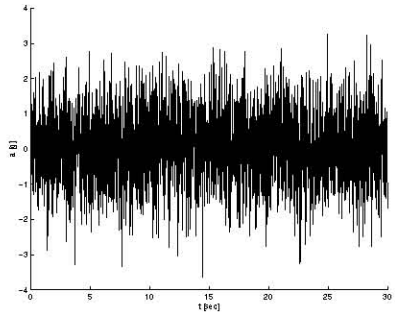


Figure 2.1: Unfiltered White Noise

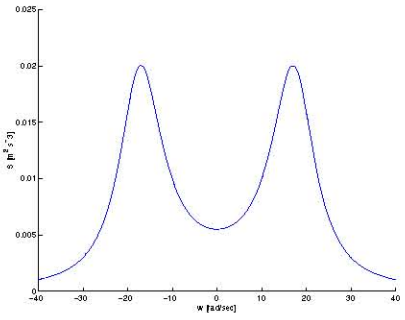


Figure 2.2: Kanai Tajimi PSD

Figure 2.3: White Noise samples

## 2.3 Non-stationary White-Noise excitation

The representations presented in chapter 2.1 and 2.2 represent a stationary process, in fact, the frequency content and the probabilistic parameters are constant during all the excitation. A generic earthquake groung motion usually presents nonstationarity features both in time and frequency domain and it is necessary to model this features in the input excitation.

Many ways of representing nonstationarities are available. Considering only a time-domain nonstationarity, the excitation assumes the form:

$$F_{NS}(t) = q(t)F_{ST}(t) \tag{2.10}$$

where $q(t)$ is a deterministic modulating function, $F_{ST}$ and $F_{NS}$ are respectively the stationary and the non-stationary processes. $F_{ST}$ is given in the 2.6 form. Furthermore, it also could be necessary to model frequency nonstationarities. Working in the frequency domain, nonstationarities change *de facto* the power spectral density in time. In the time

domain this property can be translated by the superposition of different linear filters, each one with different frequency and damping and each one related to a different modulating function. The excitation obtained by the superposition of $N$ filters is:

$$F_{NS}(t) = \sum_{k=1}^{N} c_k q_k(t) \sum_{i=1}^{n} \int_{t_{i-1}}^{t_i} h_k(t-\tau)\, d\tau u_i, \quad t_1 < t \leq t_n \tag{2.11}$$

so, each one of the filter's IRFs is scaled by a fixed deterministic parameter $c_k$, due to scale the white-noise intensity between the filters, and then it is scaled by a modulating function $q_k(t)$ which changes in time and it is due to model the different frequency content for different times. Obviously, $h_k(t)$ is the IRF of the $i$th filter.

The model can also be represented in the form 2.6 simply by changing the summation order:

$$\begin{aligned} s_i(t) &= \textstyle\sum_{k=1}^{N} c_k q_k(t) \frac{\sigma}{\Delta t} \int_{t_{i-1}}^{t_i} h_k(t-\tau)\, d\tau u_i, \quad t_1 < t,\ i = 1, ..., n \\ s_i(t) &= 0 \qquad\qquad \text{otherwise.} \end{aligned} \tag{2.12}$$

In the last case, the nonstationarity is modeled by a discretized form of the frequency content. Recently it has been developed a new model by Razaeian and Der Kiureghian [19] which considers a continuous variation in time of the parameters of only one filter's IRF. In that case, the nonstationarity is not any more discrete with respect the frequency content and one car archieve a better precision.

The model can also be respresented in form 2.6 only by solving the integral: Several modulating functions are available for this purpose. A

typical one, proposed by Amin and Ang (1966) is:

$$q(t) = \begin{cases} 0 & t \leq T_1 \\ \left[\frac{t-T_1}{T_2-T_1}\right]^2 & T_1 < t \leq T_2 \\ 1 & T_2 < t \leq T_3 \\ \exp\left(-\frac{t-T_3}{2}\right) & T_3 < t \end{cases} \tag{2.13}$$

the start time, rise time and stationary duration are controlled respectively by $T_1$, $T_2$ and $T_3$. A realization of the Amin-Ang modulating function is presented in Figure 2.5. In this work it will be also used another modulating function:

$$\begin{aligned} q(t) &= A\,(t-D)^B \exp\left[-C\,(t-D)\right] \qquad D < t \\ q(t) &= 0 \qquad\qquad\qquad\qquad\quad \text{otherwise.} \end{aligned} \tag{2.14}$$

This modulating function id usually designed as *Gamma-fcn*, $A$ represents the amplitude, $D$ represents the starting time, $B$ and $C$ are decay coefficients. A particular realization of the 2.14 is presented in Figure 2.4.

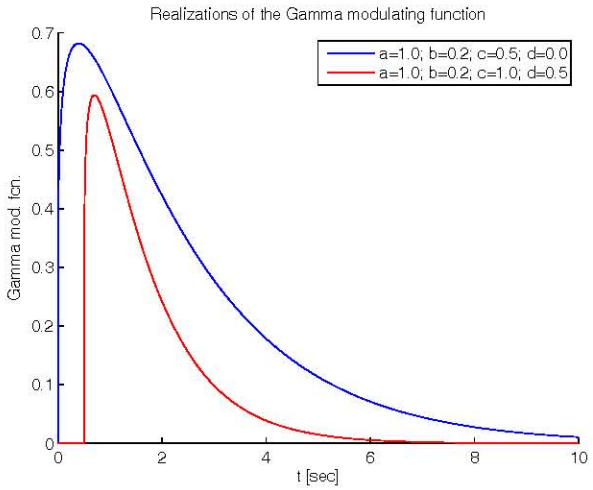


Figure 2.4: Realization of the gamma modulating function.

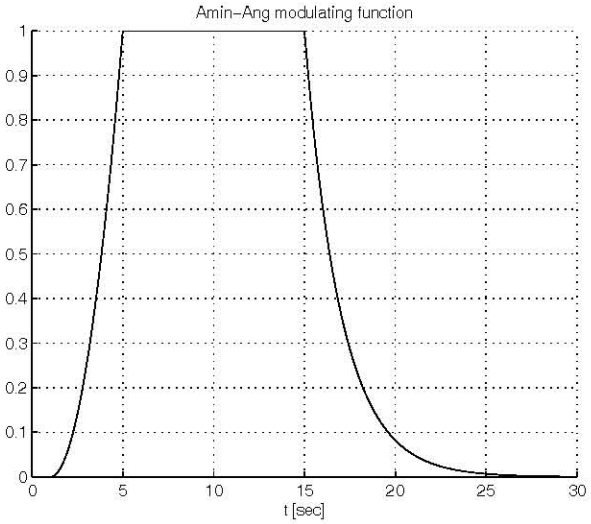


Figure 2.5: Realization of the Amin-Ang modulating function.

## 2.4 White-Noise excitation's features and properties

The employment of filtered and unfiltered white noise is a very important step in the random vibration analysis because of its peculiarity that will be briefly shown in this section.

Let us define a process $X(t)$ with constant power spectral density $\Phi_{XX}(\omega) = \Phi_0$, the first thing that ome may notice is that the auto-spectral density is not integrable and then, because its integral is the process' variance:

$$\sigma_X^2 = \int_{-\infty}^{\infty} \Phi_{XX}(\omega)\, d\omega \tag{2.15}$$

it comes out that the variance, and then the energy of the process, are practically infinite. For this reason, the unbounded white noise is just a theorical process and it has no effective realizations in physics, even if many processes have an high enough frequency content to be assimilated to an unbounded white noise and it can be used to approximate meaningful processes.

Because $S_{XX}$ is not integrable, the inverse Fourier transform takes the degenerate form of a Dirac delta function, giving the autocovariance function:

$$G_{XX}(\tau) = 2\pi\Phi_0\delta(\tau). \tag{2.16}$$

This is a particular form of random processes and in practice it is called Delta Correlated Process[1].

[1]The term White Noise is commonly used to refer to process of the general type of

Given two different points in time $t$ and $s$, because the autocovariance function has the only non-zero value for $\tau = t - s = 0$, the two outcomes $X(t)$ and $X(s)$ are completely uncorrelated. This last one is a really important property in order to perform TELM and FORM analysis using a white noise excitation. Two different points $X(t)$ and $X(s)$ of a physical time history are not completely uncorrelated because displacements, velocities and accelerations vary continuously, so, if $s$ is close to $t$, the $X(s)$ outcome will be influenced by the $X(t)$ one. However, the high variability of earthquake time histories, implies that the correlation between two outcomes in time, decreases very quickly as long as the interval $t-s$ becomes longer. It comes out that the autocovariance function has high values close to $\tau = 0$ and quickly decreases. An example can be shown in figure 2.6.

Because the excitation will model each point in time as a standard normal random variable, it is necessary to build the autocovariance matrix of the excitation which discretizes the autocovariance function for each couple of points in time $t_i$ and $t_j$:

$$\mathrm{G}_{XX} = \begin{bmatrix} G_{XX}(t_1 - t_1) & \cdots & G_{XX}(t_1 - t_n) \\ \vdots & G_{XX}(t_i - t_j) & \vdots \\ G_{XX}(t_n - t_1) & \cdots & G_{XX}(t_n - t_n) \end{bmatrix}. \tag{2.17}$$

In case of white noise, considering that each random variable has zero-mean and $\sigma = 1$, the covariance matrix is diagonal and unitary. In case of a quasi-delta correlated excitation, the covariance matrix is banded with

delta-correlated processes but the latter implies more general independence properties that sometimes are not satisfied by the definition of white noise as process with constant frequency content. This differences, anyway, are not related to the processes used in common earthquake engineering practice and in this work, so, the term delta-correlated will be used to refer to an unbounded white noise process.

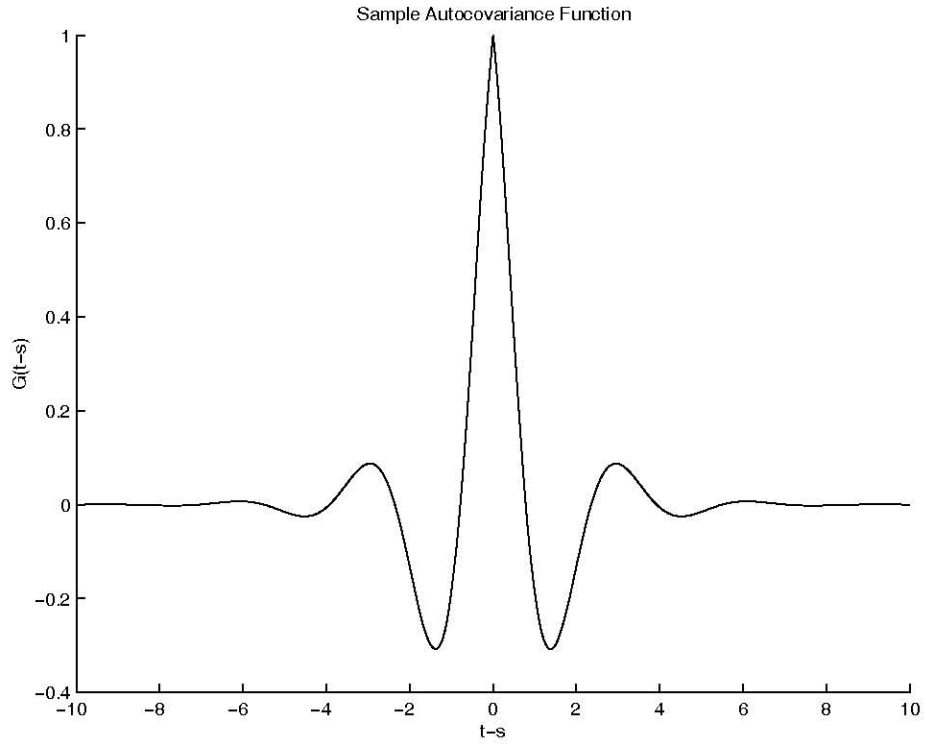


Figure 2.6: Autocovariance function sample of broad-band process

the diagonal elements close to the unity, it also has non-neglegible elements close to the main diagonal and null elements farther from it. One can gather that such kind of matrix is very close to the singularity, it is hard to get numerically its inverse and even if one can get it, it could be bad-conditioned. The drawbacks and errors that can be provoked by using a quasi-singular matrix are much higher and more dangerous than the approximation errors that one can get by using a delta-correlation instead of the real correlation of the earthquake time history.

## 2.5 TELM requirements

The model of ground motion presented in 2.1 will be applied at the TELM method wich will be presented in chapter 4. It will be shown that, in order to determine the impulse response function of the linearized system, the relation 2.6 between the process $\hat{F}(t)$ and the vector $\mathbf{u}$ of the standard normal variables must be invertible, i.e., given a realization of the process $\hat{F}(t)$ we must be able to determine the corresponding realization of the random vector $\mathbf{u}$.

The realization of the excitation process is given in vector form, given a discrete set of time points $t_i, i = 1, ..., m$ with $t_m < t_n$, the discretized process is $\hat{\mathbf{F}} = \left[\hat{F}(t_1)\ \hat{F}(t_2)\ ...\ \hat{F}(t_m)\right]^T$. It can also be written as

$$\hat{\mathbf{F}} = \mathbf{J}\mathbf{u} \tag{2.18}$$

where $\mathbf{J}$ is an $m \times n$ Jacobian matrix with $J_{ij} = s_j(t_i)$. In the TELM method, given a realization $\hat{\mathbf{F}}$ it is necessary to invert the 2.18 in order to determine the corresponding $\mathbf{u}$ and obviously it is possible only if $n =$

$m$. It means that, once that the number of random variables used to model the process is chosen, the number of time points used to model the input excitation must be the same. In the time domain analysis this requirement is easily archieved. In the frequency domain analysis, the number of frequencies used to model the process is conditioned by the number of time points. If the number of time points can be easily the same of the random variables, the number of frequencies is usually chosen in order to fit the power spectral density and the required number can depend by the features of the excitation and of the structural system. For this reason the time domain discretization is particularly suitable for the TELM analysis.

# Chapter 3

# Overwiev of Non-linear Stochastic Vibration Analysis methods

Exact solutions for non-linear stochastic systems have been found only for a relatively limited set of problems. At the same time, most of the practical analysis are based on approximated methods that are someway based on the exact solutions and the importance of the subset of non-linear problems that leads to exact results is important for, at least, two reasons. Most obvious is the circumstance in which a generic non-linear system can be approximated by an adequate enough non-linear model for which the exact solution is known so that the results can be used as approximated ones of the original system. Furthermore, the exact solution of a system can be used as a validation of different approximated methods that can be extended to more general problems.

The main drawbacks that affects non-linear dynamic problems, both in deterministic and stochastic case, is the non-applicability of the superposi-

tion of responses. Usually, the general solution for a linear system is gotten by superposition of many particular and well-known solutions. For example, let's think about the Duhamel convolution integral. It assumes that, once one knows the response of the dynamic system to a generic impulse, the excitation can be considered as a train of single impulses and the dynamic response is simply the superposition of the responses to each impulse. In this case, even if the exact analitic integral of the dynamic differential equation is hard to get, the exact solution is obtained by superposition of many well-known particular solutions. The underlying hypothesis of this method is that the response of the system to an impulse does not change in time and that the response of the sum of a set of excitation is the sum of the responses of each excitation. If there are non-linearities in the dynamic system, both hypothesis are not valid any more and it is necessary to provide alternative methods that do not require the superposition or an other property associated with linearity.

In this chapter some exact methods for non-linear stochastic dynamics will be analyzed. An important topic to start with is the derivation of general equations of stochastic moment-cumulant. In this approach, the response statistic are expressed by a set of expectation moments that completely defines the response probability distribution or, in a similar way and with the same base idea, one can define a set of general equations in terms of statistic cumulants instead of expectation moments.

The high uncertainty of earthquakes motions, forces all the analysis metods to somehow consider the stochastic characterization of the ground motion and, for linear structures, many metods have been developes. In

particular, the random characterization of acelerations or displacements can be done by power spectra defined on the base of earthquake magnitude and duration, and of the dynamic characterization of the seismic waves transmission in ground. These spectra can be used into analysis in frequency domain evaluating the maximum target response for a given excitation.

Because the dynamic response of a non-linear structure is highly dependent by the specific excitation's time history, the power and response spectra cannot be applied directly. For example, let us consider the classical modal analysis: the frequency features of the non-linear structure are changing in time, and their evolution strictly depends of the particular time history considered; it means that it is not possible to define a set of eigenvalues in the response space.

Many metods have been developed in years in order to avoid that drawback and to perform non-linear dynamic analysis, such as the Fokker-Plank equation, stochastic averaging methods or theory of perturbation. However, those metods can be very accurate but they are also largely restricted to specialized systems and particular kinds of excitation, so, they are difficult to apply to a large-scale analysis of generic practical structures. Recent developments are proposed in recent works by Roberts and Spanos [45], Lin and Cai [39] and Lutes-Sarkani [41]. The Monte-Carlo simulation [47] metod has no restrictions and is very powerful, but it is also computatinonally very demanding, so, its application is usually restricted to the validation of other random vibration metods.

The partial differential Fokker-Plank equation (FP) governs the evolution in time of the probability density function of a non-stationary response

process. Even if the equation provides exact solutions with no assumptions employed in its derivation, it only applies to a Markov-process response i.e. the case of delta correlated excitations, thus its practical application is limited. Furthermore, the complexity of the problem quickly increases as the number of degrees of freedom increases.

The stochastic averaging method defined a non-dimensional Fokker Plank equation for a set of slowly varying amplitude and phase periodic processes. The coefficients of the FP equation are defined in a simplified form because the influence of the periodic terms is replaced by its stochastic average. The method works well for lightly damped systems subjected to broad band processes but its use in case of multi degrees of freedom presents considerable difficulties.

The perturbation method expands the solution into power series of small parameters, the differential equations are defined for each term of the expansion. Even if its definition is simple, the main drawback is that the perturbation method can solve only lightly non-linear systems.

Another Fokker-Plank-derived method is the moment closure in which the equations for statistical moments of the response are derived from the FP equation but its application to non-linear systems leads to an infinite hierarchy of coupled equations that govern the statistical moments and specific techniques for approximate solutions are required. The accuracy of the solution can be improved only by increasing the complexity of the set of equation.

Some approximate metods have been developed in order to replace the non-linear system with an equivalent linear one, that can be easily used in

the classical linear analysis, generically these metod are defined as equivalent linearization metod (ELM). Chosen a non-linear system of interest, the equivalent linearization can be done in many different ways and one can get many different equivalent systems depending of the response of interest. The linearized system is defined by a set of parameters that are determined by minimizing the discrepance between the response of linear and non-linear system [9]. The mean-square error between the two responses is the most often used measure of discrepancy [2, 52], in some cases energy-based measures have also been considered [22].

## 3.1 The Fokker - Planck equation

A general approach due to get the probabilistic characterization of a non-stationary process consists in the definition of a differential equation that governs the evolution of the probability density function of the process itself. In fact, it is well known that it is possible to derive every probabilistic quantity of interest of a stochastic process if its PDF is completely known.

This generic approach is known in literature as Fokker-Plank[41] equation and its best advantage is that the derived probability density function of the process is exact and there are no approximation; nevertheless, this approach is affected by some drawbacks. Unfortunately, there must be fixed several limitations about the process characterization in order to make possible to get the integral of the Fokker-Planck equation. In this section, the underlying philosophy of the Kolmogorov and Fokker-Plank equations will be summarized[1]: even if it does not lead to efficient solutions, it remains

[1] For a complete theoretic derivation, specific applications and known solutions, one

a fundamental base for many approximated algorithms that will be shown later in this work.

Given a generic, non-stationary and multi-dimentional random process $Y(t)$, it is possible to derive its PDF by the differential Kolmogorov equation:

$$\frac{\partial}{\partial t} f_{Y(t)}(x) = \sum_{j=1}^{\infty} \frac{(-1)^j}{j!} \frac{\partial^j}{\partial x^j} \left[ C^{(j)}(x,t) f_{Y(t)}(x) \right] \tag{3.1}$$

where the $C^{(j)}(x,t)$ are the *derivate moments* or *intensity functions*; for some classes of dynamic problems, they can be directly derived in closed form. In case of multicomponent problems, the 3.1 can be written as:

$$f_{\Delta \mathbf{Y}}[\mathbf{u} - \mathbf{v} | \mathbf{Y}(t) = \mathbf{v}] = \prod_{l=1}^{n_{\mathbf{Y}}} \frac{1}{2\pi} \int_{-\infty}^{\infty} e^{-i\theta_l (u_l - v_l)} \times$$

$$\times \sum_{j_l=0}^{\infty} \frac{(i\theta_l)^{j_l}}{j_l!} E\left[ (\Delta Y_l)^{j_l} | \mathbf{Y}(t) = \mathbf{v} \right] d\theta_l \tag{3.2}$$

that leads to the proper Fokker-Plank equation:

$$\frac{\partial}{\partial t} f_{\mathbf{Y}(t)}(\mathbf{u}) = \underbrace{\sum_{j_1=0}^{\infty} \cdots \sum_{j_{n_{\mathbf{Y}}}=0}^{\infty}}_{\text{except} j+1=\cdots=j_{n_{\mathbf{Y}}}=0} \frac{(-1)^{j_1+\ldots+j_{n_{\mathbf{Y}}}}}{j_1! \ldots j_{n_{\mathbf{Y}}}!} \frac{\partial^{j_1+\ldots+j_{n_{\mathbf{Y}}}}}{\partial u_1^{j_1} \ldots \partial u_{n_{\mathbf{Y}}}^{j_{n_{\mathbf{Y}}}}} \times$$

$$\times \left[ C^{(j_1,\ldots,j_{n_{\mathbf{Y}}})}(\mathbf{u},t) f_{\mathbf{Y}(t)}(\mathbf{u}) \right]. \tag{3.3}$$

The main drawback of the Fokker-Plank equation for non-linear systems is the evaluation of the $C^{j_1,\ldots,j_{n(Y)}}(\mathbf{u},t)$ coefficients: the solution is known only for a limited set of special cases, in particular, a solutions has been

can refer to chapters 9 and 10 of Lutes-Sarkani, [41].

provided for Markov processes, however, in general, the physical characteristics of the civil engineering systems and excitations do not satisfy the Markov hypothesys and the straigth application of the Fokker-Planck equation would lead to unsolvable differential systems or to inaccurate results.

However, the Fokker-Planck equation still represents a good base for the non-linear random vibration analysis because it completely defines the problem and it is completely exhaustive; thus, it becomes the base for many approximated methods that can work in two directions: the approximated definition of the derivate moments or the development of easier (and solvable) relationship that still maintain the underlying philosophy of the Fokker-Planck equation. Some of those methods will be summarized in the following sections.

## 3.2 State-space moment and Cumulant equations

The Moment-Cumulant analysis is based on the theoretical analysis of the statistical moments and cumulant of the non-linear equation of motion itself. Many different methods based on different hypothesis have been developed in years in order to solve the cumulant equation, however, the phylosophy of the method essentially remains unchanged. Given a generic non-linear equation of motion:

$$\dot{\mathbf{Y}}(t) + \mathbf{g}[\mathbf{Y}(t)] = \mathbf{Q}(t) \tag{3.4}$$

where $\mathbf{Y}(t)$ is the displacements vector, the dot represents the time derivative, $\mathbf{Q}(t)$ is an excitation-derived vector and $\mathbf{g}[\mathbf{Y}(t)]$ is the non-linear

force. The cross covariance can be written as:

$$\frac{d}{dt}\mathbf{K_{YY}}(t,t)+\mathbf{K_{gY}}(t,t)+\mathbf{K_{Yg}}(t,t)=\mathbf{K_{QY}}(t,t)+\mathbf{K_{YQ}}(t,t) \tag{3.5}$$

considering only the time $t$, a lighter notation can be used: $\mathbf{Y}=\mathbf{Y}(t)$; for higher order cumulants the relationship is:

$$\frac{d}{dt}\kappa_j\otimes[\mathbf{Y},\ldots,\mathbf{Y}]+\sum_{l=1}^{j}\kappa_j\otimes\left[\underbrace{\mathbf{Y},\cdots,\mathbf{Y}}_{l-1}\mathbf{g}(\mathbf{Y})\underbrace{\mathbf{Y},\cdots,\mathbf{Y}}_{j-l}\right]=$$

$$=\sum_{l=1}^{j}\kappa_j\otimes\left[\underbrace{\mathbf{Y},\cdots,\mathbf{Y}}_{l-1}\mathbf{Q}(t)\underbrace{\mathbf{Y},\cdots,\mathbf{Y}}_{j-l}\right] \tag{3.6}$$

The equations 3.5 and 3.6 define exact descriptions of the general situation of the system, their solution is easy to get in case of delta-correlated excitation, however, for generic processes the solution is usually very hard to get and some approximations are needed.

One common approximation consists in the evaluation of the cumulants under the hypothesys of Gaussian behavior. In this care, closed forms of each cumulant and statistical moment are known and it is possible to write the equation in function of the mean and the covariance of the input process and it becomes possible to solve the equation.

This approach is addressed as *Gaussian Closure* and it has been one of the most employed approximated methods in non-linear random vibration analysis.

## 3.3 The Probabilistic Linearization

A recently developed method developed by Polidori and Beck [42] and Lacquaniti and Ricciardi [36] is based on the linearization of the Fokker-Plank equation and can be considered as a general method for approximate solution for non-linear systems subjected to additive and multiplicative excitations. The Fokker-Plank equation of the original non-linear system is replaced with an equivalent one relative to a linear system subjected to external excitation only which is somewhat equivalent to the original model [42]. The equivalent system is determined by means of the general scheme of wheighted residuals, the error must be orthogonal to a set of linearly independent wheight functions, defined in [10].

The equivalent system provides a Gaussian solution that can be considered as an approximation of the non-linear solution. The Probabilistic Linearization leads to residual error expressed in therms of the unknown coefficients of the linear system, obtained first satisfying the Fokker-Plank equations of the non-linear and linear systems, and then, applying the wheighted residual technique.

The coefficients of the equivalent system depend on the probability density function of the excitation and on the adopted wheight functions. In the particular case of Gaussian distribution of the response and by choosing in a suitable way the wheight functions, the probabilistic linearization leads to the same solution of the Gaussian Closure.

The method highly depends on the wheight functions, however, unlike the classical methods, a universal strategy does not exists but it must be

defined for the specific case application.

## 3.4 The Path-Integral Solution

Among the approximated procedures, the Path Integral method [44] is a non-parametric algorithm that avoids to define an equivalent linearized system and it works directly on the response statistics.

It consists in a step-by-step procedure in which, at each time step, the PDF is approximated for the entire domain of definition. The method greatly depends on the approximation schemes and many different procedures are available, such as polynomial approximations or cubic splines [20].

In general, the random variables are represented in therms of complex moments; the dynamic response is written in therms of the Chapman-Kolmogorov equation so that the Path Integral consists in a discrete time integration of that equation which governs the evolution of the probability density function of the response.

The response PDF is written, at each step $t + \tau$, in therms of total probability rule using the conditional PDF of the response at time $t + \tau$ given the response PDF at time $t$ and, obviously, the marginal PDF of the response at time $t$:

$$f_X(x, t+\tau) = \int_{-\infty}^{\infty} f_X(x, t+\tau|\bar{x}, t)\, f_X(\bar{x}, t)\, d\bar{x}. \tag{3.7}$$

If the increment $\tau$ is small enough, the conditional PDF is approximated by a Gaussian distribution such that the system is considered linear inside

the time step:

$$f_X\left(x, t+\tau|\bar{x}, t\right) = \frac{1}{\sqrt{2\pi q\tau}} \exp\left[-\frac{\left(x - y\left(\bar{x}, \tau\right)\right)^2}{2q\tau}\right]. \tag{3.8}$$

Further details are available in [44] and [4]. The core of the algorithm is the solution of the integral in 3.7, in order to semplify this procedure, many different approaches have been developed, such as the fractional calculus by Cottone, Di Paola and Pirrotta [13], where the PI method involves fractional moments and it has been also extended to MDOF systems.

However, the main drawback of the method is the huge numerical effort due to handle multi degrees of freedom systems which highly increases with the number of DOFs leading to a dramatic loss of accuracy in the solution in time due to interpolation schemes, in fact, the PDF is well approximated with a limited number of complex moments but it becomes computationally demanding as long as the number of the variables increases. In any case, the PI method is able to get very good results for limited cases, a comparison with the duffing oscillator solution shows how the approximated solution provided by the PI is almost undistinguishable from the exact one.

## 3.5 The Equivalent Linearization methods

The widest family of approximated methods for non-linear random vibration consists in the equivalent linearization (ELM), also addressed as Gaussian closure or Gaussian Statistical Linearization.

The core of the method consists in the definition of an equivalent linear system whose coefficient are calibrated by minimizing the difference between the non-linear and linear responses. The most common way to do

that is to implement the mean-square of the responses' difference as error function.

Unlike other methods for non-linear random vibrations, ELM is easy to implement, is computationally efficient and it is subjected to a few costraints. The differences between the various formulations of the ELM consist in the equivalence condition and in the strategy used to minimize the error; details on those techniques are available in the book by Roberts and Spanos [45].

The first formulations [7, 9] are relatively simple, since the introduction of the method, a further steps have been made in order to improve its efficiency and accuracy. Much work in the field has focused on refining the method and extending it to specific cases such as multi degrees of freedom and non-stationary excitations [2].

Ahn and Di Paola [1] developed a new procedure that, instead of simplifying a non-linear expression appearing in differential equations, apparently complicates the equation by replacing the therms with higher-order ones. Then, the higher-order therms are replaced by a linear approximation in several steps. The indirect linearization certainly is more demanding than the standard formulation, however, it still takes into account the higher order statistics and it results more efficient in capturing the real behavior of the system. The procedure has also been extended by Elishakoff *et al.* [23] replacing the classical mean-square of the error by the ortogonal condition, superimposed to the higher-therms procedure.

Other remarkable improvements have been made by Falsone *et al.* [24] that developed a modified strategy in order to account colored noise exci-

tations for duffing oscillator.

Focusing on the topic of Bouc-Wen constitutive model, Hurtado and Barbat [34] analyzed the sources of the errors of the classical ELM method applied to the Bouc-Wen model under the hypothesis of joint Gaussian behavior. Afterwards, a linearized method based on the Dirac and Gauss densities has been developed and applied to the Bouc-Wen model under a variety of conditions and it is able to get excellents estimations of the response statistics without increasing the computational effort required by the classical ELM. However, the method has been developed under the hypothesis of symmetric behavior of the material.

The criteria so far proposed, however, all share the characteristic that they reflect global properties of the system, so that the linearization coefficients obtained can be expected to express approximately the global stochastic properties of the response, such as are described by its statistic moments. However, in many reliability problems, what is of interest is the probability of the response (or its modulus) exceeding some given threshold $x$ addressed as *Tail Probability* that will be defined properly in chapter 4.

Casciati *et al.* developed an improved ELM procedure [8]. The failure probability is measured by the stationary upcrossing rate at the critical threshold $x$. The upcrossing rate can be calculated from the joint stationary probability of the response and its derivative[2] at time $t$. A good remark is that the technique can be extended to a variety of cases by using the stochastic averaging method and focusing on the stationary upcrossing to

[2]For further details on the upcrossing rate, see chapter 5.

the envelope process[3] expecially in presence of narrow band excitations.

Still, the ELM procedure is affected by some drawbacks. In order to determine the parameters of the linearized system, the response statistics of the equivalent linearized system itself are used, which, in turn, depend on its own parameters. Thus, a set of non-linear equations for the calibration of the parameters arises. Moreover, the linearized system subjected to Gaussian excitations provides responses that are also Gaussian whereas the actual response should be nongaussian. Consequently, the response power spectral density corresponding to the ELM solution will contain only frequencies inherent in the excitation, while the actual response power spectral density of the non-linear system may contain frequencies outside the excitation's spectrum (Donley ans Spanos, [21]). Finally, the ELM does not guarantee the uniqueness of the solution, as shown by Fan *et al.* [25] and Roberts [46].

Further considerations about the reasons that lead to propose a non-parametric linearization method as alternative of ELM for some applications, will be discussed in chapter 4.

[3] Also, for further details about the envelope process, see chapter 5.

# Chapter 4

# Tail-Equivalent Linearization Method (TELM)

Let us focus on the equivalent linearization method which have been briefly summarized in chapter 3. The easiest way to define an equivalent linear model of a nonlinear one is to define a set of physical parameters such that the response of the linear system matches somehow the one of the non-linear model. It is necessary to define an equivalence condition so that an error function, depending on the physical parameters, can be evaluated. The calibration of the physical parameters is conducted minimizing the error function.

Many equivalence condition are available in practice. The most common one defines the error as the mean-square of the difference between the linearized and the non-linear response. Regardless of the equivalence condition, these methods are addressed as Equivalent Linearization Methods (ELM).

Defined the error function, a minimization algorithm leads to a set of

physical parameters that completely defines the system. Some general consideration can already be made. First of all, the specific set of parameters obviously depends on the properties of the non-linear model but also on the features of the specific input excitation. This is a first drawback of the ELM methods, because it is necessary to define a different linear model, and then to run a minimization algorithm, as long as the input excitation is modified. Furthermore, the definition of the error function depends on the specific goal of the performed analysis and then the ELM could be needed to be performed several times for different targets.

However, the ELM applies to a wide range of non-linear tipologies and the main advantage is that the method's complexity does not increase significantly as the number of degrees of freedom becomes larger. Although, still it is affected by some drawbacks. First, the definition of a whole linearized system leads to an hypothesis about the probability distribution of the response at a given times; for example, if the input excitation has Gaussian distribution, also the response would be Gaussian[1]. For this reason, the probability of the response can be inaccurate especially in the tail region and the evaluation of many entities of interest for the random vibration analysis, such as crossing rates, first passage probability, can be inaccurate at high thresholds.

Furthermore, the parameters of the linearized system are function of the second-moment of its response (i.e. the mean square of the error of the response), thus, there is a double dependence: the response depends

[1] Of course, different probability distribution can be used for the input excitation and they would lead to different response distributions.

on the parameters and the parameters' definition depends on the response, thus, there is an implicit relationship and the set of parameters can be evaluated only by an iterative scheme that can be computational demanding expecially if, in order to get a high accuracy, a large set of parameters is required.

In order to address a better solution that does not assume the Gaussian distribution, an alternative solution has been proposed by Casciati *et al.* [8]. The equivalence between the equivalent linear and non-linear systems is expressed by equating their mean level crossing rates but the knowledge of the joint probability of the response and its first derivative is required and it can be extremely difficult to define for general non-linear systems as long as the number of DOF increases.

A different class of linearization methods has been developed thanks to the application of the First-Order Reliability Method (FORM) in order to avoid the dependence of the linearized system by a set of parameters. The approach was proposed by Li and Der Kiureghian (1995) and it has been applied and extended by Der Kiureghian (2000), Koo and Der Kiureghian (2003), Franchin (2004), Koo *et al.* (2005) and Fujimura and Der Kiureghian (2006). The stochastic excitation si discretized in terms of a finite number of random variables as shown in Chapter 2 and it is possible to express the state limit function that the target response exceedes a given threshold at a given time as an implicit function of the random variables. The FORM method is applied and it gives back the first-order approximation of the tail probability. The definition of tail probability and the reasons that lead to its implementation are better explained in section

4.1. The limit state surface, defined in the space of the random variables, is approximated by an hyperplane which is tangent to the surface at the design point. Each point of the random variables space defines a particular realization of ground motion and each point of the state limit surface defines a particular realization of ground motion that leads the non-linear system response to reach the given threshold at the given time. The design point satisfies that property and it correspond to the most likely ground motion realization that implies the limit state event. It will be shown that the linearized system corresponds to the tangent hyperplane and that it is possible to extract its IRF only by the knowledge of the design point ad without the needing to define any system parameter.

Numerical analysis have already shown that this approach leads to a better accuracy compared to the classical equivalent linearization methods. The latter-developed form of the method has been improved in this work and validating numerical samples have been provided.

## 4.1 Tail Probability and equivalence conditions

Let us consider an input random process $F(t)$ defined, for example, in term of ground acceleration. The response of a generic oscillator ca be defined as $X(t)$. The statistic of both processes is completely defined by the cumulative probability distribution (CDF) and its firs derivative: the probability density function (PDF); for example, the $F(t)$ process will have:

$$F_F(t_n, f^*) = \Pr[F(t_n) \leq f^*] \tag{4.1}$$

the PDF can also be defined as:

$$f_F(t_n, f^*)\, df = \Pr\left[f^* - \frac{df}{2} < F(t_n) \leq f^* + \frac{df}{2}\right] \tag{4.2}$$

where $df$ represents a small differential of $f$. Both CDF and PDF can change in time, the stationary processes have the property that their statistical characterization does not change in time, so both the CDF and the PDF would only be dependent of $f$ but not of $t_n$.

The excitation process defined in chapter 2.1 is Gaussian with zero mean, i.e., the PDF has the form:

$$f_F(t_n, f) = \frac{1}{\sqrt{2\pi}\sigma_F(t_n)} \exp\left[-\frac{1}{2}\frac{f^2}{\sigma_F(t_n)^2}\right]. \tag{4.3}$$

In the same way, the PDF in time of the response $X(t)$ can be defined. It is important to note that, even if $f_F(t_n, f)$ is Gaussian, the PDF of the response $f_X(t_n, f)$ is not Gaussian unless the dynamic system is linear. For generic non-linear systems neither the shape nor the equation of the PDF are known.

The probability of response at a given time is not the most interesting result in structural engineering. In order to evaluate the structural reliability under earthquake excitation, usually it is useful to choose a target response, such as a specific displacement, the interstory drift or the global base force. The collapse of the structure, or in general a limit state, can be defined as a specific threshold of the target response (such as a maximum vaue of the interstory drift, etc.). The random vibration analysis can provide the probability that the structural response exceedes the threshold during a given interval of time large enough to contain all the earthquake duration.

Let $E$ be the collapse event, $T$ the duration of the earthquake and $\hat{x}$ the collapse threshold, phisically, the probability of structural collapse should be defined as:

$$\Pr\left[E|T\right] = \Pr\left[\max\left(X\left(t\right)\right) \geq \hat{x}\right], \qquad t \leq T \tag{4.4}$$

but this definition, even if phisically correct, is not often useful in random vibration analysis and in particular it cannot be applied with the FORM and the TELM methods. In fact, recalling that the response process $X\left(t\right)$ depends on the excitation process $F\left(t\right)$, the FORM method would search the most likely realization of $F\left(t\right)$ that satisfies the condition $\max\left(X\left(t\right)\right) \geq \hat{x}$. The FORM method is iterative on a set of trial realizations of $F\left(t\right)$ and, at each step, it evaluates the response $\max\left(X\left(t\right)\right)$ and its gradient with respect to $F\left(t\right)$. In order to archieve the convergence, it is required that the gradient is continuous over all the domain, and this collapse condition does not satisfy this requirement; because of this reason, the probability 4.5 cannot be used.

In order to get a continuous gradient, it is useful to consider the so-called *Tail Probability*:

$$\Pr\left[E'|T\right] = \Pr\left[X\left(T\right) \geq \hat{x}\right] \tag{4.5}$$

the event $E'$ is not the event of collapse, but a subset of it: it defines that the structure collapses at the end of the earthquake duration. The event that the system response is greater than the threshold for $t < T$ *but not* at $t = T$ is simply $E - E'$. Note that $E'$ and $E - E'$ are not mutually exclusive because in general if the system does not collapse at $t = T$ it does

not mean that it did not collapse for $t < T$, as shown, for example, in figure 4.1.

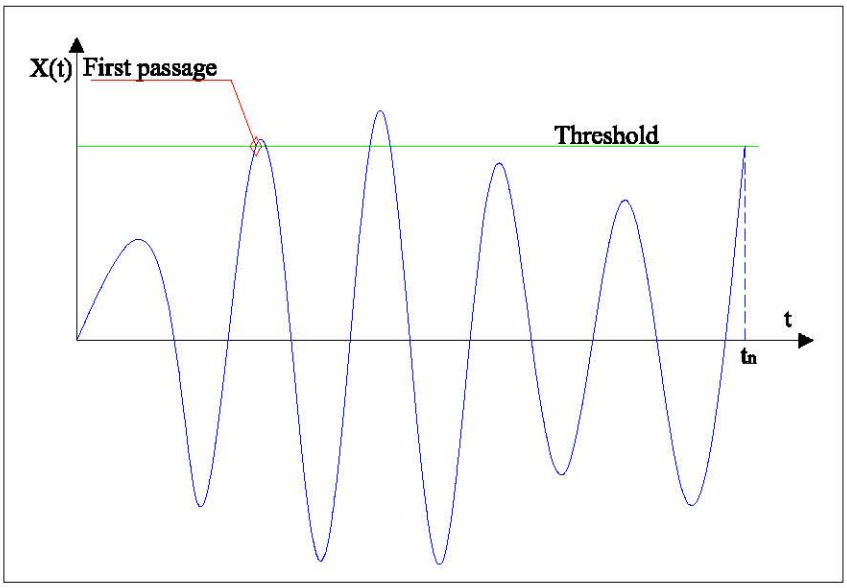


Figure 4.1: Realization of first excursion before $t_n$

Even if the tail probability leads to approximate results, they are accurate enough to be employed if practice. Numerical analysis show that the event $E'$ has a probability of occurrence bigger that the event $E - E'$, thus, fixed an interval $T$ most likely the collapse will occur at the end of the interval. A deeper treatment about this topic is shown in [29] in which the employment of the tail probability is also validated by a set of Monte Carlo simulation. Only to understand the phisical meaning, the figure 4.2 shows the structural response of an oscillator and its probability distribution, because the process is stationary, the PDF remains the same during all the $T$

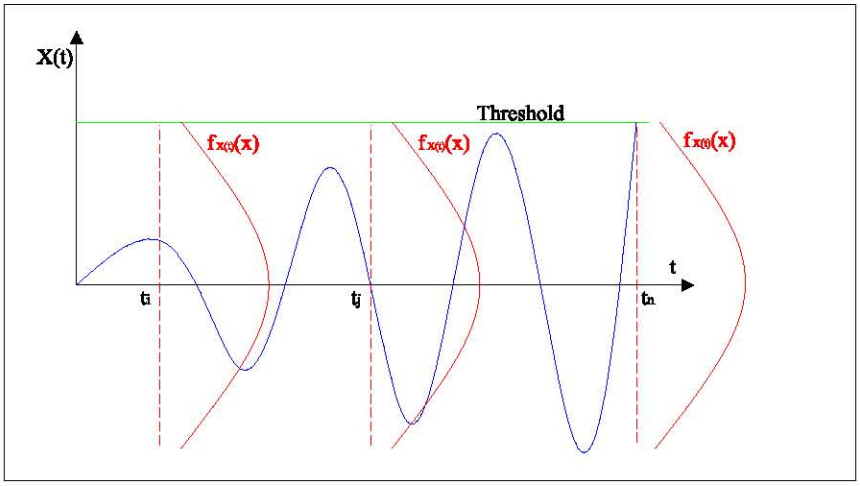


Figure 4.2: Stationary response statistic in time

interval, thus, the likelyhood of the peaks occurring during the interval $T$ are as high as the peak is short, so, because the influence of each peak on the response at $t = T$ is as smaller as the peak occurs early in the interval, the peaks gradually grew in time and lead to the final, highest value of the response at $t = T$. Of course, it is necessary to consider different intervals $T_i$ in order to consider the case of shorter earthquake and the case of collapse occurring early in time. Evermore in [29] it is shown that accurate enough results are given by a set of analysis performed ad different times fixed from 0 and then every 5 seconds until the entire earthquake duration.

### 4.1.1 Equivalence conditions

The underlying idea under all the linearization methods is to replace a non-linear system with a conveniently chosen linear system. This convenience lays into an equivalent condition, in fact, fixed a non-linear system, it is

possible to define several equivalent linear ones, each one of them on the base of a different entity of interest. Of course, each linear system has its own application field and effectiveness domain.

Because the entity of interest of the TELM is the tail probability, the condition of equivalence is defined in terms of if. Given a threshold and at a given time, the tail probability of the equivalent linear system is fixed to be the same of the first-order approximation of the tail probability of the non-linear system, evaluated by a FORM.

Both probabilities are defined in the space of the standard-normal random variables, then the tail probability is completely defined by a design point. In the following sections, the equivalence will be set in terms of design point and reliability index.

## 4.2 Characterization of linear systems

Let us define a dynamic linear system in terms of a set of differential equations:

$$\mathbf{M}\ddot{\mathbf{y}}(t) + \mathbf{C}\dot{\mathbf{y}}(t) + \mathbf{K}\mathbf{y}(t) = \mathbf{P}f(t) \tag{4.6}$$

where $\mathbf{M}$, $\mathbf{C}$ and $\mathbf{K}$ are respectively the mass, damping and stiffness matrix, $\mathbf{P}$ is a load distribution factor, $f(t)$ is the excitation, $\mathbf{y}(t)$ is the displacement vector and the dots represents derivatives with respect the time. The stiffness matrix is constant in time and, fixed the initial conditions:

$$\begin{aligned} \ddot{\mathbf{y}}(0) &= \mathbf{a_0} \\ \dot{\mathbf{y}}(0) &= \mathbf{v_0} \\ \mathbf{y}(0) &= \mathbf{d_0} \end{aligned} \tag{4.7}$$

it is possible to get the solution $\mathbf{y}(t)$. Many computational methods have been developed for this purpose, but it is also well known that a stable linear oscillator can be completely defined by the so-called Impulse Response Function (IRF).

Defined a pair excitation-response[2] $f_i(t)$, $x(t)_j$ the IRF is defined as:

$$h(t) = x(t) \qquad \text{with } f(t) = \delta(t) \tag{4.8}$$

where $\delta(t)$ is the Dirac's function; so, the IRF is the response of the system for an impulse at $t = 0$. It only depends by the specific chosen pair excitation-response, it is invariant in time and with respect the scale of the excitation. Because the system is linear, the superposition of the responses of different excitation is simply the sum of the individual responses, this property leads to the well known Duhamel's integral that, if the IRF is defined, evaluates the response of the system for any excitation:

$$x(t) = \int_o^t h\left(t-\tau\right) f\left(\tau\right) d\tau \tag{4.9}$$

the IRF of a SDOF oscillator has the expression:

$$h(t) = \frac{1}{\omega_D} \exp\left(-\zeta\omega_0 t\right) \sin\left(\omega_D t\right) \qquad \text{for } t > 0 \tag{4.10}$$

where $\omega_0$ is the natural frequency of the oscillator, $\zeta$ is the damping ratio and $\omega_D = \omega_0\sqrt{\zeta - 1}$ is the damped frequency.

[2]If the system is multi-degrees of freedom and the excitation is multi-component and/or multi-support, it is necessary to define one target response, such as a specific displacement or a force, and a specific component and/or support excitation.

The system is defined as stable if its free vibration response approaches zero after a long enough time, independently of the initial conditions. Necessary and sufficient condition for the stability of a system is the following:

$$\lim_{t\to\infty} h(t) = 0 \tag{4.11}$$

it is easy to verify that the SDOF oscillator with IRF 4.10 is stable as long as $\zeta > 0$.

As long as the system is stable, it has a steady-state and it is possible to define the Frequency Response Function (FRF), $H(\omega)$ as the steady state response amplitude when $f(t) = \exp(i\omega t)$:

$$\lim_{t\to\infty} x(t) = H(\omega)\exp(i\omega t). \tag{4.12}$$

The FRF of a system is the Fourier transform of its IRF:

$$H(\omega) = \int_0^\infty h(\tau)\exp(-i\omega\tau)d\tau. \tag{4.13}$$

Both functions will be useful in the random vibration analysis. At this point it is important to note that the IRF or the FRF completely define a linear system, even if the matrixes **M**, **C** and **K** are not known.

### 4.2.1 Relationship between IRF and Performance Point

Let us consider the SDOF linear oscillator with IRF defined in 4.10 subjected to a single-component-and-support excitation $F(t)$ defined in the form 2.2, the capital letters denotes a random process, in fact $F(t)$ is function of a set of standard-normal random variables **u**. The response at a given time $t$ is given by the Duhamel's integral:

$$X(t) = \int_o^t h(t-\tau)F(\tau)d\tau \tag{4.14}$$

substituting $F(t)$ with its discretized form 2.2 and changing the integration-summation order, it leads to:

$$X(t) = \int_o^t h(t-\tau) \sum_{i=1}^{n} s_i(\tau)\, u_i d\tau = \mathbf{a}(t)\, \mathbf{u} \tag{4.15}$$

where the generic component of the array $\mathbf{a}(t)$ is:

$$a_i(t) = \int_0^t h(t-\tau)\, s_i(\tau) d\tau. \tag{4.16}$$

It follows that the response process is the scalar product of a deterministic row vector $\mathbf{a}(t)$ and the random vector $\mathbf{u}$.

Now, fixed a threshold $x$ for the response, in the space of the standard-normal variables the locus of all realizations that give rise the response $X(t) = x$ at time $t = t_n$ can be defined; it is given by the equation:

$$x - \mathbf{a}(t_n)\, \mathbf{u} = 0 \tag{4.17}$$

and it defines an hyperplane in the standard-normal space with normal vector $\mathbf{a}(t_n)$. The 4.17 is also defined as Ultimate State Limit Function (USL). The projection of the origin of the space on the hyperplane is defined as Performance Point (PP) and it is denoted as $\mathbf{u}^*(x, t_n)$, as shown in figure 4.3 for only two dimentions of the standard normal variables set. The performance point has the minimum distance from the origin over all the points of the hyperplane, thus, it also has the maximum likelyhood.

Because there is one and only one performance point for each given couple $(x, t_n)$ and there is one and only one vector $\mathbf{a}(t_n)$ fixed $t_n$, it is

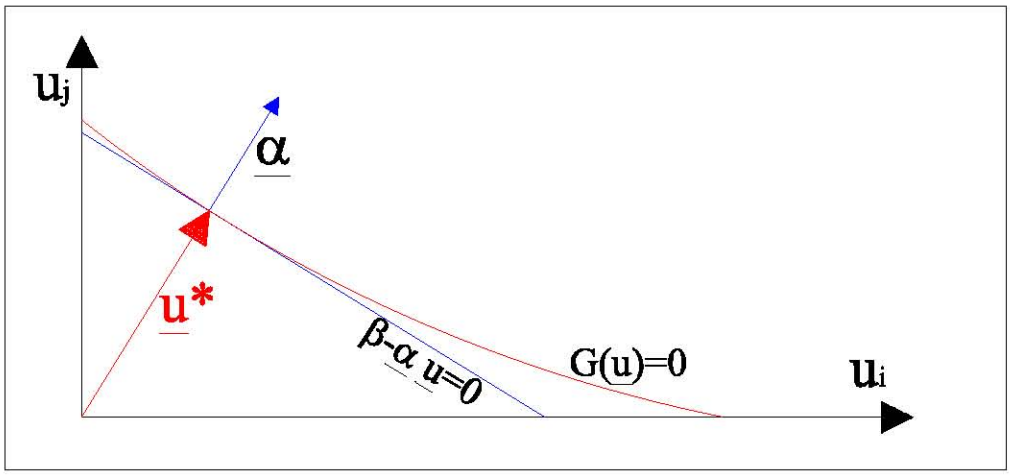


Figure 4.3: Performance Point

possible to express the performance point in terms of the threshold and $\mathbf{a}(t_n)$ vector. By geometric considerations:

$$\mathbf{u}^*(x, t_n) = \frac{x}{\|\mathbf{a}(t_n)\|} \frac{\mathbf{a}(t_n)^T}{\|\mathbf{a}(t_n)\|} \tag{4.18}$$

and the equation can be inverted and it gives:

$$\mathbf{a}(t_n) = \frac{x}{\|\mathbf{u}^*(x, t_n)\|} \frac{\mathbf{u}^*(x, t_n)^T}{\|\mathbf{u}^*(x, t_n)\|}. \tag{4.19}$$

It is clear that, if the performance point $\mathbf{u}^*(x, t_n)$ is known, it is possible to determine the gradient vector $\mathbf{a}(t_n)$.

Because this last one vector is deterministic and it only depends on the excitation covariance structure, given by $s_i(\tau)$, and on the IRF of the system, it is possible to invert the relation 4.16 and get the IRF itself. In order to do that, the IRF can be discretized and approximated as a set of

rectangular responses and then the integral 4.16 becomes the summation:

$$a_i(t_n) \cong \sum_{j=1}^{n} h\left(t_n - t_j\right) s_i\left(t_j\right) \Delta t \tag{4.20}$$

which represents a set of $n$ linear equations where the only unknown quantities are the $h\left(t_n - t_j\right)$. Note that, thanks to the properties of the IRF and because the time step is constant in time, each solution of the 4.20, $h\left(t_n - t_j\right)$ corresponds to the IRF of a specific point in time:

$$h\left(t_n - t_j\right) = h\left(t_{n-j}\right) \tag{4.21}$$

furthermore, assuming the particular form of the $s_i\left(t_j\right)$ as defined in section 2.2, the characteristic matrix of the system defined above is triangular in form and in the particular case of unfiltered and unbounded white noise, it is in diagonal form and the equation are uncoupled:

$$h\left(t_n - t_j\right) = \frac{a_j\left(t_n\right)}{\sigma \Delta t} \tag{4.22}$$

Thus, the systems 4.20 and 4.22 are easily invertible. It is obvious that a long enough response time $t_n$ has to be considered in order to capture the whole decaying tail of the IRF and a small enough time step $\Delta t$ has to be used in order to avoid too much large approximations about the rectangular-shape discretization of the IRF defined in the 4.20 and so to get a high enough resolution. Specifically, as shown previously in section 2.2, the discretization of the input excitation cuts its PSD and, even if an unbounded white noise has been defined, it will be *de facto* upper-bounded at the approximative frequency $1/\left(2\Delta t\right) Hz$, thus, it is necessary

to consider a small enough $\Delta t$ value in order to have a cutoff frequency much higher than the significant frequencies of the dynamic system, so that one can avoid to loose not neglectible contributions at high frequencies.

Finally, the system is always invertible if the excitation has always non-zero variance over all the interval $[0, t_n]$, i.e., the $s_i(t_j)$ on the main diagonal of the matrix are non-zero values. The seismic excitation commonly used in practice usually satisfy this last requirement.

Summarizing, at that point, given the performance point of the linear system $\mathbf{u}^*(x, t_n)$ of a specific time $t_n$ and threshold $x$, and fixed the excitation, it is possible to get the $\mathbf{a}(t_n)$ functions and, then, the rectangular-approximated discretized IRF of the linear system. The figure 4.4 shows the IRFs of a SDOF oscillator with $f = 1Hz$, $\zeta = 0.02$, the firs one is the IRF obtained from the exact solution given by the equation 4.10, the second one is obtained applying the procedure just described with a unitary white noise excitation, $x = 1$, $t_n = 30sec$ and a time step $\Delta t = 0.02sec$, one can notice that the approximated IRF perfectly matches the theorical one.

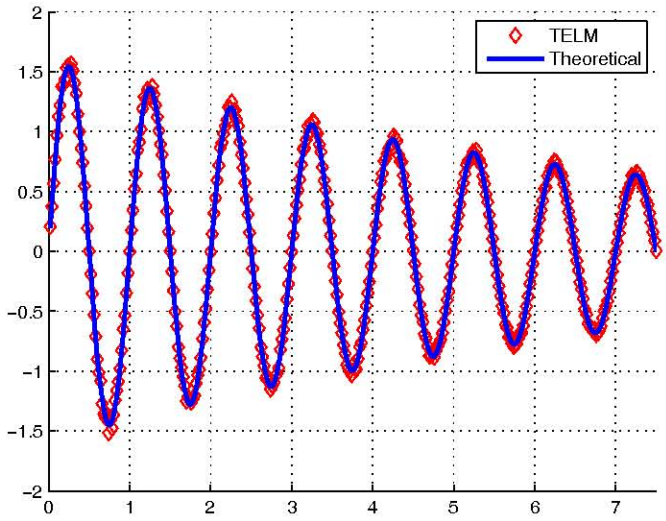


Figure 4.4: Impulse Response Function linear SDOF oscillator, $f = 1Hz$

## 4.3 Tail Probability of the non-linear system and Tail-Equivalent Linearized System (TELS) definition

Let us consider a multi-degree-of-freedom (MDOF) non-linear system, it can be defined by the 2nd order differential equation:

$$\mathbf{M}\ddot{\mathbf{Y}} + \mathbf{C}\dot{\mathbf{Y}} + \mathbf{R}(\mathbf{Y}, \dot{\mathbf{Y}}) = \mathbf{P}F(t) \tag{4.23}$$

where $\mathbf{Y}$ denotes the displacement vector, $\mathbf{M}$ is the mass matrix, $\mathbf{C}$ denotes the viscous damping matrix, $\mathbf{R}$ denotes the restoring force vector and it depends by both displacements and velocities, and finally $\mathbf{P}$ is a load distribution factor. The MDOF system is subjected to a stochastic excitation $F(t)$ which is in the form defined in section 2.2 with null initial

conditions $\dot{\mathbf{Y}}(0) = 0$ and $\mathbf{Y}(0) = 0$. In this section the case of a single-component excitation process, subsequently, the case of multi-component process will be developed.

The restoring force vector $\mathbf{R}(\mathbf{Y}, \dot{\mathbf{Y}})$ depends by the displacement and the velocity vectors and it allows the system to have a non-linear hysteretic behavior. Many different models of restoring forces are available, in the present work the Bouc-Wen model has been used.

The system response $X(t) = X\left(\mathbf{Y}, \dot{\mathbf{Y}}\right)$ is usually defined as a non-linear function of the nodal displacements and velocities; common quantity of interest are the interstory drifts, the top displacement or the global horizontal force. Defined $F(T)$ as in 2.2, the domain variables vectors $\mathbf{Y}$ and $\dot{\mathbf{Y}}$ are implicit function of the standard-normal variables $\mathbf{u}$, it follows that the system response can be defined as dependent by the time and the random variables, as $X(t, \mathbf{u})$.

Fixed a threshold $x$ and an excitation time $t_n$ similarly as the previous section, the tail probability of the $X$ response is defined as:

$$\Pr\left[x \leq X\left(t_n, \mathbf{u}\right)\right] \tag{4.24}$$

and it corresponds to a limit state function:

$$G\left(x, t_n, \mathbf{u}\right) = x - X\left(t_n, \mathbf{u}\right) \tag{4.25}$$

and the 4.24 becomes:

$$\Pr\left[x \leq X\left(t_n, \mathbf{u}\right)\right] = \Pr\left[G\left(x, t_n, \mathbf{u}\right) \leq 0\right]. \tag{4.26}$$

Provided that $G$ has continue firs derivative with respect to $\mathbf{u}$, the equations 4.23 and 4.26 become a standard structural component reliability

problem with loads randomply defined by $\mathbf{u}$ and limit state parameters defined by $t_n$ and $x$. In order to get the tail probability, many methods can be applied, the one of interest is the First-Order Reliability Method (FORM) because the equivalence condition between the non-linear and equivalent linear system defined in section 4.1.1 impose the equality between the tail probability of the equivalent linear system and the first-order approximation of the tail probability of the nonlinear system. This latter one is directely provided by the FORM.

In the standard normal space, the limit state function 4.25 is related to the limit state surface:

$$G\left(x, t_n, \mathbf{u}\right) = 0 \tag{4.27}$$

each point of it corresponds to a particular realization of excitation $F(t)$ that leads the system response $X$ to reach the threshold $x$ at time $t_n$, now, the first-order probability approximation is obtained by linearizing the limit state surface in the standard normal space at the point which is closest to the origin and, for this reason, has the maximum likelyhood. This point, again designed as "design point", is the solution of the following constrainted optimization problem:

$$\mathbf{u}^{*}\left(x, t_n\right) = \arg\min\left[\|u\| \;\; |G\left(x, t_n, \mathbf{u}\right) = 0\right] \tag{4.28}$$

and it is related to the firs-order tail probability given by the joint Gaussian cumulative probability function $\Phi$:

$$\Pr\left[x \leq X\left(t_n, \mathbf{u}\right)\right] = \Pr\left[G\left(x, t_n, \mathbf{u}\right) \leq 0\right] \cong \Phi\left[-\beta\left(x, t_n\right)\right] \tag{4.29}$$

where $\beta(x, t_n)$ is the reliability index given by:

$$\beta(x, t_n) = \boldsymbol{\alpha}(x, t_n)\, \mathbf{u}^*(x, t_n) \tag{4.30}$$

in which $\boldsymbol{\alpha}(a, t_n)$ is the normalized negative gradient vector of he limit state surface at the design point:

$$\boldsymbol{\alpha}(x, t_n) = -\frac{\nabla G(x, t_n, \mathbf{u}^*)}{\|\nabla G(x, t_n, \mathbf{u}^*)\|}. \tag{4.31}$$

The reliability index and the negative gradient completely define the hyperplane tangent to the limit state surface at the design point by the equation:

$$\beta(x, t_n) - \boldsymbol{\alpha}(x, t_n)\, \mathbf{u} = 0. \tag{4.32}$$

It is important to note that both quantities $\mathbf{ff}(a, t_n)$ and $\beta(x, t_n)$ are univocally defined by the performance point, *i.e.* the knowledge of $\mathbf{u}^*(x, t_n)$ completely defines both the first-order tail probability and the tangent hyperplane to the state limit surface. This important property allows to apply the equivalence condition between the equivalent linear and non-linear system defined in 4.1.1 in terms of performance point instead of, more strictly, tail probability.

### 4.3.1 Tail-Equivalent Linearized System (TELS) definition

As shown in section 4.2.1, a linear system is defined, in the standard normal space, by an hyperplane and the projection of the origin on it is the performance point. Also, the performance point of the linear system $\mathbf{u}^*_{LS}(x, t_n)$ is related to the tail probability given time $t_n$ and threshold $x$.

Furthermore, as shown in section 4.3, a non-linear system defines a limit state surface in the standard normal space, the first-order approximation performance point $\mathbf{u}^*_{NL}(x, t_n)$ is the one on the limit state surface with the maximum likelihood of occurrence; the hyperplane tangent to the limit state surface at the performance point is completeli defined by $\mathbf{u}^*_{LS}(x, t_n)$ and in turn it completely defines the first-order approximation of the tail probability. The equations of the two hyperplanes are totally analogous:

$$\beta_{NL}(x, t_n) - \boldsymbol{\alpha}_{NL}(x, t_n)\, \mathbf{u}^*_{NL} = 0 \tag{4.33}$$

for the non-linear system, and

$$\beta_{EL}(x, t_n) - \boldsymbol{\alpha}_{EL}(x, t_n)\, \mathbf{u}^*_{NL} = 0 \tag{4.34}$$

for the linear system.

It is clear that, if the equivalent linear and non-linear tail probabilities have to coincide, also the hyperplanes have to be the same. In order to archieve this equivalence note that, because threshold, time and excitation are the same for both systems, it is necessary, and at the same time sufficient, that also the performance points are equal.

Thus, the equivalence condition defined in section 4.1.1 in terms of tail probability, can be proposed in terms of performance points; so, the Tail-Equivalent Linearized System (TELs) can be defined as the linear system that leads to:

$$\mathbf{u}^*_{EL} = \mathbf{u}^*_{NL}. \tag{4.35}$$

We now have all the elements to get an equivalent linear system given:

- the threshold $x$
- the excitation time $t_n$
- the excitation $s_i(t)$

and, of course, the physicl characteristics of the system. The TELM procedure can be summarized as:

1. Performing the FORM method on the non-linear system, it gives back the performance point $\mathbf{u}^*_{NL}$, the reliability coefficient $\beta_{NL}(x, t_n)$ and the normal vector $\boldsymbol{\alpha}_{NL}(x, t_n)$;
2. Setting the equivalence between the performance points $\mathbf{u}^*_{EL} = \mathbf{u}^*_{NL} = \mathbf{u}^*$
3. Evaluation of the $\mathbf{a}(t_n)$ vector by $\mathbf{a}(t_n) = \frac{x}{\|\mathbf{u}^*(x,t_n)\|} \frac{\mathbf{u}^*(x,t_n)^T}{\|\mathbf{u}^*(x,t_n)\|}$;
4. Inversion of the system 4.20 in order to get the impulse response function of the equivalent linear system.

Note that the obtained IRF is reliable only for the specified time and threshold $t_n$ and $x$, its dependence by the excitation structure and scale will be analyzed in the next section. However, the TELs permits the performance of a random vibration analysis and the parameters of the linearized system, such as mass, stiffness and damping, are not even needed. The implementation of the TELs in the most common random vibration methods will be analyzed in chapter 5.

## 4.4 Features and peculiarities of the Asymmetric TELM

In order to apply the TELS in random vibration analysis it is useful to briefly analyze its features and its physical admissibility. In this section, the TELS dependance on the physical parameters will be analyzed, then, the requirements for its existence and uniqueness will be shown.

It is important to emphasize that the properties explained in [28] only apply to the classical formulation of TELM, for this reason, in the following sections the corresponding properties related to the specific asymmetric material defined in chapter 6 will be analyzed. The implementation of different kinds of materials can compromize some of this features and the TELS properties must be analyzed for the specific implemented constitutive model.

### 4.4.1 Physical admissibility of TELS

In order to employ the obtained TELS in engineering applications, its physical admissibility has to be archieved. The only way to do it is to investigate if the IRF of the TELS satisfies all the fundamental requirements of the IRF of a generic and stable system.

The first property, as mentioned earlier, is that it must result $h(t) = 0$ for each $t < 0$. The set of equations in 4.20 does not involve any value of the IRF for negative times, therefore this requirement is satisfied for any hyperplane in the standard normal space.

Furthermore, it is required that the system is stable, *i.e.*, the IRF has fi-

nite value of the integral over all the positive domain $[0, \infty[$: $\int_0^\infty h(t)dt < \infty$ which also implies that the IRF must decay to zero after a long enough interval of time: $\lim_{t\to\infty} h(t) = 0$ but this requirement is harder to archieve because some hyperplanes in the standard normal space may lead to unstable systems. For example, fixed a white noise excitation (*i.e.* the 4.20 system has its characteristic matrix as a multiple of the unitary matrix), if the gradient of the hyperplane has equal components, it leads to a constant IRF, regardless of the length of the considered time interval, so, its integral and its limit are not zero.

It is not possible to make sure that the TELM leads to a stable system and it is necessary to check the IRF properties anytime the TELM is applied, however, Fujimura [28] shows how, for most of the practical applications, the symmetric formulation of TELS is stable. Also, the TELS related to the applications of the present work are always made of admissible IRFs; for this reason, it is reasonable to say that, in general, TELM provides physically admissible results but a deeper analysis of the solution is required in order to assure that each IRF of the TELS corresponds to a stable linearized system.

### 4.4.2 Influence of the threshold

In order to investigate the dependence of the TELS on the response thresholds, it is useful to consider the Impulse Response Functions (IRFs) and the Frequency Response Functions (FRFs) of the TELS for different thresholds $x$.

A set of IRFs for negative and positive thresholds are shown respectively

in figures 4.5 and 4.6. Some observations are noteworthy. First, the rate of decay in the amplitude of the IRF increases with increasing threshold of the response. This is because higher thresholds lead to bigger hysteresis loops and, therefore, the system dissipates more energy. Furthermore, the predominant period of the oscillation tends to increase with increasing response threshold. This is due to softening of the connecting element with increasing threshold. However, this two phenomena are common to symmetric hysteretic behavior as well. A more inter-esting observation is made by comparing the IRFs for symmetric thresholds, such as those shown in figure ?? for the threshold of +0.1m and 0.1m.

As can be seen in figure 4.9, the TELSs for positive and negative thresholds of equal magnitude are distinctly different. The IRF of the TELS for the negative threshold (compression side) decays more rapidly and exhibits a longer predominant period than the IRF of the TELS for the positive threshold. These are because of the asymmetry of the hysteresis law of the material. With decreasing magnitude of the thresholds, the two IRFs become similar and approach the IRF of the linear system corresponding to the case of $\alpha = 1$.

Similar considerations can be made on the FRFs which are obtained taking the Fourier transform of the corresponding IRFs. A set of FRFs have been plotted togheter in figures 4.7 and 4.8 respectively for negative and positive thresholds. As the threshold increases, the dominant peak of the FRF shifts to the lower frequencies and decreases in intensity. Also, the frequency containt near the origin slowly increases. It means that, fixed the parameter properties, the linearized system becomes softer as the threshold

increases. This behaviour depends on two factors: the shifting to the lower frequencies depends on the smaller stiffness of the Bouc-Wen material as long as the displacements increase; the smaller value of the FRF depends on the higher dissipation of elastic energy during the hysteresis as long as force and displacement become larger and so the cycles becomes wider.

It is clear that there is a high dependance of the TELS on the threshold, and it results the biggest one. In order to get the non-Gaussian probability distribution of the non-linear response, this behaviour forces the evaluation of the IRFs for a range of threshold of interest while, for example, it is not necessary, in case of symmetric material.

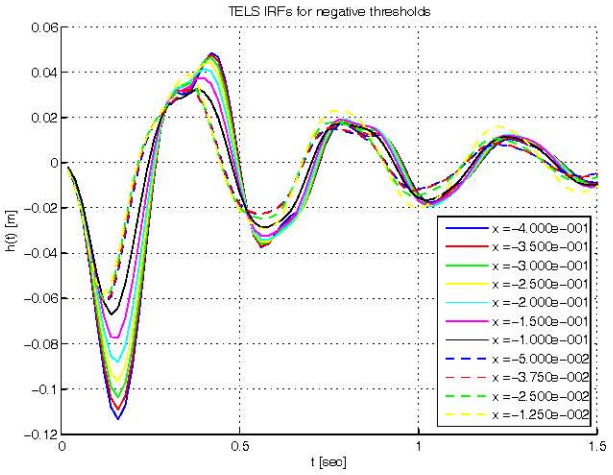


Figure 4.5: Impulse response functions for negative thresholds

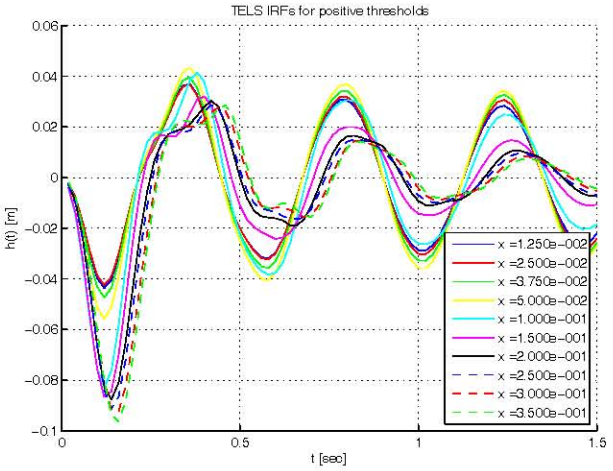


Figure 4.6: Impulse response functions for positive thresholds

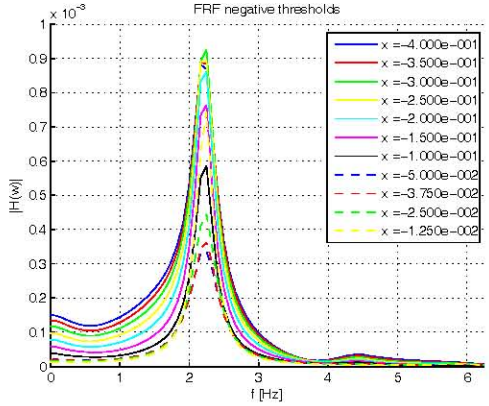


Figure 4.7: Frequency response functions for negative thresholds

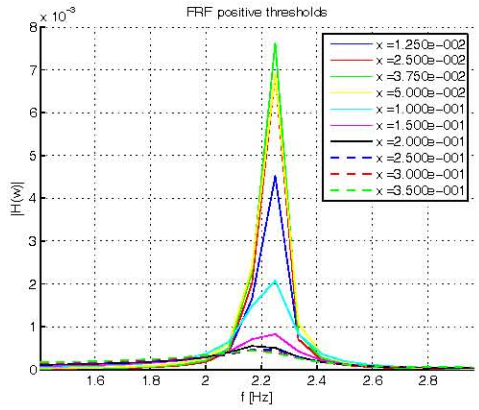


Figure 4.8: Frequency response functions for positive thresholds

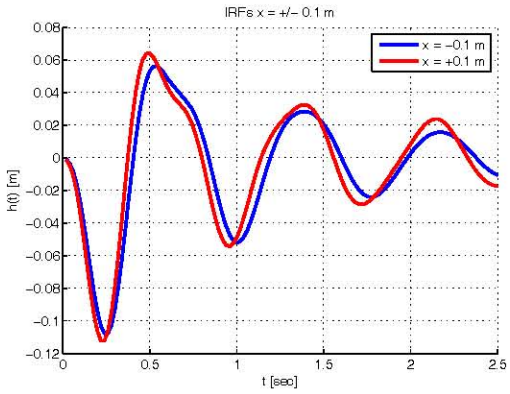


Figure 4.9: Impulse response functions for $x = \pm 0.10m$

### 4.4.3 Existence and uniqueness

The existence of the TELS directly depends on the existence of the design point and its tangent hyperplane. This implies that the limit state surface must be differentiable with respect to $\mathbf{u}$ at the design point. Furthermore, because the FORM is an iterative method and at each step it determines the value of the limit state function and its gradient, it is convenient that the limit state surface, and then the dynamic response of the non-linear system, are differentiable in any point of the space.

As shown in [32], the differentiability is archieved if the costitutive model of the employed material is smooth, *i.e.* its first derivative is always continuous. The generalized Bouc-Wen model used in this work is smooth, many materials used in engineering practice have some derivative discontinuities. The drawback can be easily solved by smoothing the model with transition archs[3].

The uniqueness of the TELSs requires that there must be one and only one design point. It is possible to get limit state surfaces with more than one point at the same minimum distance from the origin, and this case cannot lead to a unique TELS[4], in this case the first order approximation is non accurate enough in case of multiple performance points and all the procedure would not be reliable.

Furthermore, the FORM method cannot distinguish between the global

[3]The implementation of the Smoothed-Generalized Bouc-Wen material, described in chapter 6, has been made in order to archieve this specific requirement.

[4]In general, the specific limit state surface employed in this work presents many than a single convergence point because the limit state is archieved if the response at $t_n$ is equal to a threshold, regardless of the responses in the previous step in time, then, there would be several time histories that correspond to a local minimum on the surface.

and the local minimum distance points, then, the evaluated TELS could not correspond to the global minimum. It is well known that the speed and the accuracy of the FORM convergence highly depend on the first trial value of the random variables array, in this work, the *start point excitation.* In order to investigate the convergence to different minimum points, the TELM has been performed with different starting points in the standard normal space. In particular, for a generic threshold $x_j$:

1. Perf. Point excitation of the linear system for the same threshold $x_j$;

2. Perf. Point excitation of the non-linear system for the symmetric threshold $-x_j$;

3. Perf. Point excitation of the non-linear system for the threshold $x_{j-1}$;

4. *Hot starting point* $\hat{\mathbf{u}}^*$ defined by Koo *et al.* [35] as:

$$\hat{\mathbf{u}}^* = \mathbf{u}^*(x_{j-1}, t_n) + \lambda \frac{\mathbf{u}^*(x_{j-1}, t_n) - \mathbf{u}^*(x_{j-2}, t_n)}{\|\mathbf{u}^*(x_{j-1}, t_n) - \mathbf{u}^*(x_{j-2}, t_n)\|} \tag{4.36}$$

5. Random white noise excitation;

6. Sinusoid excitation defined as:

$$u_i = q \sin(\omega_0 t_i + \theta) \tag{4.37}$$

where $i$ is the index of the generic element of the $\mathbf{u}$ vector, $\omega_0$ is the first natural frequency of the system neglecting its non-linear behavior (*i.e.*, setting $\alpha = 1$), $q$ is an amplitude coefficient[5] and $\theta$ is a phase

[5] In this work it is always $q = 1$.

angle.

The simulations show how, for the application that will be presented in chapter 7, the starting point excitations corresponding to the items 1, 2, 4 and 5 always lead to the same TELS but with highly different convergence speeds. The conventions 3 and 6 present some cases of non-convergence, expecially for high thresholds. However, the fastest conventions have been the 4 for large thresholds and 4 for small thresholds while the 5 presents an intermediate behavior and the 2 seems to be the slowest one.

A reasonably good strategy to find the performance points could employ the linear start point (item 1) to find the performance points of the smallest two thresholds (respectively, the two smallest positive thresholds and the two largest negative ones), and then the *hot starting point* can be used moving farther from the zero.

In case of non-convergence of the FORM, first the linear starting point (item 1) and then the white-noise starting point (item 5) should be used.

In case of convergence to a non reasonable performance point, it would be appropriate to lightly modify the value of the threshold and to check the new convergence trend or to construct an approximated model by interpolation of the nearest reliable TELS.

# Chapter 5

# Non-linear Random Vibrations analysis

As shown in the previous chapters, the IRFs and then the FRFs completely define a linearized system for a fixed threshold at a given time; the TELM so far also provides the tail probability for given threshold and time. The two sets of IRFs and FRFs may be implemented into a deeper random vibration analysis in order to evaluate other stochastic quantities of interest.

The *failure problem* can be considered the main interest in engineering, it simply consists in the analysis of the system's behavior to make sure that it will be able to carry out its purpose under exercise actions. In the particular case of civil and earthquake engineering, the events of failure can be separated in two broad categories. The *fatigue failure* occurs due to an accumulation of damage in time; the *first-passage failure* is related to the first up-corssing of a critical value of a specific response, such as displacements, strains or forces.

The purpose of this chapter is to introduce some methods due to es-

timate the likelihood of failure of a mechanical system (or its reciprocal likelihood of survival) under the effect of random dynamic excitations. In the common practice of civil engineering the event of failure of a structure usually belongs to the fisrt-passage class, the limit state can be the occurrence of large stresses or displacements but also brittle fracture, buckling or instability.

A stochastic analysis of failure requires study of the extreme values of the response process. Two kinds of extreme problems can be defined, the *local* extreme and the *global* one . In the first case there will be analyzed the response's behavior in a neighbourhood of a fixed time $t$ so that this case assumes an *instantaneous* meaning; it will be also used the term *peak* to refer to the local extrema of a process. The global case considers the extreme values distribution over a longer time window such as $T_1 \leq t \leq T_2$ and it will be used the term *extreme distribution* to refer to this more general case.

The occurrence and the likelihood of a first-passage global extrema is of course related to the statistics of the local peaks, this chapter shows the application with TELM of three entity of interest related to both local and global extrema, in particular, there will be analyzed the *Peak Probability Distribution*, the *Up-Crossing Rates* and the *First Passage Probability* or the corresponding *First Passage Time*.

The dynamics of the system are involved only marginally because, as shown previously, the system is completely defined by the set of IRFs and FRFs and, furthermore, the presented procedures are generically applicable to any kind of dynamic system because they only concern about the FRFs.

It is important to emphasize that the Gaussian characterization of the excitation leads to many semplifications. In fact, the non-linear system has been replaced by a set of linear systems and it is well known that the response of a linear system subjected to a stationary, Gaussian process, is Gaussian itself. Thus, each one of the linearized system, singularly, has a response that can be characterized by a standard-normal CDF, its mean and its variance, and the same happens for other derived problems such as the local peaks, the up-crossing rate and the first passage probability.

Once the TELS is defined, it is not necessary that the excitation used to get it in the TELM, must be the same used into the random vibration analysis. Usually, the TELM uses an unfiltered white-noise excitation and it has already been shown how the TELS is independent on the white-noise scale.

The excitation that will be used in the random vibration analysis can be as general as possible and its only requirement is that the excitation must be given in the form defined in chapter 2 and since now it will be called *design excitation.*

The described procedures are accomplished using a MatLab package developed on purpose.

## 5.1 Response probability distribution at a given time

The dynamic response of the system is defined as $\hat{X}(t_i, \mathbf{u})$ for a given time $t_i$; fixed a threshold $x$, let $E_{res}$ denote the event that the response at $t_i$ is bigger than the threshold. As shown previously, the vector $\mathbf{u}$ completely

defines the input stochastic excitation. The probability distribution of the response at the given time $t_i$ can be defined in terms of CDF as:

$$\Pr\left[E_{res}\right] = \Pr\left[x \leq \hat{X}\left(t_i, \mathbf{u}\right)\right] \tag{5.1}$$

.

As long as the system is non-linear, it is impossible to guess the shape or the mathematical expression of the 5.1; however, the system has been linearized and it is possible to replace the $\hat{X}\left(t_i, \mathbf{u}\right)$ response of the non-linear system with the response $X\left(t_i, \mathbf{u}\right)$ of the linearized one because the first-order tail probability is exactly the same. Thus, the first-order response probability approximation will be Gaussian:

$$\Pr\left[E\right] \approx \Pr\left[x \leq X\left(t_i, \mathbf{u}\right)\right] = \Phi\left[-\beta\left(x, t_i\right)\right] \tag{5.2}$$

where $\Phi\left[\cdot\right]$ is the standard normal CDF and $\beta\left(x, t_i\right)$ is the reliability index for a fixed threshold $x$ at the given time $t_i$.

Thus, the distribution of the response for a given time, in terms of CDF, can be defined as:

$$F_{X(t_i)}\left(x\right) \cong \Phi\left[\beta\left(x, t_i\right)\right] \tag{5.3}$$

and the corresponding PDF can be obtained by derivation:

$$f_{X(t_i)}\left(x\right) \cong \phi\left[\beta\left(x, t_i\right)\right] \frac{\partial \beta\left(x, t_i\right)}{\partial x} \tag{5.4}$$

where $\phi\left[\cdot\right]$ is the standard normal PDF.

Also, it has been shown in [18] and [28] that the first derivative of the $\beta$ is reciprocal to the norm of the response gradient:

$$\frac{\partial \beta\left(x, t_i\right)}{\partial x} = \frac{1}{\left\|\nabla_{\mathbf{u}} X\left(t_i, \mathbf{u}\right)\right\|} \tag{5.5}$$

and it is evaluated at the design point. However, if the design point is not available, the PDF can be also evaluated by numerical differentiation of the CDF.

However, this approach requires the knowledge of the design point excitation that, sometimes, is not available. In fact, the TELM provides the RSFs and FRFs of the linearized system evaluated thanks to a white-noise excitation and it has been shown in [28] how those functions can be employed even with noticeably different excitations, such as modulated white-noise, non-stationary excitation or, more in general, excitations that have a a different amplitude or shape of the power spectral density. For this reason, the knowledge of the design point excitation may not be available and a numerical approach is required. A first way to determine it is the time domain approach that will be presented in the following subsection but, in case of stationary excitations, a frequency domain approach can be more useful and it will be presented in section 5.2.1.

### 5.1.1 Time domain approach

The time-domain approach is able to determine by numerical evaluation the performance point of a system given time and treshold, through a numerical IRF, and the statistics of the train-pulse excitation, through the $\mathbf{s}$ vector and the probabilistic distribution of each time pulse, through the $\mathbf{u}$

vector. In the present work, the **s** vector can model filtered and unfiltered white noises and, more in general, nonstationary excitations, the **u** vector is usually made of standard normal variables.

As shown in section 5.1, the knowledge of the reliability coefficient $\beta$ is required in order to get the response distribution for a given time. The $\beta$ is, more in general, part of the solution of a reliability problem which gives back a performance point excitation $\mathbf{u}^*$ which is equivalent to its reliability coefficient $\beta$ and the gradient of the limit state surface $\alpha(x, t_n)$ at the performance point.

These values can be directly evaluated by the TELM but, in many cases, we need to evaluate them by a numerical way because the TELS is already known by its IRFs and the excitation is different by the one used to perform the TELM.

It has been already shown in chapter 4.2.1 that:

$$\sum_{j=1}^{n} h_{t_n,x}(t_n - t_j)\, s_i(t_j)\, \Delta t = a_i(t_n) \tag{5.6}$$

this relation has been used to determine the IRFs at given time and threshold and the $a_i(t_n)$ are related to the performance point of the FORM problem over the white-noise random variables. In the previous case, the performance point was known and the 5.6 was used in order to get the IRFs.

When TELS is already known, the same relation can be applied in order to get the $a_i(t_n)$ and its knowledge leads to the performance point and reliability coefficient. It is enough to determine the $s_i(t_j)$ of the design excitation and the 5.6 leads to the $a_i(t_n)$ for fixed time $t_n$ and threshold $x$.

Now, the design point of the design excitation will be:

$$\mathbf{u}^{*}\left(x,t_n\right)=\frac{x}{\left\|\mathbf{a}_x\left(t_n\right)\right\|}\frac{\mathbf{a}_x\left(t_n\right)^T}{\left\|\mathbf{a}_x\left(t_n\right)\right\|} \tag{5.7}$$

.

The reliability coefficient is:

$$\beta\left(x,t_n\right)=\alpha\left(x,t_n\right)\times\mathbf{u}^{*}\left(x,t_n\right) \tag{5.8}$$

where $\alpha\left(x,t_n\right)$ is the negative normalized gradient of the limit state surface at the design point:

$$\alpha\left(x,t_n\right)=-\frac{\nabla G_{\mathbf{u}^{*}}}{\left\|\nabla G_{\mathbf{u}^{*}}\right\|} \tag{5.9}$$

the limit state surface is:

$$G\left(x,t_n,\mathbf{u}\right)=x-X\left(t_n,\mathbf{u}\right) \tag{5.10}$$

now, the response is:

$$X\left(t_n,\mathbf{u}\right)=\mathbf{a}_x\left(t_n\right)\,\mathbf{u} \tag{5.11}$$

.

Collecting the 5.11, 5.8 and 5.9 we can determine the reliability coefficient:

$$\beta\left(x,t_n\right)=\frac{\mathbf{a}_x\left(t_n\right)}{\left\|\mathbf{a}_x\left(t_n\right)\right\|}\frac{x}{\left\|\mathbf{a}_x\left(t_n\right)\right\|}\frac{\mathbf{a}_x\left(t_n\right)^T}{\left\|\mathbf{a}_x\left(t_n\right)\right\|} \tag{5.12}$$

and finally:

$$\beta\left(x,t_n\right)=\frac{x}{\left\|\mathbf{a}_x\left(t_n\right)\right\|} \tag{5.13}$$

in case of double bounded threshold, beta has to be independent on the algebric sign of the threshold:

$$\beta\left(x,t_n\right)=\frac{|x|}{\|\mathbf{a}_x\left(t_n\right)\|}. \tag{5.14}$$

Now, we have all the elements to apply the procedure described in the section 5.1 in order to get the response distribution at a given time for both stationary and non-stationary excitations and responses. The time domain approach requires more computational resources than other methods that will be shown, but it has the great advantage that it is possible to apply it to any possible case, even if the system is not stable or if the stationarity is not archieved, or if the knowledge in time of the IRFs is only partial.

## 5.2 Stationary response statistic

An important class of stochastic process $X\left(t\right)$ is referred to the stationarity of the processes. In general, the probabilistic description of a generic process evolves in time, in some cases one or more characteristic of the process are constant in time and the process is defined as stationary. Depending on the invariant characteristic, it is possible to define many different kinds of stationarity.

The most strict type of stationarity is archieved if the complete probability structure is invariant of a shift in the parameter origin:

$$f_{X(t_1)\ldots X(t_n)}\left(x_1,t_1;\ldots;x_n,t_n\right)=$$

$$=f_{X(t_1+h)\ldots X(t_n+h)}\left(x_1,t_1+h;\ldots;x_n,t_n+h\right);\ \forall n,h \tag{5.15}$$

.

If only a subset of the probabilistic characterization is invariant in time, the stationarity can be defined in *weak sense*. Many different convenctions are available, Lutes and Sarkani [41] generalize the weak stationarity as:

- mean stationarity

$$\mu_X(t) = \mu_X \tag{5.16}$$

- autocorrelation stationarity

$$\phi_{XX}(t,s) = R_{XX}(t-s) \tag{5.17}$$

- autocovariance stationarity

$$K_{XX}(t,s) = \Gamma_{XX}(t-s) \tag{5.18}$$

With more than one stochastic process, it is also possible to introduce the concept of *joint stationarity* and the property refers to the joint probabilistic characterization. Given two processes $X(t)$ and $Y(t)$, they are jointly weakly stationary if each one is weakly stationary and:

- joint autocorrelation stationarity

$$\phi_{XY}(t,s) = R_{XY}(t-s) \tag{5.19}$$

- joint autocovariance stationarity

$$K_{XY}(t,s) = \Gamma_{XY}(t-s) \tag{5.20}$$

The strict or weak stationarity is an important stochastic property in practical applications. The simple archievement of the 5.17 or 5.18 leads to easier calculations because the autocorrelation, or autocovariance, can be treated as univariate functions and this property simplifies the integral evaluations in time. Also, in order to define the power spectral density as in chapter 2.2, the stationarity is a fundamental requirement[1] and it leads to the applications of the procedures presented in sections 5.2.1, 5.2.2 and 7.2.2.

### 5.2.1 Stationary response probability distribution at a given time; frequency domain approach

It is useful to notice that each one of the FRFs corresponds to a different linear system. Because the input excitation is Gaussian, the response of each one of the linearized systems will be Gaussian as well. Furthermore, if the excitation is stationary, the response of each one of the linearized systems will be stationary as well. Thus, the numerical evaluation of the response probability is possible recalling that, given the power spectral density of the excitation $\Phi_{FF}(\omega)$ the corresponding PDF of the response will be:

$$\Phi_{XX}(\omega) = \Phi_{FF}(\omega) |H_{x,t}(\omega)|^2 \tag{5.21}$$

[1] It is also possible to define models of frequency domain analysis for non-stationary excitations and response by the *instantaneous PSD*, the *physical spectrum*, the *evolutionary PSD* [43, 38] or parametric PSD [54]. However, it will be shown that excitation has to be stationary in order to provide the invariance in time of the linearized system once that stationarity is archieved, thus, only the stationary PSD will be used in this work.

where $H_{x,t}(\omega)$ is the FRF for a fixed threshold $x$ at a given time [2] $t$. The cumulative probability of the response is defined as:

$$F(x) = \Pr[x \leq X(t) | 0 \leq t \leq T] \tag{5.22}$$

and recalling that the response is also gaussian for fixed $x$ and $t$, we obtain:

$$F(x) = \Xi(x)\,\sigma_{X(t)} \tag{5.23}$$

where $\Xi[\cdot]$ indicates the standard normal CDF and $\sigma_{X(t)}$ is the standard deviation of the response at time $t$. This latter one can be easily evaluated by the PSD:

$$\sigma_{X(t)} = 2\int_0^\infty \Phi_{XX}(\omega)\,d\omega = 2\int_0^\infty \Phi_{FF}(\omega)\,|H_{x,t}(\omega)|^2\,d\omega \tag{5.24}$$

and finally:

$$F(x,t) = \Xi(x)\,2\int_0^\infty \Phi_{XX}(\omega)\,d\omega = 2\int_0^\infty \Phi_{FF}(\omega)\,|H_{x,t}(\omega)|^2\,d\omega \tag{5.25}$$

.

Recall that the integral in the 5.25 is in effect a summation because the FRFs are available only in the form of a set of points in the frequency domain. For this reason is absolutely required for the FRFs to be consistent with the original model, *i.e.* they must cover a large enough frequency domain and the Fourier transform from the IRFs must be accurate. For

[2] In case of stationary response, the FRFs does not depend on time as long as the stationarity is archieved but, in the more general case of non-stationary response, it is necessary to consider different IRFs and FRFs as long as the response statistics evolves in time. In order to give a more general meaning to the procedure, the dependance on $t$ will be shown.

this purpose it is necessary that the IRFs are defined in a large enough time window so that it will be noticeable the decay to zero in order to avoid big approximations into the Fourier integral by cutting a non neglectible tail.

### 5.2.2 Mean up-crossing rate

An important measure of the process' stochastic is the so-called *mean up-crossing rate*[3] which already presuppose a global meaning of the process, because its value changes in time, but it is also still has a local interpretation, because it defines the crossing rate with instantaneuos meaning. Its main purpose is to lead from the local analysis to a more general global one, *i.e.* the first passage problem.

Let $\nu_X(x^+, t)$ be the expected rate of occurrence of the up-crossing event: $X(t) = x \cap \dot{X}(t) > 0$, and let $\nu_X(x^-, t)$ be the expected rate of occurrence of the down-crossing event $X(t) = x \cap \dot{X}(t) < 0$[4] of the same level $X = x$, as shown in figure 5.1; the expected number of up-crossing during an interval will be the integral of $\nu_X(x^+, t)$ over the integral itself, so the mean rate can be defined as a limit value over a small enough interval as follows:

$$\nu_X(x^+, t) = \lim_{\Delta t \to 0} \frac{\Pr\left[X(\tau) = x \cap \dot{X}(\tau) > 0 | t \leq \tau \leq t + \Delta t\right]}{\Delta t} \tag{5.26}$$

.

The theoretical value of the fraction's numerator that appears in the 5.26 can be developed from the joint PDF of the response and its first derivative.

[3] Or *mean down-crossing rate*

[4] Note that this down-crossing definition is intended with respect the $+x$ level, as shown in the figure. In other cases, when there is a symmetric bound, it will be considered the down-crossing of the $-x$ level

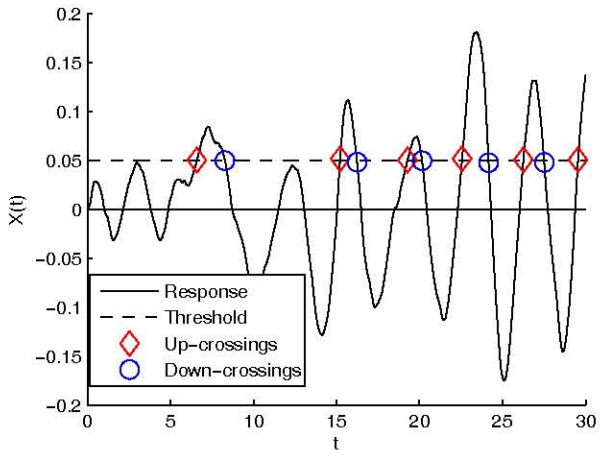


Figure 5.1: Crossings of the level $X(t) = x$.

The event of up-crossing can be defined as $UC(t, \Delta t) = X(\tau) = x \cap \dot{X}(\tau) > 0, t \leq \tau \leq t + \Delta t$ and its probability of occurrence will be:

$$\Pr[UC(t, \Delta t)] = \int_0^{\infty} \int_{x - v\Delta t}^{x} f_{X(t),\dot{X}(t)}(w, v)\, dw\, dv \tag{5.27}$$

taking the limit for $\Delta t \to 0$, the mean up-crossing rate is:

$$\nu_X(x^+, t) = \int_0^{\infty} v\, f_{X(t),\dot{X}(t)}(u, v)\, dv \tag{5.28}$$

.

This formulation is not rigorous: the JPDF is unbounded with respect $\dot{X}(t)$ that can assume arbitrarily large values, but, in this case, the integration interval $[x - v\Delta t, x]$ should be conveniently chosen and it is possible to prove that the limiting process is legitimate despite this drawback. However, in common practice, approximate formulation of the up-crossing rate

are used because it is difficult to deal directly with the JPDF of the response and its derivative.

In case of stationary-Gaussian processes, it is possible to express the mean crossing rates as functions of the standard deviations of the response and first-derivative processes:

$$\nu_X\left(x^+,t\right)=\frac{1}{2\pi}\frac{\sigma_{\dot{X}(t)}}{\sigma_{X(t)}}\exp\left[-\frac{1}{2}\left(\frac{x}{\sigma_{X(t)}}\right)^2\right] \tag{5.29}$$

known as Rice's formulation (1943) [41]; it may be applied to any type of excitation as long as it's stationary and Gaussian. Because the analysis usually involves the employment of the power spectral density of the response process, it is useful to rewrite the 5.29 using the spectral moments instead of the standard deviations because the response variance $\sigma_{X(t)}$ corresponds to the zero-order spectral moment $\lambda_0$ and the first-derivative variance $\sigma_{\dot{X}(t)}$ corresponds to the second-order one $\lambda_2$.

As long as the power spectral density of the response is known, the spectral moments are defined as:

$$\lambda_m=\int_0^\infty \omega^m G_{XX}\left(\omega\right)\,d\omega \tag{5.30}$$

where $G_{XX}\left(\omega\right)$ is the single-side PDF, defined as:

$$G_{XX}\left(\omega\right)=2\Phi_{XX}\left(\omega\right)\qquad \omega\geq 0 \tag{5.31}$$

and it is easily evaluable by the 5.21. The 5.29 becomes:

$$\nu_X\left(x^+,t\right)=\frac{1}{2\pi}\sqrt{\frac{\lambda_2}{\lambda_0}}\exp\left[-\frac{1}{2}\frac{x^2}{\lambda_0}\right] \tag{5.32}$$

.

However, the Rice's formulation presents a tricky drawback. The 5.32 descends by a limiting process and does not consider the global behavior of the response process, *i.e.* it does not consider if the response at a certain time $t$ is already over the considered threshold $x$. In case of white-noise or broad-band processes the very irregular behavior of the response does not provoke big errors, the 5.32 works well and it can be applied without any care.

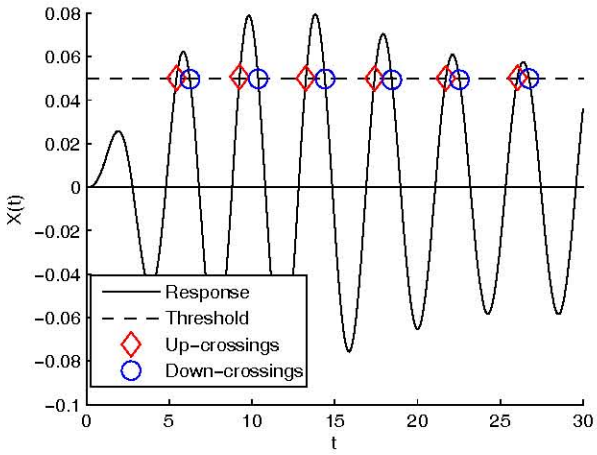


Figure 5.2: Crossings of the level $X(t) = x$ for a Narrow-Band excitation.

In case of narrow band processes the approximations becomes not neglegible any more, let's for example consider the narrow-band realization in figure 5.2. The most regular behavior of the response process implies that, if the response $X(t)$ is already over the threshold $x$, it is impossible to have another up-crossing if the response do not goes back under the threshold

again, thus, in the up-crossing formulation must be considered the likelihood that $X(t) > x$ already and then the likelihood that a down-crossing occurs before the next up-crossing.

### 5.2.3 First passage probability

The extreme value analysis shown in sections 5.1 and 5.2.2 lead to the main first-passage failure problem. As shown in the introduction of this chapter, the failure problems in civil engineering can be differentiated in two categories: the *fatigue* and the *first-passage* failure. Usually this latter one occurs when one particular entity such as a displacement or a force in the model crosses for the first time a critical value that will be considered as a threshold. The purpose of this section is to evaluate the probability that, during a particular interval of time $[T_1, T_2]$ the response overcrosses the critical value.

Let us set a safety threshold $x$, and a stochastic process with one realization shown in figure 5.3. The upcrossing probability of a stochastic process, given the threshold $x$ in the interval $[t_i, t_i + \delta t]$, is defined as:

$$\Pr[\text{upcr.}] = \Pr\left[X(t) < x \cap X(t + \delta t) > x \cap \dot{X}(t) > 0\right] \tag{5.33}$$

with $t \in [t_i, t_i + \delta t]$. Substituting $X(t + \delta t) = X(t) + \dot{X}(t)\,\delta t$ we obtain:

$$\Pr[\text{upcr.}] = \Pr\left[x - \dot{X}(t) < X(t) < x \cap 0 < \dot{X}(t)\right] \tag{5.34}$$

so, if the joint PDF of $X$ and $\dot{X}$ is known, it is possible to evaluate the istantaneous upcrossing probability. However, this probability distribution is related to a specific istant in time, the first excursion is more general.

Selected $x$ and $\tau$, the *First Passage Probability* is defined as the probability that the first excursion of $X(t)$ above $x$ occurs for $t \leq \tau$. Defined the peak process $X_\tau = \max_{0 \leq t \leq \tau} X(t)$ the FPP is defined as:

$$FPP(x, \tau) = \Pr[X_\tau > x]. \tag{5.35}$$

However, the exact value of the first-passage probability is hard to obtain due to evaluate the process $X_\tau$ but some approximate solutions are available. An upper bound developed by Bolotin for stationary broad-band excitations and high threshold is the following:

$$\Pr[X_\tau > x] \leq 1 - F_{X(t)}(x, 0) + \int_0^\tau \nu(x^+, t)\, dt \tag{5.36}$$

where $F_{X(t)}(x, 0)$ is the probability that the process is already above level $x$ at time zero, and $\nu(x^+, t)$ is the mean up-crossing rate of level $x$. The two-sides[5] analogous equation is:

$$\Pr[X_\tau > x] \leq 1 - F_{X(t)}(x, 0) + \int_0^\tau \nu(x^+, t)\, dt + \int_0^\tau \nu(-x^-, t)\, dt. \tag{5.37}$$

A further solution available is based on the assumption that the crossing of the specified threshold is a Poisson's process:

$$\Pr[X_\tau > x] = 1 - F_{X(t)}(x, 0) \exp[-\nu_X(x^+)\tau] \tag{5.38}$$

for one side and stationary response, and:

$$\Pr[X_\tau > x] = 1 - F_{X(t)}(x, 0) \exp\left[-\int_0^\tau \nu_X(x^+, t)\, dt - -\int_0^\tau \nu_X(-x^-, t)\, dt\right] \tag{5.39}$$

[5] Useful if the threshold $-x$ is a limit state as well as $+x$.

for two-sides and non-stationary processes.

This approximation assumes a simplified form for Gaussian process and it can be shown that it becomes close to the Gumbel distribution, however, because the purpose of TELM is to get the distribution of non-Gaussian response, it is not useful and it will not be presented.

The Poisson's approximation is able to catch the distribution of a broad-band excitation at high thresholds because each crossing becomes a point of a Poisson's process and its statistics do not consider the correlation that each crossing can have with respect other crossings. Physically, given a time instant $t_i$, the probability of an up-crossing depends on the state of the process itself: if the response is already above the threshold level, obviously it has to came down under it before we can have another up-crossing; thus, the up-crossing probability of the process above the threshold $x$ is minor than its probability when it is under $x$. In case of high thresholds and broad-band processes, the crossings are weakly correlated[6] and the error of the Poisson's process is negligible; for narrow-band processes or low thresholds, the peaks of the process are strongly correlated[7] and the Poisson's approximation does not work.

In order to avoid this drawback, a better approximation has been developed by Vanmarcke (1975) [51] which defines an envelope process of the response and defines the statistics of its crossings. A realization of the envelope process is shown in figure 5.4.

[6] In the extreme case of white-noise, each point of the process is completely uncorrelated from the others.

[7] In the extreme case of a single periodic component, each point of the process is completely correlated with all the others.

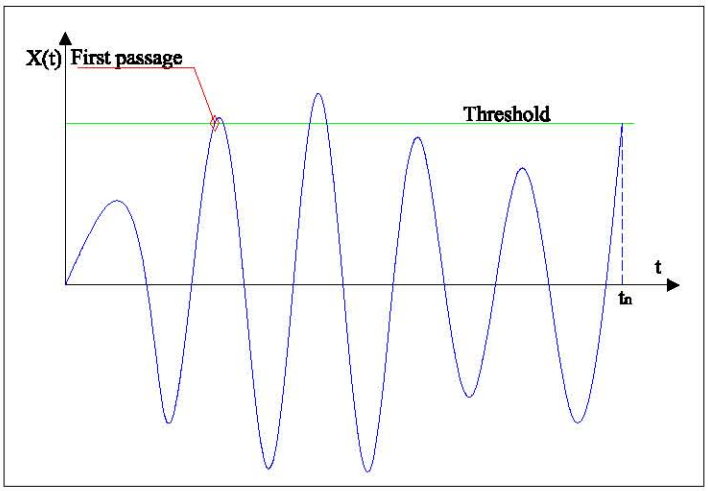


Figure 5.3: First passage of a stochastic process

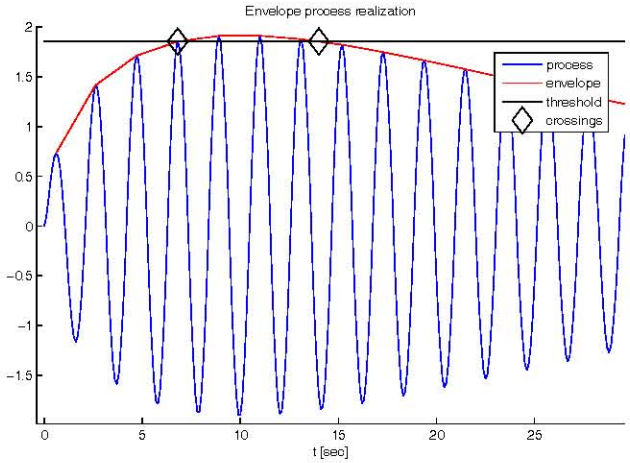


Figure 5.4: Realization of the envelope process $A(t) = x$.

The envelope process has been introduced first by Rice (1944) but it has many definitions, one of the most applied formulations has been developed by Stratanovic (1963-67) and it is:

$$A^2(t) = X^2(t) + \hat{X}^2(t) \tag{5.40}$$

where $A(t)$ is the envelope process, $X(t)$ is the narrow-band process and $\hat{X}(t)$ is a conjugate of $X$ obtained by a linear transformation:

$$\hat{X}(t) = I_c(t)\sin(\omega_m t) + I_s(t)\cos(\omega_m t) \tag{5.41}$$

where $\omega_m$ is the midpoint frequency of the narrow-band process and $I_c$ and $I_s$ are coefficients obtained by an Hilbert transform.

The number of crossings of the narrow-band process is usually higher than the envelope's one, because the narrow-band crossings are usually grouped in clusters or clumps like shown in figure 5.5. It can happen for extremely high thresholds that the envelope process has unqualified crossings (Figure 5.6) because there are no crossings of the narrow-band process. Vanmarcke's formulation of the first passage probability accounts for the envelope statistics, for the clusters' size and for possible unqualified crossings.

The final form of the Vanmarcke's distribution of extreme peaks is:

$$F_{X(\tau)}(x) = \left[1 - \exp\left(-\frac{x^2}{2}\right)\right] \exp\left[-\nu_X(0^+)\,\tau \frac{1 - \exp\left(-\sqrt{2\pi}\delta^{1.2}x\right)}{\exp\left(\frac{x^2}{2}\right) - 1}\right] \tag{5.42}$$

where the exponent 1.2 is an experimental correction factor, $x$ is the threshold and $\delta$ is a *regularity factor* that characterizes the $X(t)$ process:

$$\delta = \sqrt{1 - \frac{\lambda_1^2}{\lambda_0 \lambda_2}} \tag{5.43}$$

and it involves up to the second spectral moment. Furthermore, it must be $0 \leq \delta \leq 1$ and if $\delta$ is close to 1, then the process is broad-band, on the other way, when it is closer to 0, the process is narrow-band.

The Vanmarcke's formulation is very useful for stationary processes because, even if the design excitation is broad-band or even white noise, it is filtered by the model and its response usually shows a narrow-band behavior, thus, the Poisson's approximation can result inaccurate.

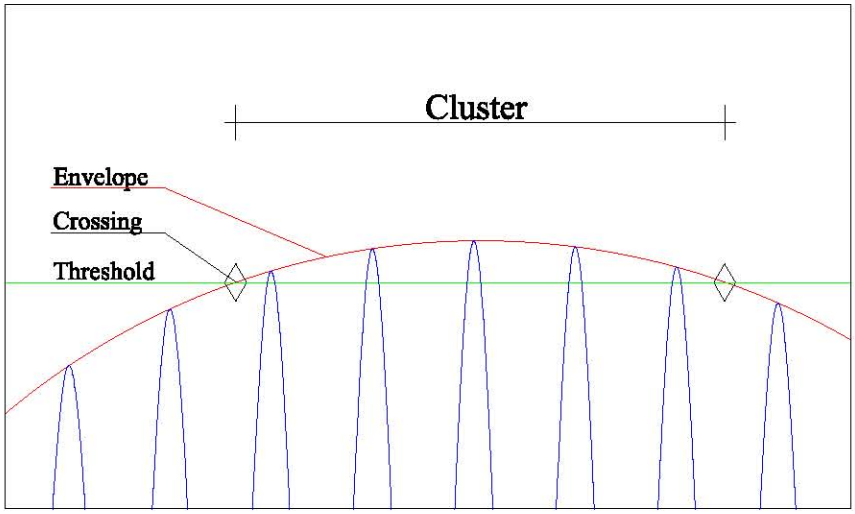


Figure 5.5: Cluster of an envelope process

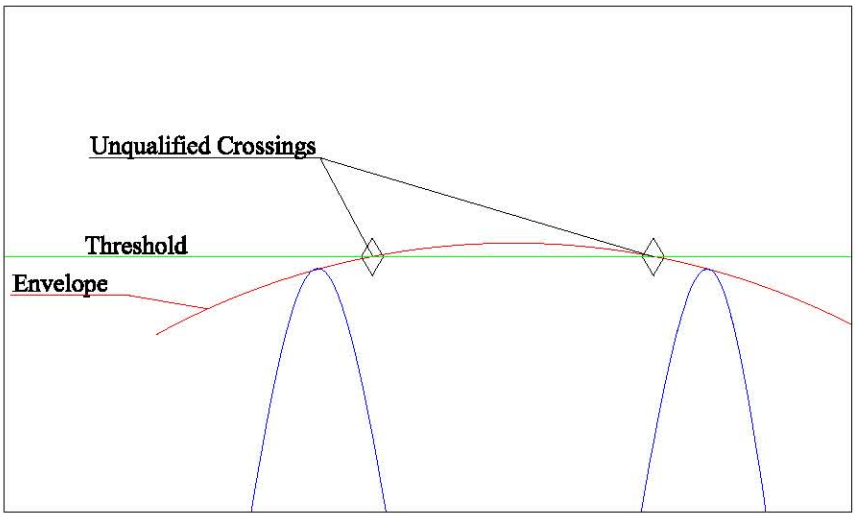


Figure 5.6: Unqualified crossing of an envelope process

## 5.3 Non-stationary response statistic

The response statistics of a non-stationary process is more difficult to obtain because it is not possible to apply the first passage probability formulations shown in section 7.2.2. Note that, in this section, the non-stationarity refers only to the response process and not necessairly to the design excitation. A non-stationary design excitation usually leads to a non-stationary response, it can happen that, for specific constitutive models, also a stationary excitation has a non-stationary response.

The first passage probability of a non-stationary process is usually evaluated by discretizing the time interval $[0, t_n]$ into a sequence of time steps $t_i$ and considering the response at discrete times only. Of course, because the excitation has already been discretized and the IRFs of the TELS are avail-

able only in discrete time points, the same discretization will be considered. The first passage probability, in this case, is the union of the probabilities that, at each time step, the response exceedes the threshold:

$$\Pr\left[x \leq \max_{0\leq t\leq t_n} X\left(t,\mathbf{u}\right)\right] = \Pr\left[\bigcup_{i=0}^{n} x \leq X\left(t_i,\mathbf{u}\right)\right] \tag{5.44}$$

this formulation is properly a lower-bound of the first passage probability, because the maximum can occur somewhere in between two consecutive time steps, of course, the smaller the time step, the closer lower bound is to the exact solution.

The left side of the 5.44 is a series-system reliability problem. It is possible to solve the problem using a FORM metod; the solution is given by the complement of the $n+1$-dimensional multinormal probability:

$$1 - \Phi_{n+1}\left(\mathbf{B},\mathbf{R}\right) \tag{5.45}$$

where $\mathbf{B} = \left[\beta\left(x,t_0\right)\ \beta\left(x,t_1\right)\ \ldots\ \beta\left(x,t_n\right)\right]$ is the set of the reliability indexes for each time step, and $\mathbf{R}$ is the correlation matrix having elements $\rho_{ij} = \alpha\left(x,t_i\right)\alpha\left(x,t_j\right)^T$, with $\alpha\left(x,t_i\right)$ defined earlier.

The multi-normal probability is easily computed by an algorithm developed by Au and Beck [3], furthermore, all the series-system problem can be solved by an algorithm implemented in FERUM by Song that also requires the definition of the limit state function for each time step.

Because the IRFs are known, the best way to do it is to compute a Duhamel convolution integral in discrete form:

$$x\left(t_n,\mathbf{u}\right) = \sum_{i=1}^{n} f\left(t_i,\mathbf{u}\right) h\left(t_n - t_i\right) \Delta t. \tag{5.46}$$

The implemented FERUM object will be used in this work for the applications that requires a non-stationary evaluation of the first passage probability.

## 5.4 Linear response analysis

In order to verify the results of the non-linear analysis, a linear random vibration analysis will be performed. The $\alpha$ parameter of the restoring force will be set equal to one so that only the linear part of the response will be considered. It is important to consider the limit case of linear behavior because it has an already known and analytical solution.

For each model, a frequency domain analysis will be performed and the case of multi degrees of freedom will be shown is this section. It can be easily extended to the case of single degree of freedom simply considering scalars instead of matrixes, furthermore, the analysis will be performed using a Matlab code due to take advantage of its matrix calculus features.

Each model is defined in terms of a well-known differential equation of motion:

$$\mathbf{M}\ddot{\mathbf{y}} + \mathbf{C}\dot{\mathbf{y}} + \mathbf{R}\left(\mathbf{y}, \dot{\mathbf{y}}, z\right) = -\mathbf{L}f\left(t\right) \tag{5.47}$$

in each one of the implemented material, the restoring force, in case of $\alpha = 1$, it becomes:

$$\mathbf{M}\ddot{\mathbf{y}} + \mathbf{C}\dot{\mathbf{y}} + \mathbf{K}\mathbf{y} = -\mathbf{L}f\left(t\right). \tag{5.48}$$

The frequency response function of a linear, multi degrees of freedom

system is:

$$\mathbf{H}(\omega) = \left[\mathbf{K} - \omega^2\mathbf{M} + i\omega\mathbf{C}\right]^{-1}. \tag{5.49}$$

Given the power spectral density function of a stationary excitation $\Phi_{FF}(\omega)$, the response will be stationary itself and its power spectral density will be:

$$\Phi_{XX}(\omega) = \mathbf{H}(\omega)\,\mathbf{MR}\Phi_{FF}(\omega)\,\mathbf{R}^T\mathbf{M}^T\mathbf{H}(\omega)^T \tag{5.50}$$

and it leads to the covariance matrix of the response which is:

$$\Sigma = \int_{-\infty}^{\infty} \Phi_{XX}(\omega)\, d\omega \tag{5.51}$$

in the particular case of two degrees of freedom it is:

$$\Sigma = \begin{bmatrix} \sigma_{11}^2 & \sigma_{12} \\ \sigma 21 & \sigma_{22}^2 \end{bmatrix}. \tag{5.52}$$

Let us consider a sample 2-DOF model, shown in figure 5.7, with mass, damping and stiffness as:

$$\mathbf{M} = \begin{bmatrix} 553.9 & 0 \\ 0 & 276.9 \end{bmatrix} Kg \tag{5.53}$$

$$\mathbf{C} = \begin{bmatrix} 696 & 0 \\ 0 & 1740 \end{bmatrix} \frac{Kg}{s} \tag{5.54}$$

$$\mathbf{K} = \begin{bmatrix} -125.73 & 147.6 \\ -147.6 & 420.93 \end{bmatrix} \frac{kN}{m}. \tag{5.55}$$

The Frequency Response Function is shown in figures 5.8 and 5.9, the real part results symmetric and the imaginary part results antisymmetric.

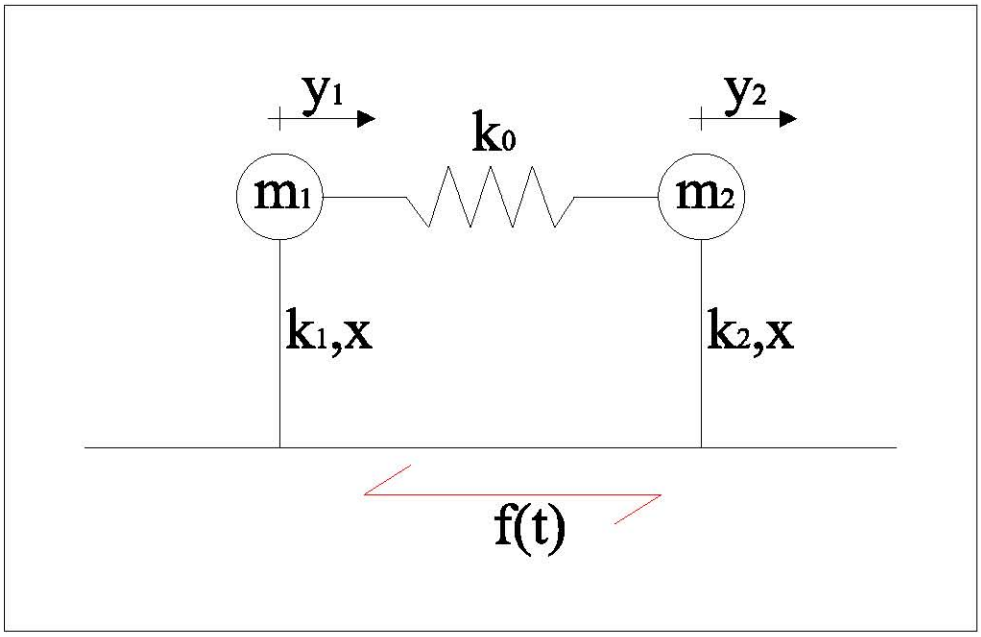


Figure 5.7: Two degrees of freedom linear oscillator

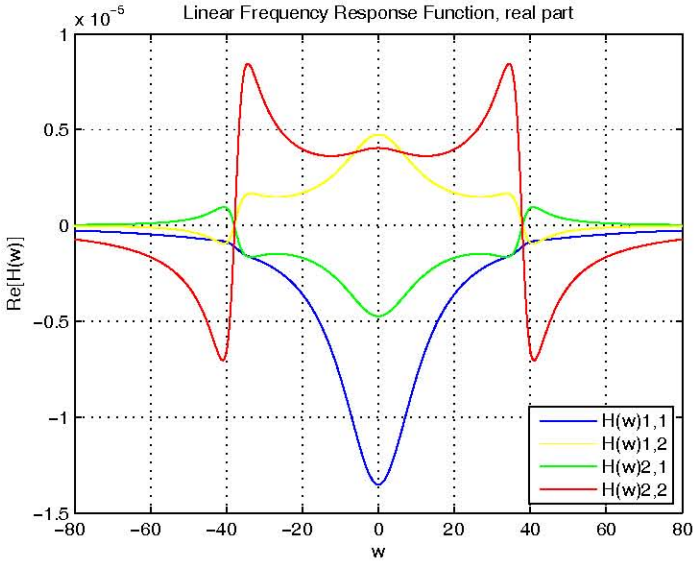


Figure 5.8: Frequency Response Function, real part

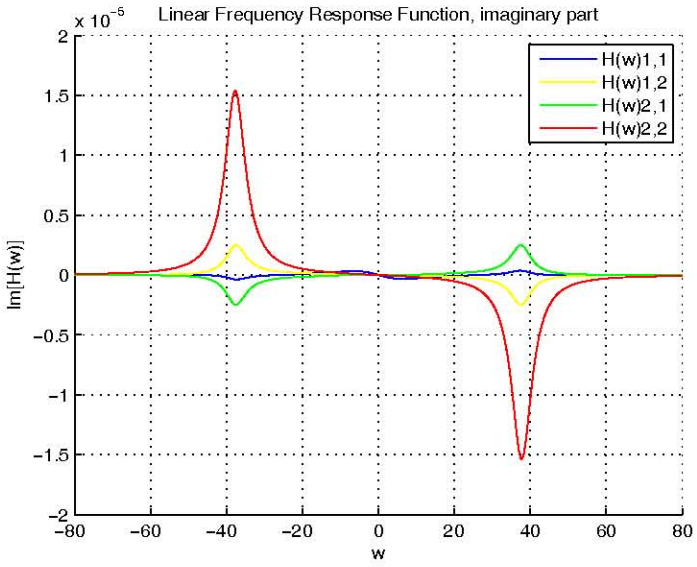


Figure 5.9: Frequency Response Function, imaginary part

The generic $i, j$ component of the FRF is defined as the steady-state response of the degree of freedom $i$ with excitation applied to the degree of freedom $j$.

Fixed a Gaussian white-noise excitation with $\sigma_{WN} = 2g$, the power spectral density of the response is shown in figures 5.10 and 5.11; and the

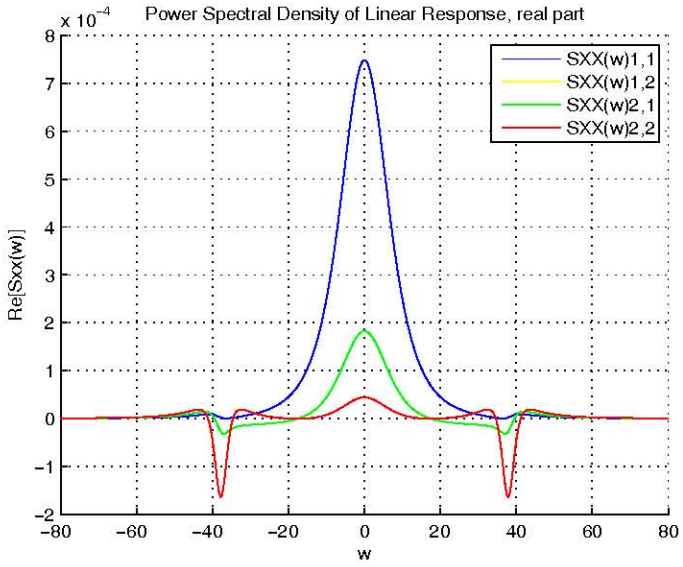


Figure 5.10: Response Power Spectral Density, real part

covariance matrix is:

$$\Sigma = \begin{bmatrix} 0.0136 & 0.0024 \\ 0.0024 & 0.0002 \end{bmatrix}. \tag{5.56}$$

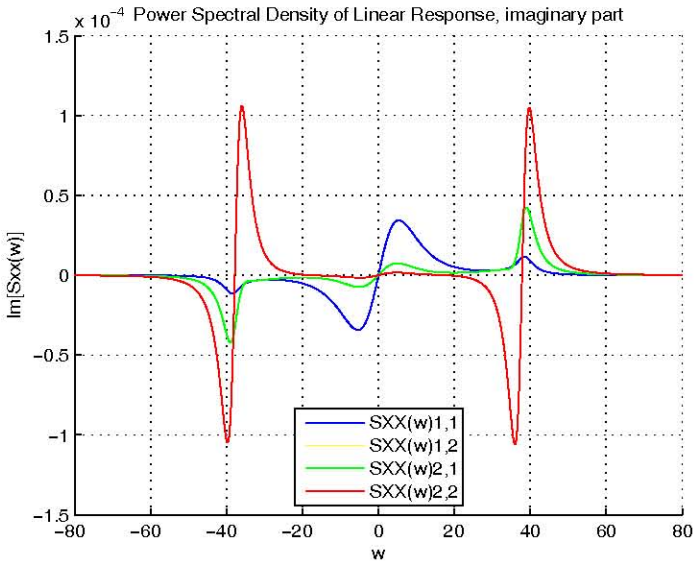


Figure 5.11: Response Power Spectral Density, imaginary part

# Chapter 6

# Uniaxial Smoothed-Generalized Bouc-Wen material

According to the model of oscillator proposed in chapter 4, it is necessary to define a costitutive model for the non-linear restoring force and its sensitivity response. Obviously, the choosen model must satisfy all the TELM requirements in terms of consistency, regularity and differentiability.

The Bouc-Wen model is a well-known smooth hysteretic material developed by Bouc (1971) and Wen (1976); it has been extended in many directions in order to introduce degrading behaviour, pinching and asymmetric hysteresis. In any case, the common feature is that it has a continue first derivative that avoids gradient discontinuities that could compromize the convergence of the FORM methods.

In order to consider a non symmetric behavior of the hysteretic model, a generalized material has been defined and calibrated by Song and Der Kiureghian (2006) on the base of the underlying phylosophy of the Bouc-Wen

material. The generalized Bouc-Wen model presents a sufficient flexibility in shape control to describe highly asymmetric hysteresis loops.

The main purpose of the new model is to describe the behavior of flexible strap connectors (FSCs) which are inserted for thermal expansion between electrical substation equipment items connected by a rigid bus (RB). The model has been calibrated on experimental data provided by the Pacific Gas & Electric Company (PG&E). A rigid bus typically consists of an aluminium pipe connected between two electrical equipment items for conductions. The FSCs are U-shaped spring elements made of three straps, each one consisting of two copper bars, inserted at one or both ends of the rigid bus. In case of severe earthquake excitations, the relative displacement demand betqeen the two interconnected equipments in general causes huge inelastic deformations of the spring elements, whose behavior presents large and non symmetric hysteresis loops.

The specific shape of the straps governs the shape and the extension of the hysteretical loops; in the common practice, PG&E employes three specific classes of connectors whose shapes are shown in figures 6.2, 6.4 and 6.6. Further details about connectors' dimensions and features can also be found in [15, 17].

In order to employ the generalized Bouc-Wen model in the TELM analysis, a further step is required. In fact, the original model does not satisfy all the requirements of the FORM analysis already summarized in section 2.5, in particular, the hysteresis loop is affected by discontinuities of its first derivatives at $z = 0$ and $u = 0$, *i.e.* at the zero-crossings of the restoring

force[1] and/or the displacement[2]. Thus, the definition of the constitutive model requires the implementation of a smoothing therm that provides the continuity of the hysteresis' first derivative.

In this chapter, the theoretic definition and the incremental formulation of the *Smoothed-Generalized Bouc-Wen* material are provided. Furthermore, its implementation in TELM requires an iterative Newton's algorithm and a sensitivity analysis with respect the displacements, both topics are discussed in the following sections; also, the constitutive parameters for each connector class are summarized.

[1] Or of the axial stress in case of single fiber.
[2] Or of the axial strain in case of single fiber.

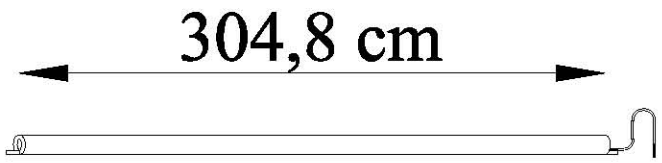


Figure 6.1: Rigid bus with asymmetric strap connector

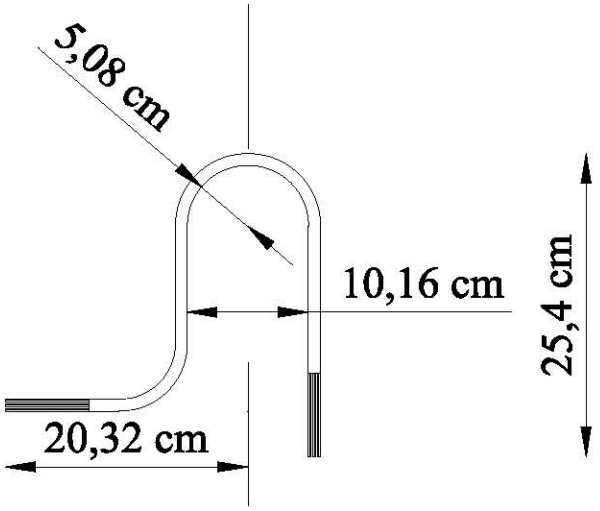


Figure 6.2: Dimensions of FSC No. 30-2021

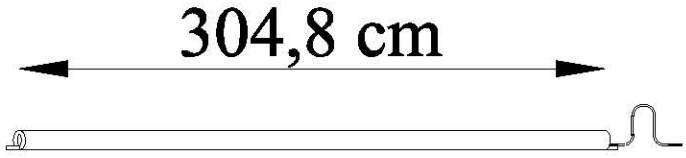


Figure 6.3: Rigid bus with asymmetric strap connector

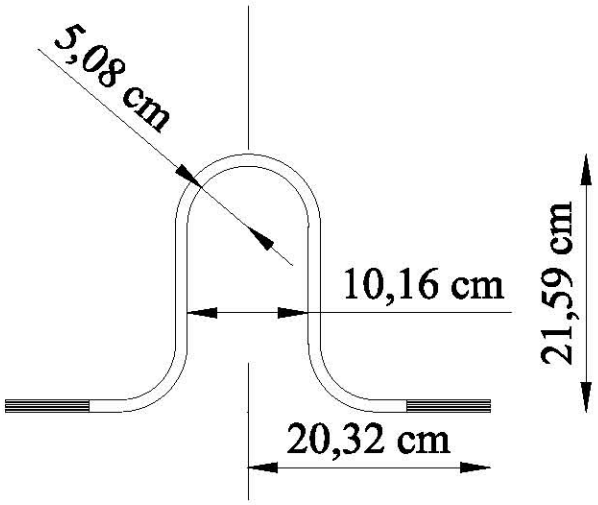


Figure 6.4: Dimensions of FSC No. 30-2022

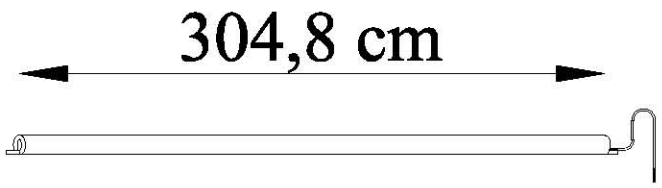


Figure 6.5: Rigid bus with asymmetric strap connector

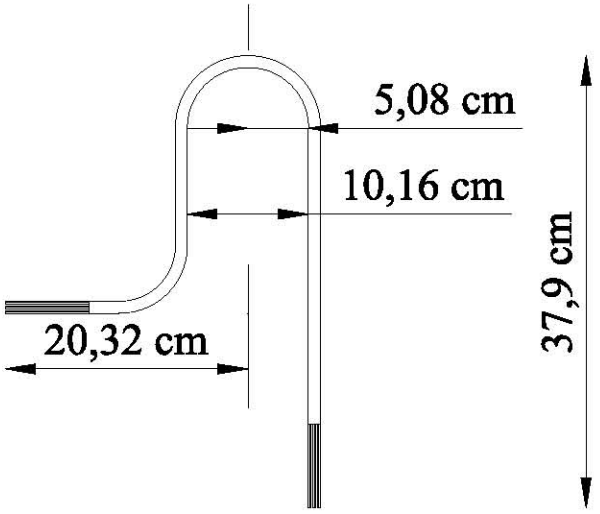


Figure 6.6: Dimensions of FSC No. 30-2023

## 6.1 Model definition

The generalized Bouc-Wen model can be implemented in order to define the restoring force of a non-linear oscillator or the stress of a uniaxial fiber. In the first case, the current displacement and the historical variables (such as displacements, velocity and dissipated energy) are known, the second case only differs from the first one because the strain is defined instead of the displacement and its first derivative with respect the time is defined instead of the velocity.

In fact, the restoring force of the oscillator can be considered like the strain of a unitary-area and unitary-length fiber so that the integrals of stress and strain (which give back respectively the total force and the displacement) are exactly the stress and the strain. To avoid confusion, the material will be defined in therms of force and displacement, respectively $R$ and $y\left(t\right)$.

The restoring force is defined as the sum of a linear and a hysteretic part:

$$R = \alpha k_0 y\left(t\right) + \left(1-\alpha\right) k_0 z \tag{6.1}$$

where $\alpha$ is the ratio of the post-yielding to the linear stiffness, $k_0$ is the initial linear stiffness and $z$ is the hysteretic displacement that is defined by the following differential equation:

$$\dot{z} = A\left(\epsilon\right) - \left|z\right|^n \psi\left(y, \dot{y}, z\right) \dot{y}. \tag{6.2}$$

The shape of the hysteretic loop is defined by $n$ and $\psi$. This last one has

been defined by Song [49] and it is capable of modelling highly asymmetric loops with constant parameters. The auxiliary equation is:

$$\begin{aligned}\psi(y,\dot{y},z) = \beta_0 + \beta_1 \mathrm{sgn}(\dot{y}z) + \beta_2 \mathrm{sgn}(y\dot{y}) + \beta_3 \mathrm{sgn}(yz) + \\ + \beta_4 \mathrm{sgn}(\dot{y}) + \beta_5 \mathrm{sgn}(z) + \beta_6 \mathrm{sgn}(y)\end{aligned} \quad . \tag{6.3}$$

However, this last formulation of $\psi$ is affected by an important drawback. As long as the *sign* operator appears in the expression, there will be discontinuities where its argument crosses the zero. In order to assure the convergence of the FORM algorithm, it is necessary that the costitutive law has continuous first derivative with respect the displacements $y$ in the load and unload phases. Thus, the 6.3 must be modified in order to avoid these discontinuities. It is possible to use another algebric function instead of the *sign* operator, in this case the function that appears to match best the original one, is the hyperbolic tangent, so, the following approximation can be defined:

$$\mathrm{sgn}(x) \approx \tanh(kx) \tag{6.4}$$

where $x$ is a generic argument and $k$ is a coefficient that governs the shape of the hyperbolic tangent and, particularly, its slope. In figure 6.7 several realizations of the 6.4 for different valuer of $k$ are shown.

because the first derivative's continuity is required only with respect to $y$, the smoothed sign operator will be used only for $\beta_1$, $\beta_2$, $\beta_3$ and $\beta_6$ and only for $y$ and $z$. Furthermore, because:

$$\mathrm{sgn}(ab) = \mathrm{sgn}(b)\,\mathrm{sgn}(b)\,, \tag{6.5}$$

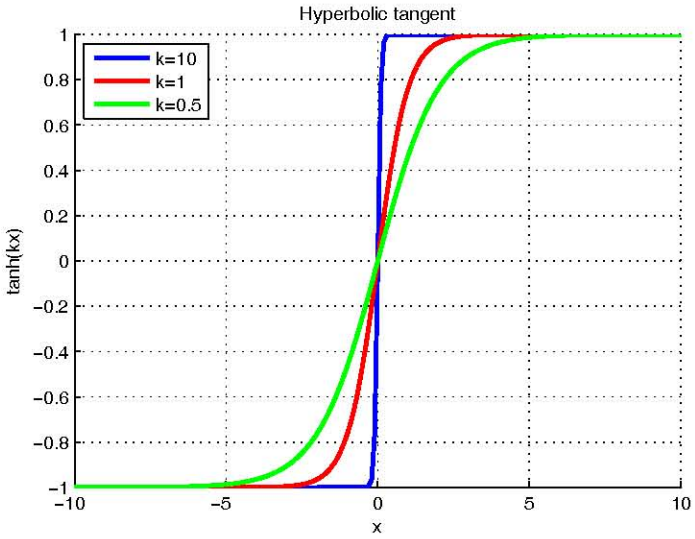


Figure 6.7: Hyperbolic tangent parametrized on $k$

the 6.3 becomes:

$$\begin{aligned}\psi\left(y,\dot{y},z\right) = \beta_0 + \beta_1 \mathrm{sgn}(\dot{y})\tanh(kz) + \beta_2 \tanh\left(ky\right)\mathrm{sgn}(\dot{y}) + \\ + \beta_3 \tanh\left(kyz\right) + \beta_4 \mathrm{sgn}(\dot{y}) + \beta_5 \tanh(z) + \beta_6 \tanh\left(ky\right)\end{aligned} \quad . \tag{6.6}$$

A realization of the hysteresis loop of the restoring force is shown in figure 6.8, note that, fixed the input excitation, three different loops have been plotted corresponding to different values of $k$. The parameters of the material can be found in table 6.1. Also, it is important to notice that the $k$ parameter has a big influence on the loops, expecially in the regions close to the origin; in fact, note that, for $k = 10$ the hysteresis loop remains almost coincident with the one of non-smoothed material. In this work, the parameter has been set $k = 0.5$ for two reasons: first, physically the transition between the positive and negative half does not

show any kink and the material gradually smooths; second, even if the first derivative is continuous, it is important that the FORM analysis can "feel" the continuity. In fact, for short time steps, the material can behave like if there is a kink in the origin even if the hyperbolic tangent has been used because the restoring force jumps the smoothing region. If this phenomenon happens, then some convergence problems could affect the FORM analysis.

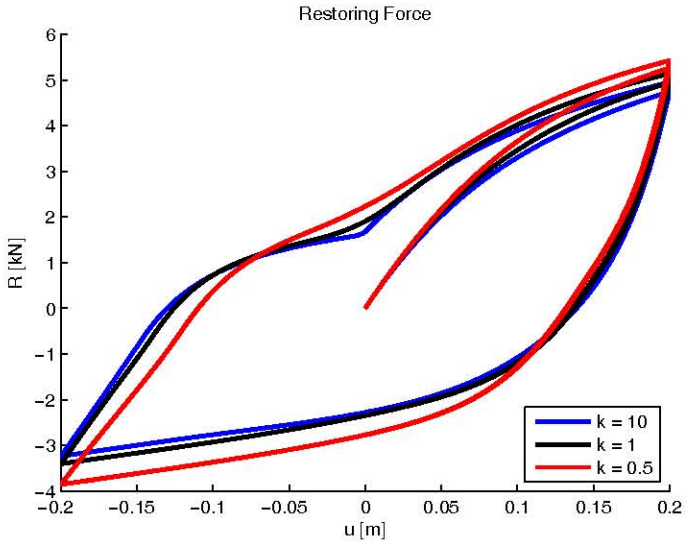


Figure 6.8: Smoothed-generalized Bouc-Wen restoring force

| | PG&E 30-2021 | PG&E 30-2022 | PG&E 30-2023 |
|---|---|---|---|
| $k_0$ (kN/m) | 147.60 | 106.80 | 33.30 |
| $\alpha$ | 0.10 | 0.10 | 0.10 |
| $A$ | 1.00 | 1.00 | 1.00 |
| $n$ | 1.00 | 1.00 | 1.00 |
| $\beta_1$ (1/m) | 18.50 | 16.50 | 11.22 |
| $\beta_2$ (1/m) | -4.65 | -7.60 | -3.61 |
| $\beta_3$ (1/m) | 1.16 | 6.85 | 1.48 |
| $\beta_4$ (1/m) | 4.53 | 3.55 | 4.17 |
| $\beta_5$ (1/m) | -4.76 | -6.14 | -2.29 |
| $\beta_6$ (1/m) | -4.41 | -2.22 | -2.19 |

Table 6.1: Parameters of the smoothed-generalized Bouc-Wen material.

## 6.2 Incremental formulation

As shown in the previous section, the solution for the Bouc-Wen restoring force given the displacement depends on an implicit first order differential equation in $z$. In order to get a robust solution, a Newton's iteration method is required.

Let us consider $j$ as the generic step in time, regardless of the integration method, it is necessary to get the value of the restoring force $R(y, \dot{y})$ given the value of the displacement $y$ and of the velocity $\dot{y}$. The non linear equivalent displacement $z(y, \dot{y})$ is the only unknown therm of the restoring force formulation and it is defined in therms of its first derivative by the equation 6.2.

The effective value of $z$ should be evaluated by time integration of the 6.2, however, a solution in closed form is hard to obtain. The easiest numerical solution is obtained simply by calculating the integral as a rectangular

summation, *i.e.*, the current value of $z$ can be written in incremental form:

$$z_{j+1} = z_j + \Delta t\dot{y} \left[A - |z_{j+1}|^n \psi \left(z_{j+1}, y_{j+1}, \dot{y}_{j+1}\right)\right]. \tag{6.7}$$

The previous equation shows how the current value of $z$ has an implicit dependance on itself, thus, in order to numerically evaluate the solution, an iterative algorithm is required. In the FERUM object, a Newton's algorithm has been implemented and it can me summarized as the following:

- Set $z_{new} = z_j$ [3]
- While $|z_{new} - z_{old}| > tol$.
  1. evaluation of $\psi \left(y_{j+1}, \dot{y}_{j+1}, z_{new}\right)$
  2. evaluation of the $f\left(z_{j+1}\right)$ as:

     $$f\left(z_{j+1}\right) = z_{new} - z_{old} - \Delta t\dot{y} \left[A - |z_{j+1}|^n \psi \left(z_{new}, y_{j+1}, \dot{y}_{j+1}\right)\right]. \tag{6.8}$$

  3. evaluation of the first derivative $f'\left(z_{j+1}\right)$
  4. the Newton's trial value is obtained as: $z_{new} = z_{old} - \frac{f(z_{j+1})}{f'(z_{j+1})}$
  5. updating of $z_{old}$
- evaluation of the restoring force.

The derivatives needed by the Newton's scheme are intended with respect $z_{new}$:

$$f'\left(z_{j+1}\right) = 1 + \Delta t\dot{y} \left[n \left|z_{new}\right|^n \operatorname{sgn}\left(z_{new}\right) \psi + \left|z_{new}\right|^n \psi'\right] \tag{6.9}$$

[3] Note that $z_{new}$ and $z_{old}$ are step values of $z_{j+1}$ *inside* the Newton's scheme at the time step $j+1$ while $z_j$ is the value at the previous time step.

$$\psi' = \beta_1 \text{sgn}\left(\dot{y}_{j+1}\right) \frac{k}{\cosh^2\left(kz\right)} + \beta_3 \frac{ky}{\cosh^2\left(kyz\right)} + \beta_5 \frac{k}{\cosh^2\left(kz\right)}. \tag{6.10}$$

Then, one can keep on the evaluation of the restoring force as defined in the previous section.

## 6.3 Model sensitivity

The implementation of the Bouc-Wen asymmetric material in the TELM requires that the Newmark oscillator previously shown in chapter 4 provides the dynamic response but also its first derivative. If a finite differences algorithm is used, the TELM loses every advantage with respect any other method, because the dynamic response would have to be evaluated so many times that a straight Monte Carlo simulation would become sustainable. Zhang *et al.* developed a lighter method that evaluates the gradient of the time response with respect a generic status variable for inelastic systems[53], the Direct Differentiation Method (DDM) and its complete implementation in OpenSees has been made by Haukaas [32, 33].

The DDM is able to evaluate the derivative or the gradient of any status variable of a dynamic system with respect any variable. As it has been shown previously, in order to get the most likeliable excitation, the TELM runs a FORM method that consists of an iteration algorithm that gradually approaches the minumum of a target function. While the FORM evaluates the $i+1$ step trial excitation, at the generic $i$ step, the response gradient is evaluated with respect of the random variables of the problem.

Regardless of the definition of those random variables, the DDM only requires the evaluation of the restoring force derivative with respect the dis-

placement. In fact, defined $h$ as the generic random variable, the restoring force derivative can be written as:

$$\frac{\partial R\left(y,\dot{y},z\right)}{\partial h}=\frac{\partial R\left(y,\dot{y},z\right)}{\partial y}\frac{\partial y}{\partial h} \tag{6.11}$$

where the gradient of $y$, $\frac{\partial y}{\partial h}$, is the unknown variable that the DDM will evaluate.

For this reason, it is necessary to define the gradient of the restoring force with respect the displacement that will be addressed as the *instantaneous tangent stiffness*. It's essential to notice that it is not sufficient to estract the theoretical derivative because it would lead to wrong values of the gradient: the restoring force implemented in the algorithm has been defined in incremental form, thus, an algoritmically consistent first derivative of the restoring force is required.

In this section, the sensitivity analysis of the asymmetric Bouc-Wen model will be shown, in order to get the required derivatives that have to be implemented in the general algorithm.

The tangent stiffness of the material is given by:

$$\frac{dR\left(y,\dot{y},z\right)}{dy}=\alpha k_0+\left(1-\alpha\right)k_0\frac{dz}{dy} \tag{6.12}$$

note that one can be tempted to evaluate the first derivative of $z$ by the 6.2 but it would lead to an error in the algorithm. The evaluated derivative must be algorithmically consistent, *i.e.*, it has to be the derivative of the expression effectively employed in order to evaluate the $z$, thus, it must be obtained directly by taking the first derivative of the 6.7. Defining:

$$\Phi=A-\left|z_{j+1}\right|^n\psi\left(z_{j+1},y_{j+1},\dot{y}_{j+1}\right) \tag{6.13}$$

the derivative of $z$ is:

$$\frac{dz_{j+1}}{dy_{j+1}} = \Delta t \frac{d\dot{y_{j+1}}}{dy_{j+1}} \Phi + \Delta t \dot{y}_{j+1} \frac{d\Phi}{dy_{j+1}}. \tag{6.14}$$

Note that in the last equation there is the therm $\frac{d\dot{y_{j+1}}}{dy_{j+1}}$, it strictly depends on the specific integration algorithm of the equation of motion. If a Newmark's scheme is implemented, then the velocity is linear combination of the displacement, velocity and acceleration at the time step $j$ but also of the current displacement $y_{j+1}$, thus, the derivative will be the specific coefficient employed in the Newmark's updating formula. This is the particular case of the implementation in FERUM. *Au contraire*, if some other integration algorithm is employed, the velocity can be written in its incremental formulation $\dot{y}_{j+1} = \frac{y_{j+1} - y_j}{\Delta t}$, then the equation 6.7 can be written only in therms of displacements and its derivative would be easier to obtain. However, in this work the complete form will be considered in order to be consistent with the implementation in FERUM and also because if the simplified form would be required, it is easy to evaluate it simply by evaluating the derivative of the velocity as $\frac{1}{\Delta t}$.

The first drivatives of $\Phi$ and $\psi$ will be:

$$\frac{d\Phi}{dy_{j+1}} = -n \left| z_{j+1} \right|^{n-1} \operatorname{sgn}\left( z_{j+1} \right) \frac{dz_{j+1}}{dy_{j+1}} \psi - \left| z_{j+1} \right|^{n} \frac{d\psi}{dy_{j+1}} \tag{6.15}$$

$$\begin{aligned} \frac{d\psi}{dy_{j+1}} &= \beta_1 \operatorname{sgn}\left( \dot{y}_{j+1} \right) \frac{k}{\cosh^2(kz)} \frac{dz_{j+1}}{dy_{j+1}} + \beta_2 \frac{k \operatorname{sgn}\left( (\dot{y})_{j+1} \right)}{\cosh^2(k y_{j+1})} \\ &+ \beta 3 \frac{kz}{\cosh^2(k y_{j+1} z_{j+1})} \frac{dz_{j+1}}{dy_{j+1}} + \beta_5 \frac{k z_{j+1}}{\cosh^2(k z_{j+1})} \frac{dz_{j+1}}{dy_{j+1}} + \beta_6 \frac{k}{\cosh^2(k y_{j+1})} \end{aligned} . \tag{6.16}$$

Collecting the therms with $\frac{dz_{j+1}}{dy_{j+1}}$ the following auxiliary therms may be

defined:

$$A_1 = 1 + \Delta t \dot{y}_{j+1} |z_{j+1}|^{n-1} n \mathrm{sgn}(z_{j+1}) \psi(y_{j+1}, \dot{y}_{j+1}, z_{j+1}) + \\ + \Delta t \dot{y}_{j+1} |z_{j+1}|^{n} \left( \beta_1 \frac{k \mathrm{sgn}(\dot{y}_{j+1})}{\cosh^2(kz)} + \beta 3 \frac{kz}{\cosh^2(k y_{j+1} z_{j+1})} + \beta_5 \frac{k z_{j+1}}{\cosh^2(k z_{j+1})} \right) \quad (6.17)$$

$$A_2 = \Delta t \frac{d\dot{y}_{j+1}}{dy_{j+1}} \Phi - \Delta t \dot{y}_{j+1} |z_{j+1}|^{n} \left[ \beta_2 \frac{k \mathrm{sgn}\left((\dot{y})_{j+1}\right)}{\cosh^2(k y_{j+1})} + \beta_6 \frac{k}{\cosh^2(k y_{j+1})} \right] \quad (6.18)$$

and the latters finally lead to the derivative of $z_{j+1}$:

$$\frac{dz_{j+1}}{dy_{j+1}} = \frac{A_2}{A_1} \quad (6.19)$$

.

# Chapter 7

# Example applications

## 7.1 Multi Degrees-Of-Freedom electrical substation equipment

The multi degrees-of-freedom application is an electrical substation made by two equipments connected by a generalized Bouc-Wen material modelled connector. Its hysteresis is non symmetric as shown in chapter 6 and its parameters will be shown in the following. The oscillator presents only two degrees of freedom but the case can be easily extended to any number of DOF changing conveniently the mass and damping matrixes and the restoring force vector.

Each equipment item can be idealized as a linear SDOF oscillator characterized by the effective mass $m_i$, damping $c_i$, stiffness $k_i$ and loading force $l_i$ regtardless of their real number of nodes and elements, so that the global model results simplified and not computationally demanding whithout compromise the final result.

The displaced shape $U_i(\Omega, t)$ of each equipment can be obtained as

$U_i(\Omega,t) = \psi_i(\Omega)\, y_i(t)$, where $\Omega$ is the domain, $y_i(t)$ is the displacement of the connection node and $\psi_i(\Omega)$ is the shape function of the linear model relative to the connected node. The virtual work principle gives the global parameters of the system as:

$$m_i = \int_\Omega \rho(\Theta)\, \psi(\Theta)^2 \, d\Theta \tag{7.1}$$

$$k_i = \int_\Omega EI_i(\Theta)\, \psi''(\Theta)^2 \, d\Theta \tag{7.2}$$

$$c_i = 2\zeta_i \sqrt{m_i k_i} \tag{7.3}$$

$$l_i = \psi(y_i) \int_\Omega \rho(\Theta)\, \psi(\Theta) \, d\Theta \tag{7.4}$$

where $\rho(\Theta)$ is the mass density, $\zeta_i$ is the damping ratio and $E$ is the Young modulus.

Based on the above idealization, the global model, showed in figure 7.1 becomes a two degrees-of-freedom non linear oscillator with equation of motion:

$$\mathbf{M}\ddot{\mathbf{y}}(t) + \mathbf{C}\dot{\mathbf{y}}(t) + \mathbf{R}(\mathbf{y}(t), \dot{\mathbf{y}}(t), z) = -\mathbf{L}\ddot{y}_g \tag{7.5}$$

where $\ddot{y}_g$ is the support acceleration and:

$$\mathbf{M} = \begin{bmatrix} m_1 & 0 \\ 0 & m_2 \end{bmatrix} \tag{7.6}$$

$$\mathbf{C} = \begin{bmatrix} c_1 + c_0 & -c_0 \\ -c_0 & c_2 + c_0 \end{bmatrix} \tag{7.7}$$

where $c_0$ is the viscous damping of the connector,

$$\mathbf{L} = \begin{bmatrix} l_1 \\ l_2 \end{bmatrix} \tag{7.8}$$

$$\mathbf{K} = \begin{bmatrix} k_1 y_1(t) - q(\Delta y, \Delta \dot{y}, z) \\ k_2 y_2(t) - q(\Delta y, \Delta \dot{y}, z) \end{bmatrix}. \tag{7.9}$$

where $\Delta y = y_2(t) - y_1(t)$ is the relative displacement between the connected nodes of the first and second equipment, $z(t)$ is an auxiliary variable representing a non-linear equivalent displacement of the Bouc-Wen material and:

$$q(\Delta y, \Delta \dot{y}, z) = \alpha k_0 \Delta y + (1-\alpha) k_0 z \tag{7.10}$$

the general meaning and the terms of the 7.10 have already been shown in chapter 6. In this case, it represents the restoring force of the Bouc-Wen connector subjected to displacement $\Delta y(t)$ and velocity $\Delta \dot{y}(t)$.

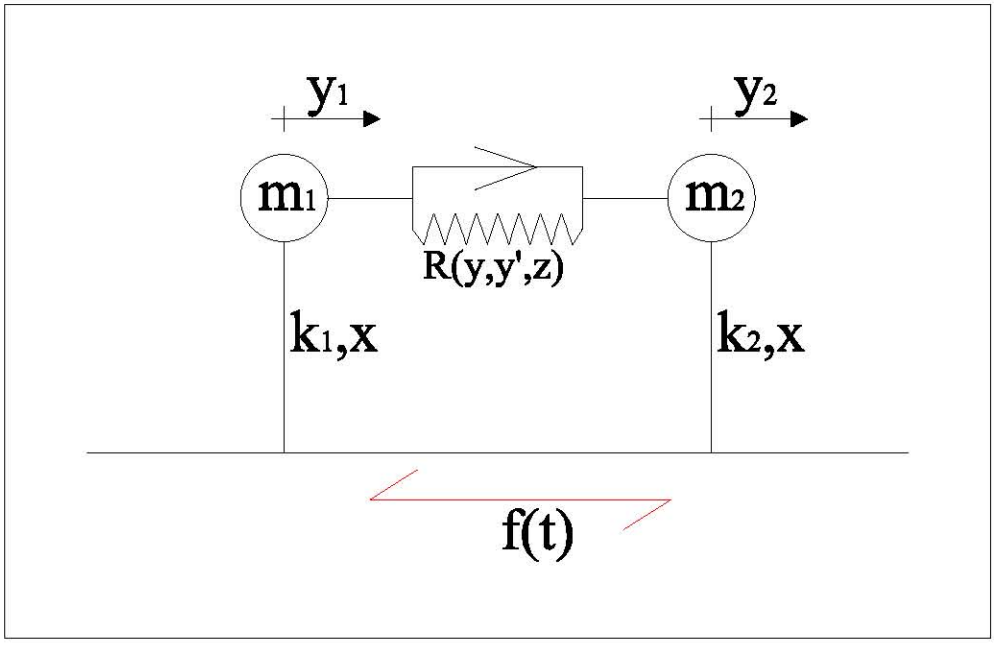


Figure 7.1: Non linear two-DOF oscillator

The equation of motion can be solved by a Newmark algorithm implemented in FERUM, in order to perform the TELM analysis. In the following section, physical parameters and results of the MDOF system will be provided.

### 7.1.1 Mechanical characterization

The system parameters have been chosen so that the results can be interpretated regardless of the specific mass, stiffness and damping of each substation. In particular, the frequencies are:

$$\begin{array}{l} f_1 = \frac{\omega_1}{2\pi} = 1\text{Hz} \\ f_2 = \frac{\omega_2}{2\pi} = 5\text{Hz} \end{array} \tag{7.11}$$

furthermore, masses, loads and initial stiffnesses are:

$$\frac{m_1}{m_2} = 2 \tag{7.12}$$

$$\frac{l_1}{m_1} = \frac{l_2}{m_2} = 1 \tag{7.13}$$

$$\frac{k+0}{k_1+k_2} = \frac{1}{2} \tag{7.14}$$

where $k_0$ is the initial stiffness of the connector. The viscous damping of the substations is $\zeta_1 = \zeta_2 = 0.02$ and the connectors' damping is neglected: $c_0 = 0$.

The connecting element is made of three single rigid-bus, flexible-connectors (RB-FCs). Thus, fixed the initial stiffness of the connector, it is possible to determine the properties of each model component using the relations 7.11, 7.12, 7.13 and 7.14. The different properties of each kind of considered connectors are summarized in Table 7.1 and 7.2.

| | PG&E 30-2021 | PG&E 30-2022 | PG&E 30-2023 |
|---|---|---|---|
| $k_0$ (kN/m) | 147.60 | 106.80 | 33.30 |
| $k_1$ (kN/m) | 21.87 | 15.82 | 4.93 |
| $k_2$ (kN/m) | 273.33 | 197.78 | 61.67 |
| $m_1$ (t) | 0.55 | 0.40 | 0.13 |
| $m_2$ (t) | 0.28 | 0.20 | 0.06 |

Table 7.1: Stiffness and mass parameters of the MDOF models.

| | PG&E 30-2021 | PG&E 30-2022 | PG&E 30-2023 |
|---|---|---|---|
| $k_0$ (kN/m) | 147.60 | 106.80 | 33.30 |
| $\alpha$ | 0.10 | 0.10 | 0.10 |
| $A$ | 1.00 | 1.00 | 1.00 |
| $n$ | 1.00 | 1.00 | 1.00 |
| $\beta_1$ (1/m) | 18.50 | 16.50 | 11.22 |
| $\beta_2$ (1/m) | -4.65 | -7.60 | -3.61 |
| $\beta_3$ (1/m) | 1.16 | 6.85 | 1.48 |
| $\beta_4$ (1/m) | 4.53 | 3.55 | 4.17 |
| $\beta_5$ (1/m) | -4.76 | -6.14 | -2.29 |
| $\beta_6$ (1/m) | -4.41 | -2.22 | -2.19 |

Table 7.2: Parameters of the smoothed-generalized Bouc-Wen material.

## 7.2 Electric substation equipment connected by PG&E 30-2021

The TELM procedure described in chapter 4 provides the tail-equivalent linearized system (TELS) as a set of impulse response functions (IRFs) shown in figures 7.2 and 7.3, on its base, some considerations can me made before the real random vibrations analysis.

First of all, fixed the value of the threshold, the asymmetric behavior of the Bouc-Wen generalized material provides two different linearized system for positive or negative excursions. For example, given $x = \pm 0.0125m$, the two IRFs, plotted in Figure 7.5, show as the decaying of the impulse response results completely different and it is higher for the negative value of the threshold. The reason of this phenomenon is due to the asymmetric hysteresis loop and to the different behavior for positive and negative displacements. Two hysteresis loops of the non-linear oscillator subjected to sinusoid exitation are shown in figure 7.4, the maximum positive displacement of the first plot (blue line) is $y^{+}_{max} = 0.20m$ and it corresponds to a maximum negative displacement of $y^{-}_{min} = -0.15m$. It is possible to increase the excitation scale in order to get a maximum negative displacement of $y^{-}_{min} = -0.20m$ (red line); in this case the maximum positive displacement is higher: $y^{+}_{max} = 0.25m$. Furthermore, it appears clear that the second loop is wider than the first one, *i.e.* fixed the absolute value of the target displacement, the dissipated energy is higher when the target is required to occur in the negative side. The higher level of dissipation of the negative target displacement, causes an higher decay of the corresponding

IRF for negative thresholds[1].

A different decay can also be noticed comparing the IRFs of the positive threshold set (or, similarly, the negative threshold set); it results directly proportional to the threshold, again, because, as long as the maximum displacement grews, the hysteresis loops become wider.

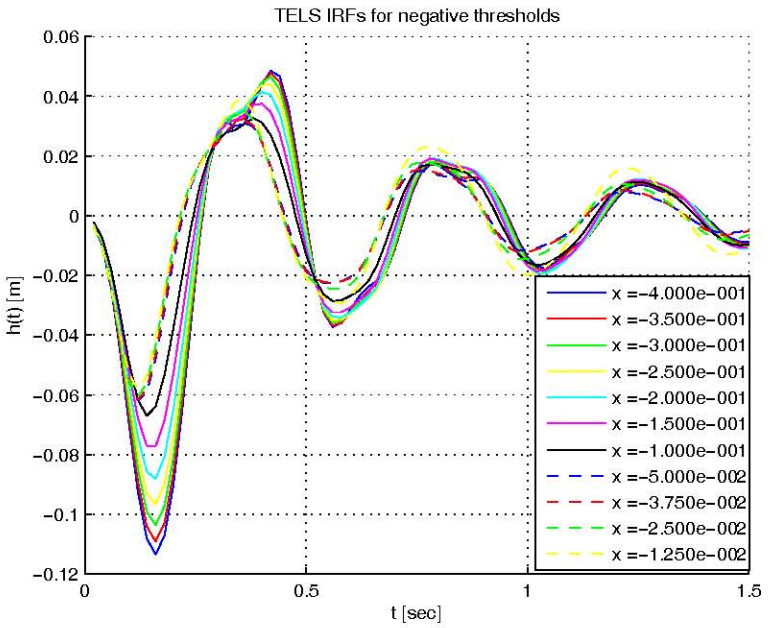


Figure 7.2: TELS Impulse Response Functions for negative thresholds

[1]This property can be easily noticed at low threshold, on the other way, high thresholds can be related to a different behavior with the positive IRF that decays faster than the negative one. The reason is related to the global behavior of the oscillator: because the system has two degrees of freedom, at high thresholds the non-linear connector becomes softer, so, the global dynamic behavior, and then the IRF, depends much more on the properties of the two connected linear oscillators that can trigger resonance phenomena and the hysteresis loop for negative thresholds can result smaller than the loops of the corresponding positive thresholds.

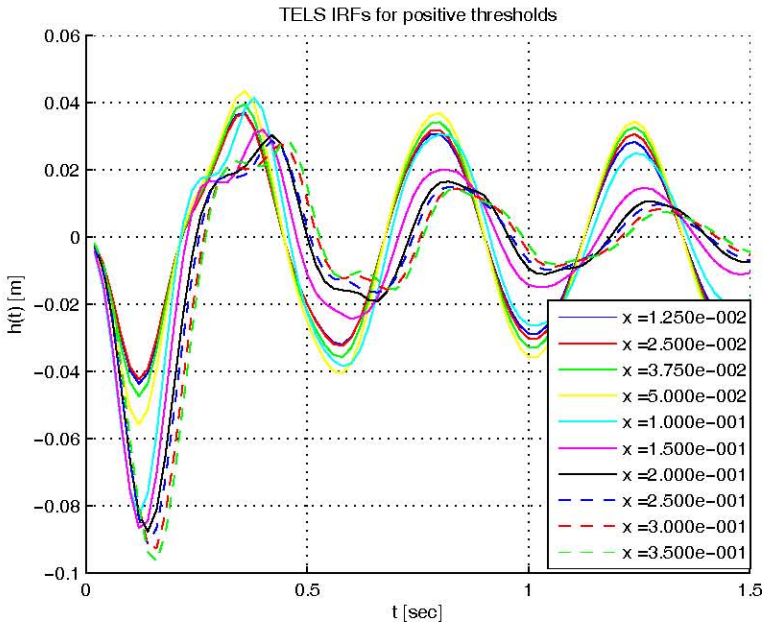


Figure 7.3: TELS Impulse Response Functions for positive thresholds

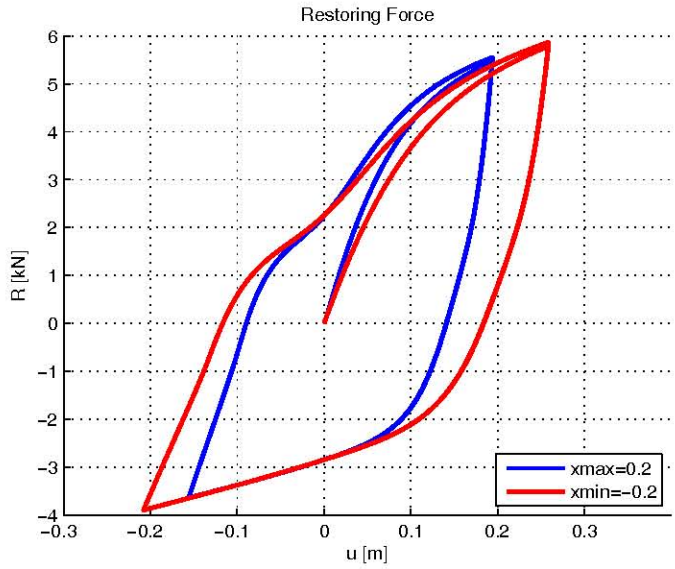


Figure 7.4: Symmetric threshold hysteresis loops

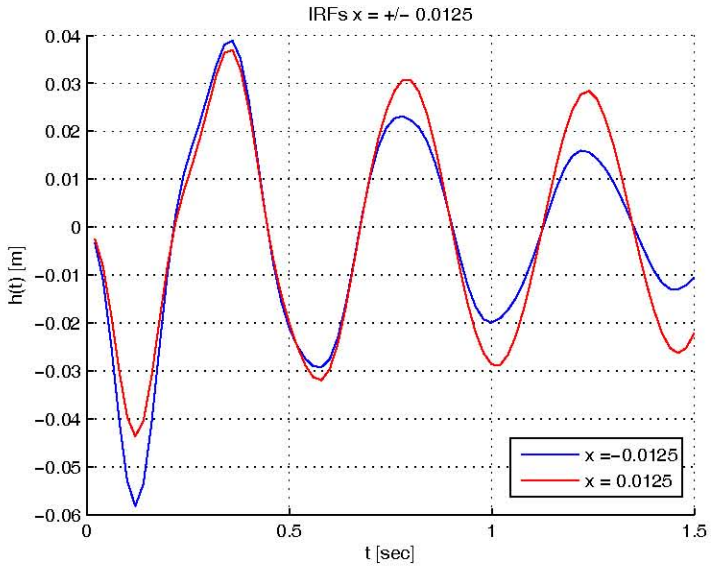


Figure 7.5: TELS Impulse Response Functions for $x = \pm 0.0125m$

It is also interesting to appreciate this latter effect analysing the fourier transform of the IRF defined as the corresponding frequency response functions (FRF). The moduli of the FRF set are provided in Figures 7.6 and 7.7. Increasing the threshold level, this time, two different effects can be noticed. The frequency content always shows a peak that corresponds to the first natural frequency of the linearized oscillator. As long as the threshold increases, the peak becomes smaller and moves to the low frequencies.

The first phenomenon is due the higher dissipation of the hysteresis loop, *i.e.* the steady-state response of the natural frequency becomes lower because of the higher level of dissipation. This effect clearly corresponds to the different decay of the IRFs.

The second effect is due the softening of the oscillator: because the stiffness of the material is inversely proportional to the displacement, as long as the threshold increases, the system becomes softer and its period is longer. This latter effect, also, amplifies the portion of FRF at low frequencies, as long as the threshold increases and it can also be appreciated in the IRFs' plot because the distances between the zeros of each IRF (which corresponds exactly to the oscillator's half-period) are noticeably different.

Note that both IRFs and FRFs tend to converge to a common function as long as the threshold becomes smaller. The reason is related to the "level" of non-linearity of the material. As shown in chapter 6, the non-linearity of the Bouc-Wen material is strongly related to the displacement. For small displacements, the influence of the linear part is high and the stiffness of the material becomes closer to the linear value. As long as the threshold decreases, then, the constitutive law becomes closer to the linear

case.

However, at the same time, the Bouc-Wen non-linear phase is completely negligible only when the displacement is exactly zero, then, even for the smallest thresholds the IRF will not be exactly the linear case which corresponds only to the limit case of zero-threshold. Even if physically the zero-threshold does not make sense[2], the linear IRF is the splitting function between the positive and negative threshold sets. This property has a consequent numerical drawback that affects the evaluation of the response at a given time for small threshold, presented in section 7.2.1.

[2]The case of zero-threshold practically corresponds to an oscillator that does not oscillate. Remember that the "target" entity is the response $X(t_n)$; even if it is always possible to find a non-zero excitation that satisfies the condition $x - X(t_n) = 0 \Rightarrow 0 - X(t_n) \Rightarrow X(t_n) = 0$, the purpose is to evaluate the most likely one. Each pulse of the excitation train has a zero-mean Gaussian distribution, then, the most likely excitation would result always the zero-excitation.

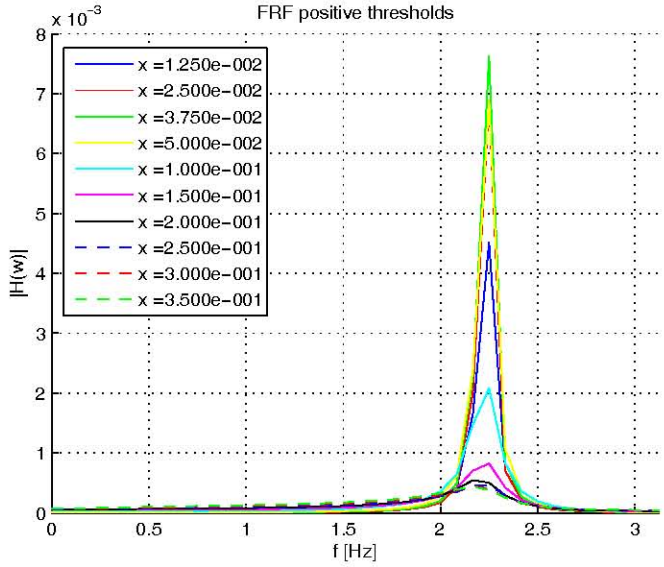


Figure 7.6: TELS Frequency Response Functions for positive thresholds

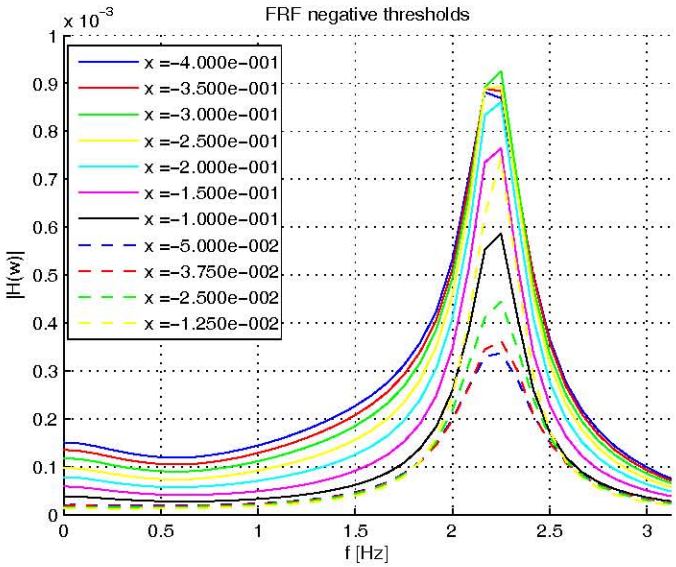


Figure 7.7: TELS Frequency Response Functions for negative thresholds

### 7.2.1 Statistics of response at given time

Once the TELS of the system has been defined, the procedures shown in chapter 5 lead to a complete random vibration analysis. The first result is about the probabilistic distribution of the response for a specified step in time. Because the excitation is stationary, once that the system has archieved the stationarity of the response, its probabilistic distribution does not change in time. Thus, the response statistics have been evaluated at $t = 12sec$ which is the time that has been considered to be enough in order to get a stationary response. Figure 7.8 shows plots of the reliability index versus threshold for response to a discretized white noise base accel-eration with a standard deviation[3] of $\sigma_{wn} = 1g$. The response considered is the relative displacement of the two equipment items, as normalized by the standard deviation of the response of the linear system ($\alpha = 1$). Four sets of results are shown: TELM by time-domain analysis (blue line), TELM by frequency-domain analysis (diamonds), Monte Carlo (MC) simulation with $10^5$ simulations (red line), and the response of the linear system (black line, $\alpha = 1$), which is Gaussian and appears as a straight line.

Several observations are noteworthy in figure 7.8. First, it is noted that the two TELM results are practically identical, thus indicating the validity of both approaches. Second, both TELM and MC results significantly deviate from a straight line, thus indicating the non-Gaussian nature of the response. Third, while the error in the TELM approximation is negligible

[3]The standard deviation $\sigma_{wn}$ refers to the white noise. Theoretically, an unfiltered and unbounded white noise has an infinite standard deviation, in this case, because there is a discretization in time, the PSD of the excitation is affected by a cut at high frequencies related to the size of the time steps as shown in chapter 2

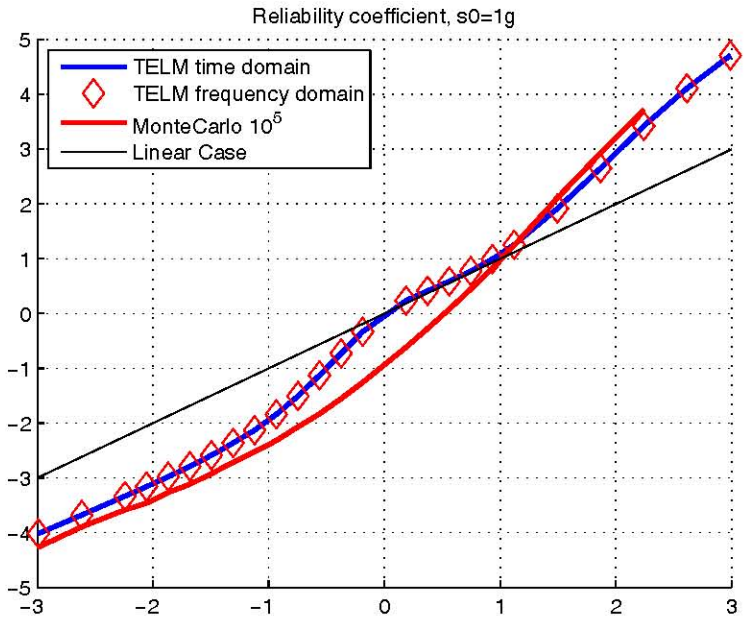


Figure 7.8: Reliability index versus normalized threshold, $\sigma_{wn} = 1g$

in the two tail regions, there is a significant error for small thresholds ($\beta$ values around zero). This is due to the asymptotic nature of the FORM approximation, as well as the convergence of the IRF of the TELS to the linear case for small thresholds. In case of zero-threshold at $t = t_n$, the limit-state surface passes through the origin and the reliability index is zero regardless of the nonlinearity of the surface (see figure 7.11). Thus, TELM produces probability 0.5 for zero threshold regardless of the shape of hysteresis loop. The correct result, of course, may correspond to a probability different from 0.5 when the hysteresis loop is asymmetric. This effect is further evident in the complementary CDF of the response, which is shown in figure 7.9. Nevertheless, it is noted that TELM produces accu-rate results in the two tail regions, which are regions of interest in reliability analysis. This is evident in figure 7.10, which shows the tails in log scale[4].

The asymmetric nature of the distribution can be seen in figure 7.10, which shows the CDF of the response for negative thresholds and the complementary CDF of the response for positive thresholds, as predicted by TELM and Monte Carlo simulations. The response of the linear ($\alpha = 1$) system is also shown. It is evident that TELM is able to capture the non-Gaussian distribution of the response in the tail regions, including the asymmetric nature of the two tails. This should be contrasted with the conventional ELM, which would essentially predict a Gaussian distribution even with an asymmetric hysteresis law. The TELM constraint of probability 0.5 at zero threshold cannot be avoided as long as the FORM approx-

[4]Note that, in figure 7.10, in order to show the tails in log scale, the left (negative) side is the CDF of the response while the right (positive) side is its complementary CDF.

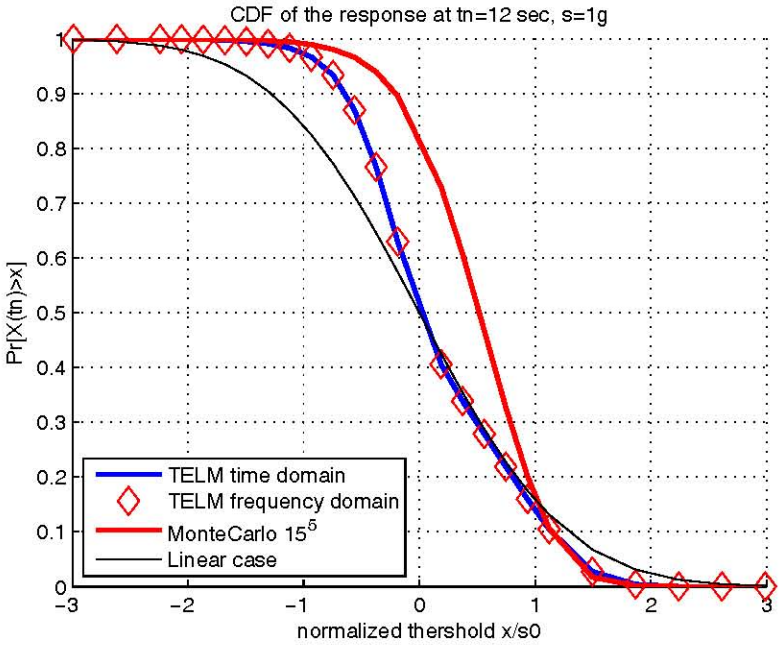


Figure 7.9: Complementary CDF at a given time versus normalized threshold, $\sigma_{wn} = 1g$

imation is used. If the low thresholds are of interest, one possible approach is to construct a second-order equivalent system. The implementation of such an approximation is currently under investigation.

Similar results have been obtained for the standard deviation of $\sigma_{wn} = 0.75g$ and are shown in appendix A together with further results for $\sigma_{wn} = 1g$.

### 7.2.2 Extreme Statistics of response for a given time

The First Passage Probability (FPP) has been evaluated following the procedures already described in section 7.2.2 which specifically are:

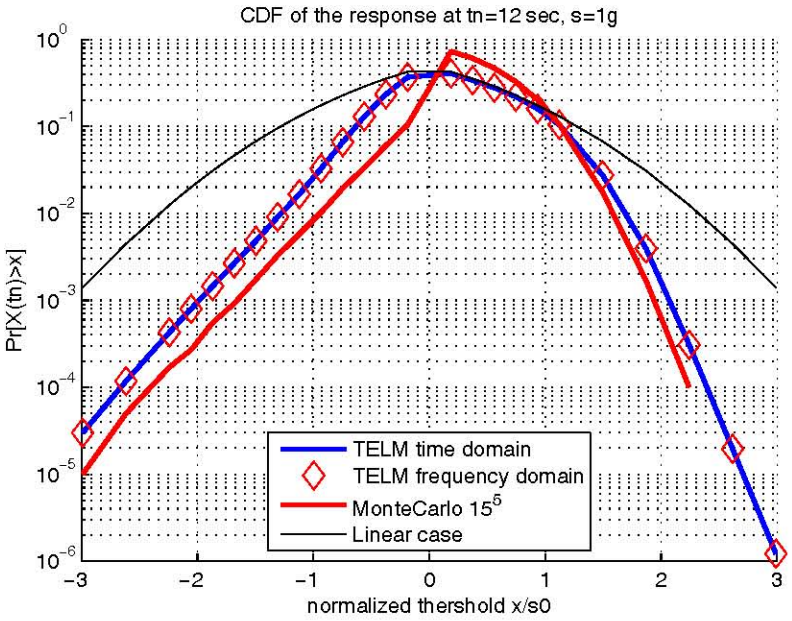


Figure 7.10: CDF and complementary-CDF of the response at a given time versus normalized threshold in log scale, $\sigma_{wn} = 1g$

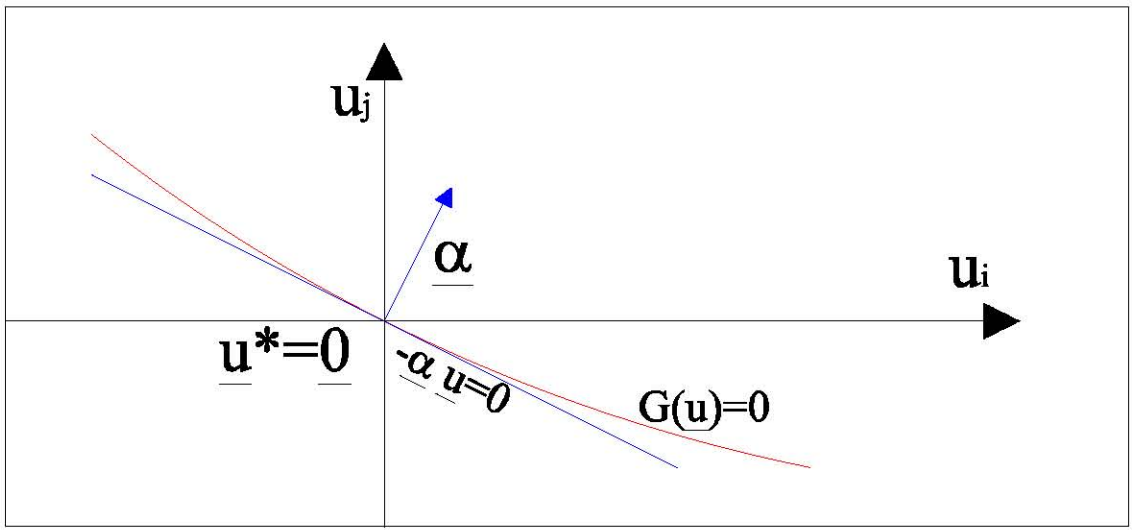


Figure 7.11: Limit state surface at zero-threshold

- Vanmarcke's formula for single bounded problems;
- Series System problem with the FERUM package.

The Poisson approximation provides results close to the Vanmarcke's formula and it's known as less accurate, then it will not be shown in the results. The first passage probabilities based on TELM have been evaluated for three different stationary time processes: $T = 3, 6$ and 10 seconds[5] and the plots are compared with Monte Carlo simulation results.

Note that, because of the asymmetry of the response distribution, it is necessary to separately evaluate the first passage probabilities for positive and negative thresholds. Furthermore, the two obtained CDFs will be

[5]In order to avoid redundance, in the present section only the results for $T = 10sec$ will be shown; further results for different time durations can be found in appendix A

plotted on the same graph, then, the right (positive) branch will correspond to the probability:

$$F_{X(\tau)}(x) = \Pr\left[X(t) \geq x | 0 < t \leq \tau\right] \tag{7.15}$$

and the negative branch will correspond to the following:

$$F_{X(\tau)}(x) = \Pr\left[X(t) \leq x | 0 < t \leq \tau\right]. \tag{7.16}$$

It is observed in figure 7.12 that the TELM results based on Vanmarcke's formula and the series-system approximation are nearly the same. Both results are somewhat higher than the MC estimates, but nevertheless good approximations for all practical purposes. Remarkably, the TELM approximation correctly predicts the asymmetric distribution of the first-passage probability. In particular, the probability of exceeding negative thresholds is much higher than that of exceeding positive thresholds of similar magnitude. This has to do with the smaller stiffness in compression, as observed in the hysteresis behavior of the connecting element.

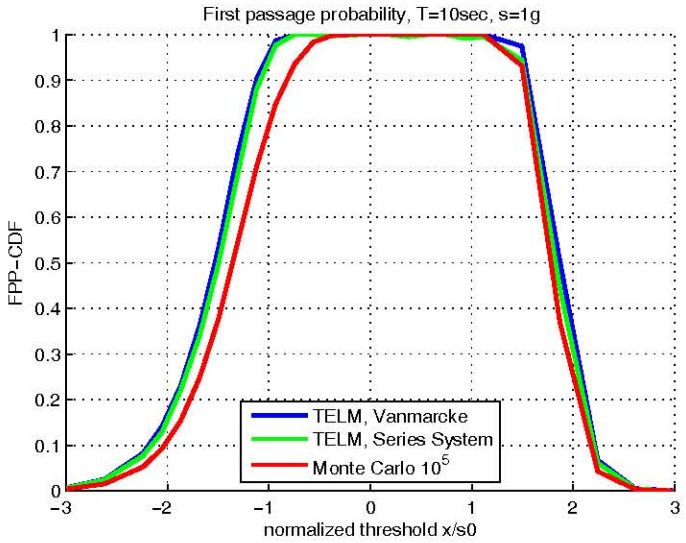


Figure 7.12: First Passage Probability, $T = 10sec$, $\sigma_{wn} = 1g$

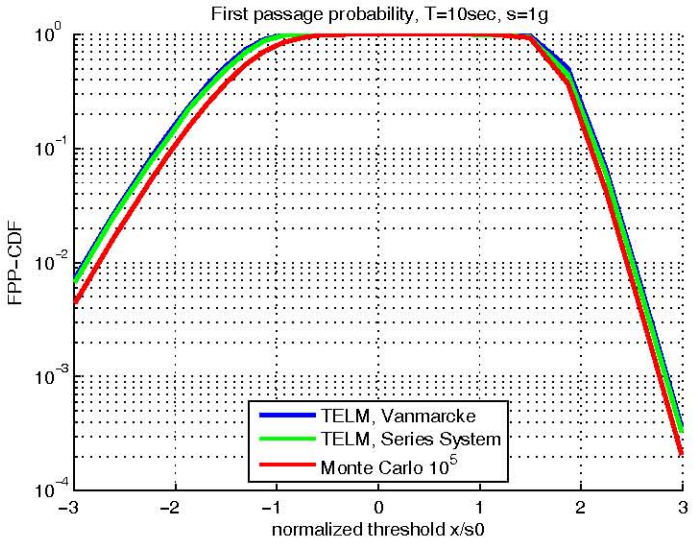


Figure 7.13: First Passage Probability, $T = 10sec$, $\sigma_{wn} = 1g$

# Chapter 8

# Conclusions

The tail-equivalent linearization method, TELM, is a non-parametric method for approximate solution of nonlinear stochastic dynamic problems. The method employs a linearization of the system response for each considered threshold, which matches the tail probability of the nonlinear response in first-order approximation. The linearized system is obtained in a non-parametric form, in terms of its impulse-response function, which depends on the considered threshold. Through this dependence, TELM is able to capture the non-Gaussian distribution of the non-linear response.

Previous studies have investigated TELM for stationary and non-stationary excitation processes, but always in presence of symmetric hysteresis loops that lead to a zero-mean and symmetric response distribution. In this work, the performance of TELM for response analysis of dynamical systems with asymmetric hysteretic behavior is investigated. For this purpose, a smoothed version of the generalized Bouc-Wen model is developed, so that the response is continuously differentiable.

It is found that TELM is able to capture the non-Gaussian and asymmet-

ric distribution of both the point-in-time response, as well as the maximum response over a time interval (the first-passage probability distribution) for large thresholds (small exceedance probabilities).

The distributions for the positive and negative thresholds are distinctly different, reflecting the difference in the behavior of the system for the two regimes. It is found, however, that TELM is unable to provide good accuracy for thresholds near zero. In particular, the cumulative probability approximation by TELM for a zero threshold is always 0.5, regardless of the shape of the hysteresis loop. This is a characteristic of FORM, which can only be overcome through a higher-order approximation method, such as SORM. Although probability values for small thresholds are not of interest in reliability analysis, work is currently in progress to construct a better approximation for small thresholds by use of SORM.

The major developments and findings of this work can be summarized as follows:

- The TELM provides a linearized system in therms of non-symmetric set of Impulse Response Functions (IRFs); in particular, the IRF of a threshold is different than the IRF of the symmetric threshold. The decay and the frequency content of the IRFs of symmetric threshold are noticeably different due to the different shapes and areas of the hysteresys loops of each threshold. Specifically, the provided application shows a higher energy dissipation for negative threshold. The diffecence between the IRFs of symmetric thresholds decreases as long as the absolute value of the threshold becomes smaller and the IRF

tend to converge to the linear case as the threshold approaches to zero.

- This latter convergence implies a costraint in the response-in-time distribution at zero-threshold, in particular, the median of the response (*i.e* 50% probability) always occurs at zero. Consequently, the error of TELM at low threshold is significant, however it does not affect the results in therms of extreme distribution.

- The TELM provides the non-Gaussian and non-symmetric response-in-time distribution, Monte Carlo simulations show that the TELM provides good approximations at high thresholds (tail region).

- The TELM also provides non-symmetric, non-Gaussian and non-zero mean extreme distribution, again, the Monte Carlo simulations show that the method provides good approximation at high thresholds (tail region) and for long enough time intervals. However, the TELM extreme distributions results more conservative than the Monte Carlo simulations.

- In order to perform the FORM analysis, it is important to determine a good starting point defined in the standard normal space. The starting point highly influence the convergence velocity of the algorithm and the convergence itself. Criteria and strategies about the starting point definition are provided.

- Objects coded in Matlab and C++ are implemented in Ferum and OpenSees and are available for further research and applications.

In summary, TELM is an alternative for nonlinear random vibration analyses, which offers a better accuracy for the tail probability for higher threshold than the ELM, which cannot provide non-symmetric distributions, and a better efficiency than the MCS. The selection of the appropriate solution method for each problem should be made by considering the required accuracy and efficiency.

## 8.1 Reccomendations for further research

In order to improve the accuracy, applicability and efficiency of TELM to non-symmetric problems, the following topics are reccomended for further research:

- Development of more efficient criteria to define the starting point in order to assure the convergence of the algorithm and a high enough speed of convergence. In particular, the fastest one of the proposed criteria, requires a high fitting of the threshold interval of interest. The proposed criteria that are not dependent on the performance points of previous thresholds still provide slow convergence speed. On the other way round, it is possible to investigate if higher tolerances for the FORM convergence still provide good enough results in therms of extreme distributions.

- Implementation of the Second Order Reliability Method (SORM) in order to avoid the *median-at-50* phenomenon. The linearized system would be defined as its tail probability mathches the second-order approximation of the tail probability of the non-linear system. In

case of o thershold, FORM always swithes the standard normal space in two perfectly equal halves, so, it leads to a probability of 50%. *Au contraire*, SORM would provide different values of the tail probability at zero threshold. This feature, would eliminate the costraint at 50% of the response-in-time distribution.

- It would be worthwhile to define and apply TELM with multi-component and multi-support excitations. It would be required a new formulation of the input excitation and the theoretical response of the linearized system (which defines the IRFs given the performance point) has to be defined on the base of the new linearized system definition.

- Because the best feature of TELM is that it bypasses the usual dependence of the response statistics on the Gaussian distribution, it could be interesting to investigate the behavior of TELM in presence of non-Gaussian input excitation. It would be required to define a new class of excitation in order to get an efficient mapping on the standard normal space that allows FORM to be performed.

- It can also be desiderable to apply TELM to complex highly nonlinear and multi degrees of freedom systems in order to emphasize the advantages of TELM with respect other conventional methods and its efficiency, as well as to investigate its drawbacks, identify shortcomings and needs for further development. It is believed that these practical applications will be beneficial for acceptance of the class of Tail-Equivalent Linearization Methods by the engineering community.

# Appendix A

# Further results of the MDOF system PG&E 30-2021

In the present appendix are shown further results about the two-degrees-of-freedom system connected with PG&E 30-2021 for values of the banded white noise of $\sigma_{wn} = 1g$ and $\sigma_{wn} = 0.75g$.

## A.1 Results for $\sigma_{wn} = 0.1g$

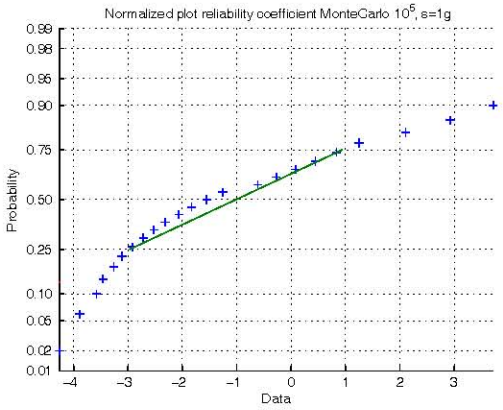


Figure A.1: Normal probability plot, MonteCarlo $10^5$ simulations, $\sigma_{wn} = 1g$

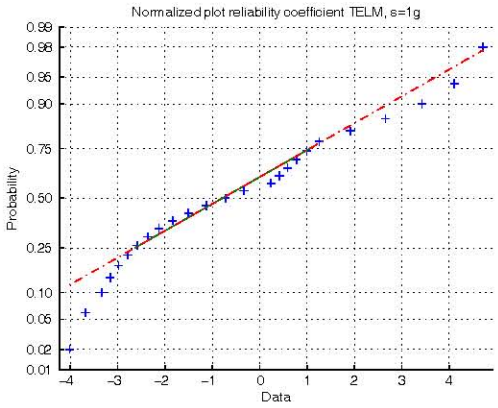


Figure A.2: Normal probability plot of TELM, $\sigma_{wn} = 1g$

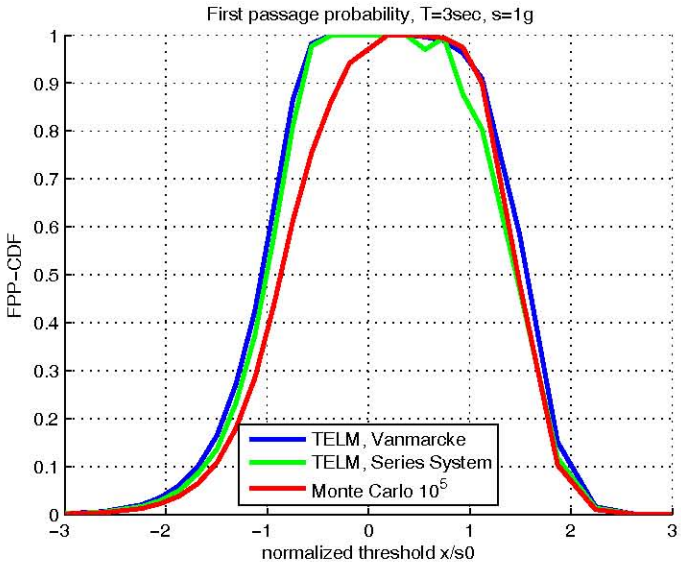


Figure A.3: First Passage Probability, $T = 3sec$, $\sigma_{wn} = 1g$

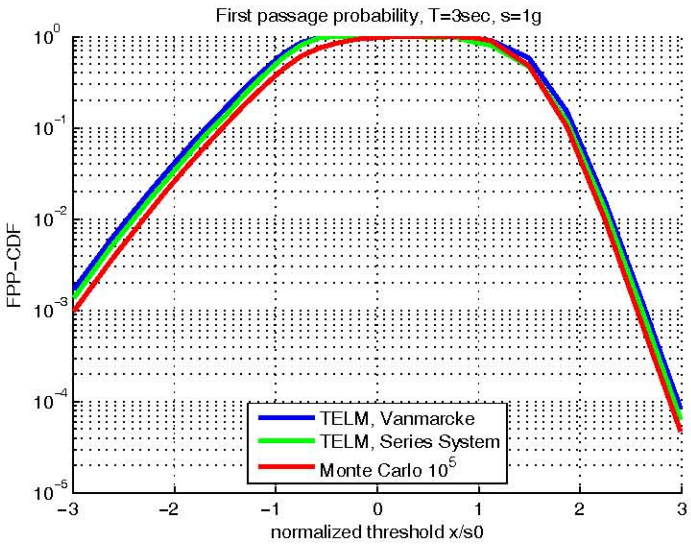


Figure A.4: First Passage Probability, $T = 3sec$, $\sigma_{wn} = 1g$

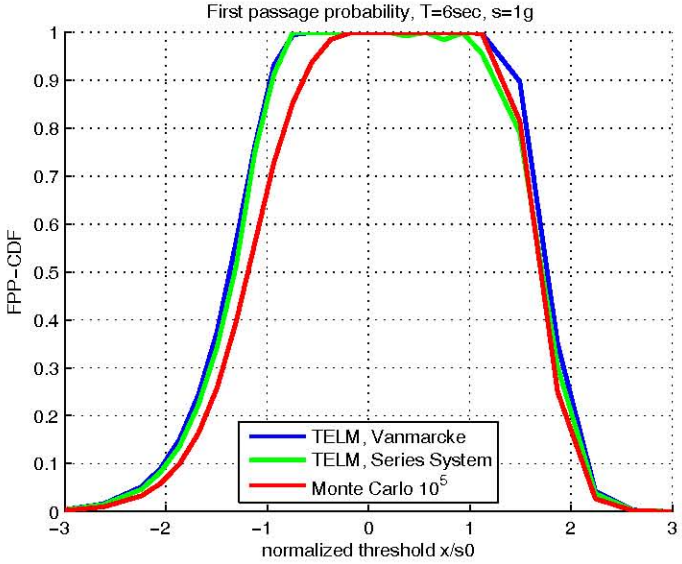


Figure A.5: First Passage Probability, $T = 6sec$, $\sigma_{wn} = 1g$

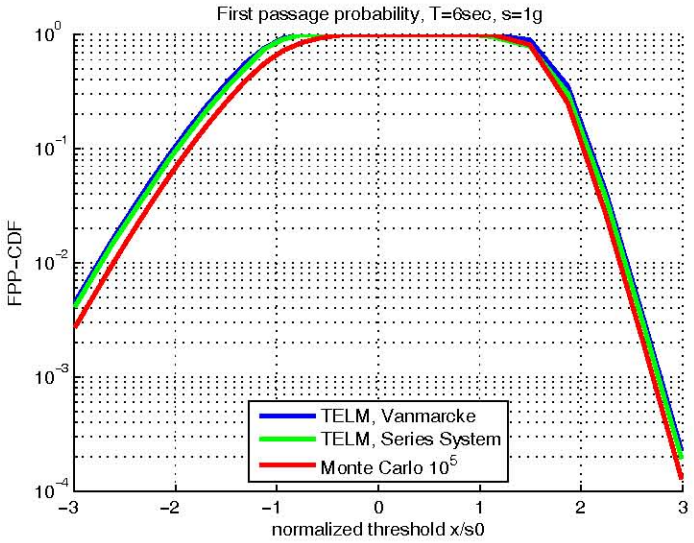


Figure A.6: First Passage Probability, $T = 6sec$, $\sigma_{wn} = 1g$

## A.2 Results for $\sigma_{wn} = 0.75g$

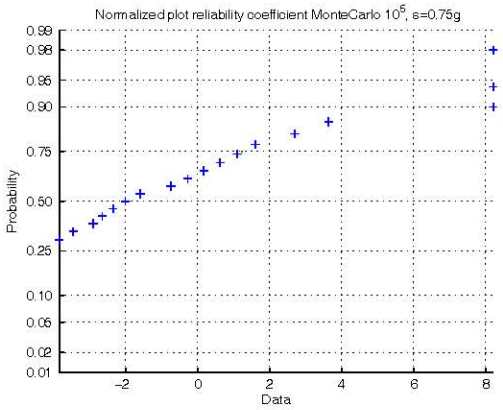


Figure A.7: Normal probability plot, MonteCarlo $10^5$ simulations, $\sigma_{wn} = 0.75g$

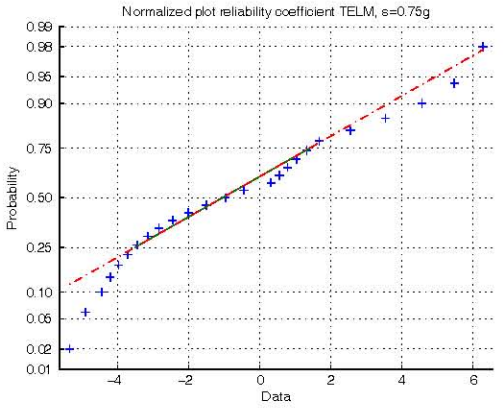


Figure A.8: Normal probability plot of TELM, $\sigma_{wn} = 0.75g$

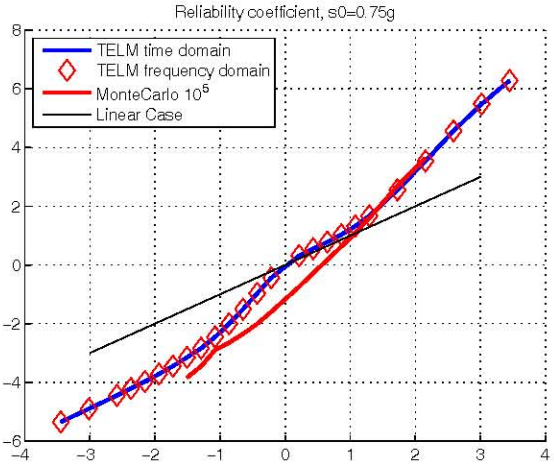


Figure A.9: Reliability index versus normalized threshold, $\sigma_{wn} = 0.75g$

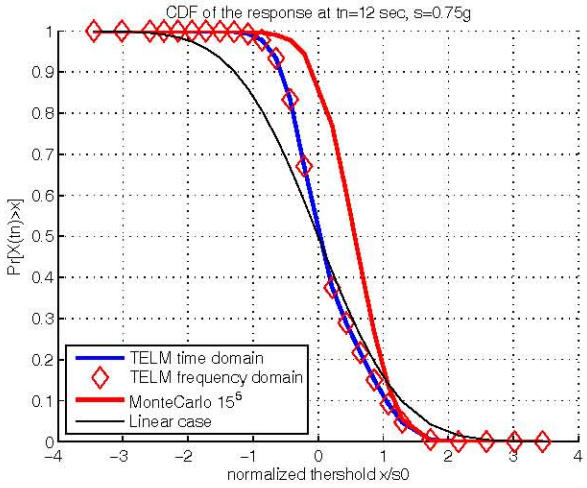


Figure A.10: Complementary CDF at a given time versus normalized threshold, $\sigma_{wn} = 0.75g$

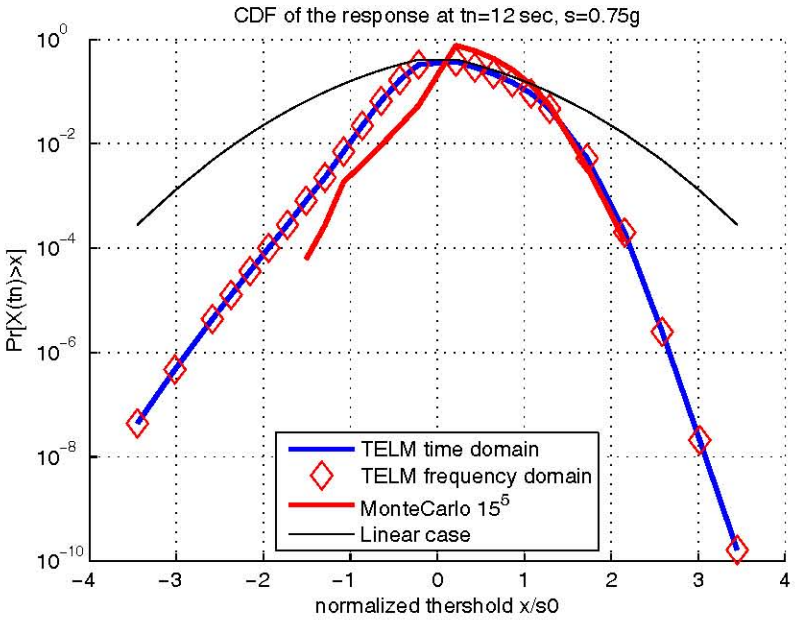


Figure A.11: CDF and complementary-CDF of the response at a given time versus normalized threshold in log scale, $\sigma_{wn} = 0.75g$

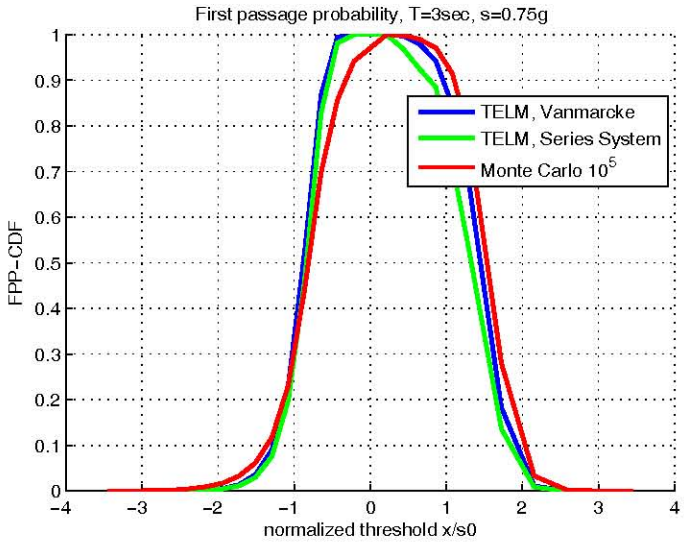


Figure A.12: First Passage Probability, $T = 3sec$, $\sigma_{wn} = 0.75g$

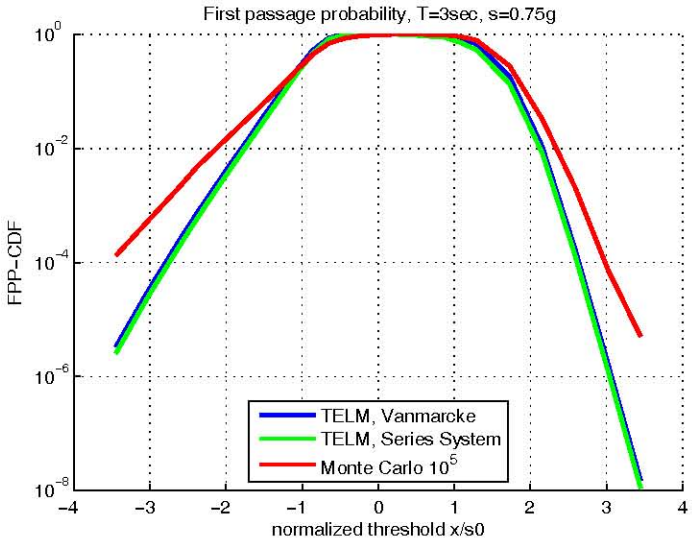


Figure A.13: First Passage Probability, $T = 3sec$, $\sigma_{wn} = 0.75g$

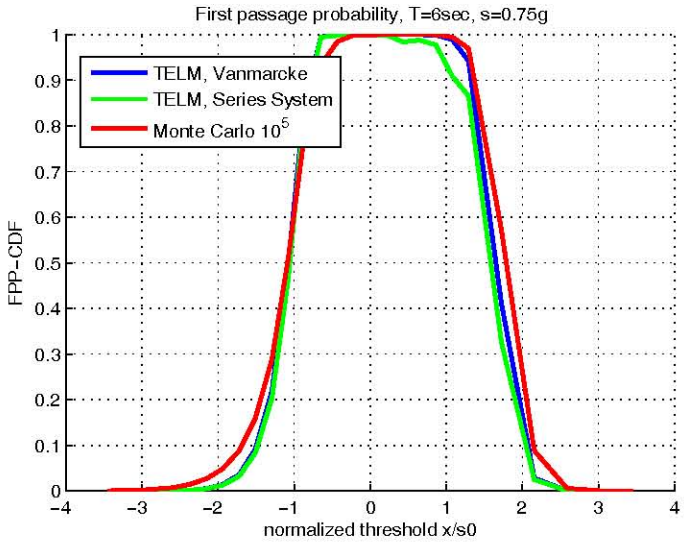


Figure A.14: First Passage Probability, $T = 6sec$, $\sigma_{wn} = 0.75g$

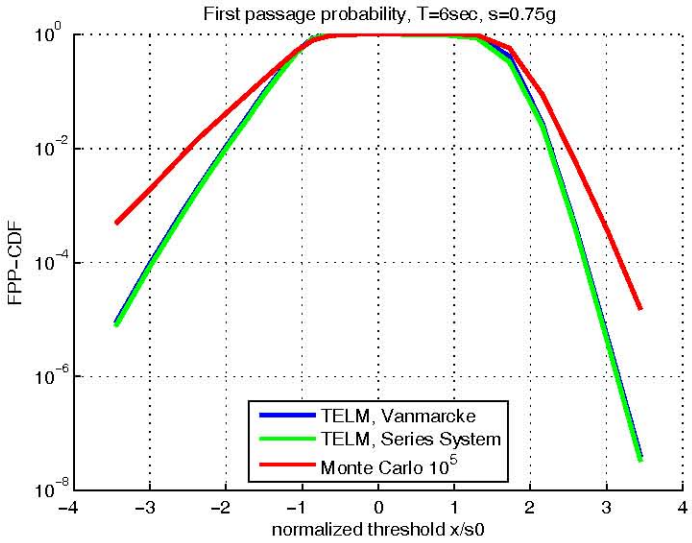


Figure A.15: First Passage Probability, $T = 6sec$, $\sigma_{wn} = 0.75g$

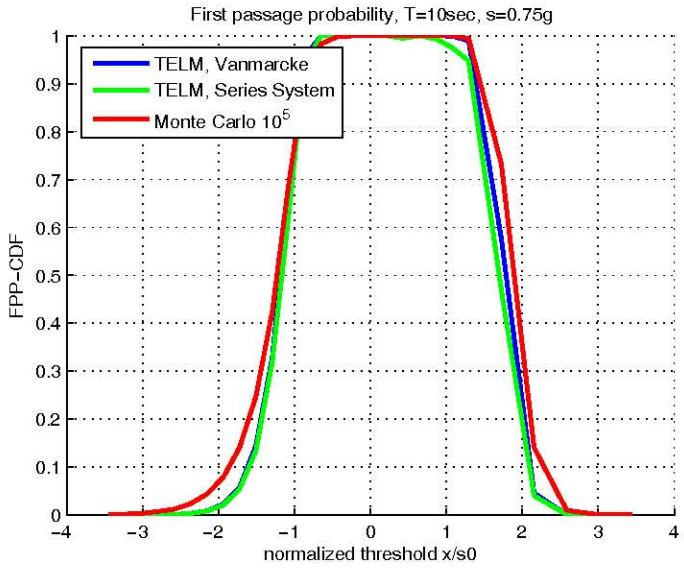


Figure A.16: First Passage Probability, $T = 10sec$, $\sigma_{wn} = 0.75g$

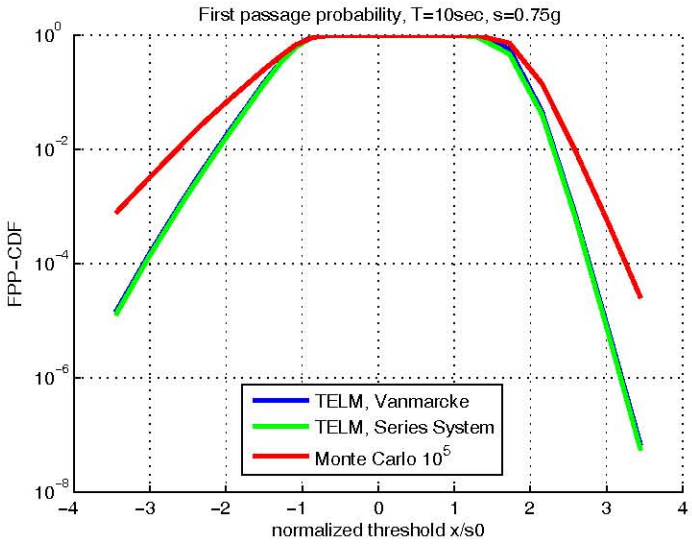


Figure A.17: First Passage Probability, $T = 10sec$, $\sigma_{wn} = 0.75g$

# Appendix B

# Implementation in OpenSees

The Smoothed-Generalized Bouc-Wen material has been implemented in OpenSees, a framework for scientific research purposes developed by the Pacific Earthquake Engineering Earthquake Research Center (PEER) and the constitutive model is available for any kind of purpose. The code has been written in C++ following the algorithm summarized in chapter 6. In this section the OpenSees definition will be shown and the main properties and methods will be explained. First, we recall the theoretical definition:

$$R = \alpha k_0 y\left(t\right) + \left(1-\alpha\right) k_0 z \tag{B.1}$$

$$\dot{z} = A\left(\epsilon\right) - \left|z\right|^n \psi\left(y, \dot{y}, z\right) \dot{y}. \tag{B.2}$$

$$\begin{aligned} \psi\left(y, \dot{y}, z\right) = \beta_0 + \beta_1 \text{sgn}(\dot{y}) \text{tanh}(kz) + \beta_2 \text{tanh}\left(ky\right) \text{sgn}(\dot{y}) + \\ + \beta_3 \text{tanh}\left(kyz\right) + \beta_4 \text{sgn}(\dot{y}) + \beta_5 \text{tanh}(z) + \beta_6 \text{tanh}\left(ky\right) \end{aligned} . \tag{B.3}$$

The definition of the material follows the command line:

```
uniaxialMaterial GenBoucWen $i $alpha $k0 $n $b1 $b2 $b3
$b4 $b5 $b6 $btan $A 1.0e-10
```

The meaning of the arguments is summarized in table B.1. Furthermore, the main methods of the C++ object are summarized in table B.2.

| Argument | Meaning |
|---|---|
| `GenBoucWen` | Name of the specific OpenSees object |
| `$i` | Progressive index of the material |
| `$alpha` | $\alpha \in [0, 1]$ in B.1 |
| `$k0` | Initial stiffness of the material in B.1 |
| `$n` | $n$ exponent in B.2 |
| `$b1 .. $b6` | coefficients $\beta_1..\beta_6$ in B.3 |
| `$btan` | smoothing coefficient $k$ B.3 |
| `$A` | $A$ coefficient in B.2 |
| `1.0e-10` | tolerance of Newton's algorithms, default $10^{-10}$ |

Table B.1: OpenSees Smoothed-Gen. Bouc-Wen material arguments meaning

| Method | Purpose |
|---|---|
| `GenBoucWenMaterial` | Creates an istance of the material. |
| `setTrialStrain` | Defines the strain value. |
| `getStress` | Evaluates the stress. |
| `getInitialTangent` | Evaluates the tangent at $\epsilon = 0$. |
| `getTangent` | Evaluates the current tangent. |
| `revertToStart` | Resets the hystory variables. |
| `getStressSensitivity` | Evaluates the stress gradient. |

Table B.2: OpenSees Smoothed-Gen. Bouc-Wen material methods

# Appendix C

# Implementation in FERUM

The Smoothed-Generalized Bouc-Wen material is implemented in FERUM, a Matlab framework for scientific research purposes. The constitutive model is available for any kind of purpose. In this section the list of objects available in FERUM will be summarized. First, we recall the theoretical definition:

$$R = \alpha k_0 y(t) + (1-\alpha) k_0 z \tag{C.1}$$

$$\dot{z} = A(\epsilon) - |z|^n \psi(y, \dot{y}, z)\, \dot{y}. \tag{C.2}$$

$$\begin{aligned} \psi(y, \dot{y}, z) = \beta_0 + \beta_1 \text{sgn}(\dot{y}) \text{tanh}(kz) + \beta_2 \text{tanh}(ky)\, \text{sgn}(\dot{y}) + \\ + \beta_3 \text{tanh}(kyz) + \beta_4 \text{sgn}(\dot{y}) + \beta_5 \text{tanh}(z) + \beta_6 \text{tanh}(ky) \end{aligned} . \tag{C.3}$$

1. `[hfcn, risFORM]=TELM(TELMparameters, Excitation, ...)`

   Evaluates a set of IRFs (hfcn) and the results of FORM for a set of times and thresholds.

2. `TELMparameters`

   Input object consisting in the following fields:

   - `threshold`: set of thresholds for which TELM is performed;
   - `times`: set of $t_n$ for which TELM is performed;

3. `Excitation`

   Excitation's parameters:

- `S0`: white noise intensity;
- `displ`: initial displacement;
- `speed`: initial velocity;
- `accel`: initial acceleration;
- `dt`: time step amplitude;
- `tn`: stationary time;

4. `[Res, grad] = gfun_betaNewmarkFFD(t, thr, u, Si, gchk, lin);`

   Non-linear oscillator object, `Res` is the response $R = x - X(t_n)$, `grad` is its gradient. It rewuires the following input arguments:

   - `t`: vector of time steps;
   - `thr`: current threshold (scalar value);
   - `u`: realization of the standard normal variables vector;
   - `Si`: deterministic matrix due to the excitation's covariance structure (cfr. 2.2);
   - `gchk`: string flag, `'no '` does not evaluate the gradient, `'ffd'` uses the finite differences method, `'ddm'` uses the direct differentiation method;
   - `lin`: linear check: if 1, the oscillator becomes linear fixing the initial stiffness, regardless of the restoring force model.

5. `[R, dR] = GetGenBoucWenA(index, u, u1, Du1, dt, step)`

   Restoring force object, it evaluates the smoothed generalized Bouc-Wen restoring force `R` and its tangent stiffness `dR`. It requires the following arguments:

   - `index`: progressive number of the material;
   - `u`: current displacement;
   - `u1`: current velocity;
   - `Du1`: derivative of the velocity with respect the displacement (in the Newmark's approximated formula);
   - `dt`: time step amplitude;

- textttstep: current time step index.

Also, the material needs to be created with the following:

6. `InitializeGenBoucWen(index, par)`

   where `index` is the progressive index of the material and `par` is an object containing the material's parameters (see tab C.1).

Further objects for random vibration analysis have been developed by the author and are available for common use. The main ones are summarized in tab C.2.

| par.* | Meaning |
|---|---|
| `alpha` | $\alpha \in [0, 1]$ in C.1; |
| `k0` | Initial stiffness of the material in C.1; |
| `n` | $n$ exponent in C.2; |
| `b` | coefficients $\beta_1..\beta_6$ in C.3 (row vector); |
| `ks` | smoothing coefficient $k$ C.3; |
| `A` | $A$ coefficient in C.2; |
| `maxiter` | maximum number of iterations allowed; |
| `toll` | tolerance of Newton's algorithms. |

Table C.1: OpenSees Smoothed-Gen. Bouc-Wen material parameters

| Function | Purpose |
|---|---|
| `GetSplineStatistics.m` | Evaluates spline CDF/PDF from discrete ones; |
| `getLinearIRF` | IRF of a linear SDOF system; |
| `getLinearFRF` | FRF of a linear MDOF system; |
| `get_FRF_from_IRF` | IRF of a linear MDOF system as FT of the FRF; |
| `StatMoments` | Probability moments given a discrete CDF; |
| `WhiteNoisePSD` | Discrete PSD of a banded white noise; |
| `KanajTajimiPSD` | Discrete Kanai-Tajimi PSD; |
| `GetPP_from_IRF` | Performance point given discrete IRF; |
| `GetDispl_from_PP` | Performance point response; |
| `GetDuhamelResponse` | Convolution Duhamel's integral. |

Table C.2: Random Vibration analysis objects

# Bibliography


[1] Ahn N.D., Di Paola M. – Some extensions of Gaussian Equivalent Linearization – *International Conference on Nonlinear Stochastic Dynamics, Hanoi, Vietnam*, 5-16, (1995).

[2] Atalik T.S., Utku S. – Stochastic linearization of multi-degree of freedom nonlinear systems – *Earthquake Engineering and Structural Dynamics*, **4**, 411-420, (1976).

[3] Au S.K., Beck J.L. – First excursion probability for linear systems by very efficient algorithm – *Probabilistic Engineering Mechanics*, **16**, 193-207, (2001).

[4] Barone G., Navarra G, Pirrotta A. – Probabilistic response of linear structures equipped with nonlinear damper devices (PIS method) – *Probabilistic Engineering Mechanics*, (to appear) (2008).

[5] Barbato M., Conte J.P. – Finite element structural response sensitivity and reliability analysis using smooth versus non-smooth material constitutive models – *International Journal of Reliability and Safety*, **1**, 3-39, (2006).

[6] Barber T.T., Noori M.N. – Modeling general hysteresis behavior and random vibration application – *J. Vib. Acoust. Stress Reliab. Des. ASME*, **108**, 411-420, (1986).

[7] Booton R. C. – The analysis of nonlinear control systems with random inputs – *IRE Transactions on Circuit Theory*, **1** 32-34 (1959).

[8] Casciati F., Faravelli L., Hasofer A.M. – A new philosophy for stochastic equivalent linearization – *Probabilistic Engineering Mechanics*, **8(3-4)**, 179-185, (1993).

[9] Caughey T.K. – Equivalent linearization techniques – *Journal of the Acoustical Society of America*, **35(11)**, 1706-1711, (1963).

[10] Cai G.Q., Lin Y.K., Elishakoff I. – A new approximate solution technique for randomly excited non-linear oscillators, part II – *Journal of Non-Linear Mechanics*, **27**(6), 969-979, (1992).

[11] Clough R.W., Penzien J. – Dynamics of structures, 2nd edition – *McGraw-Hill, New York*, 924-963, (1993).

[12] Chopra A.K. – Dynamic of Structures – *Prentice Hall*, (2007).

[13] Cottone G., Di Paola M., Pirrotta A. – Path Integral solution by fractional calculus – *Journal of Physics: conference series*, **96**, 012007 (2008).

[14] Der Kiureghian A. – A structural response to stationary excitation – *Journal of Engineering Mechanics Division*, **106**(6), 1195-1213, (1980).

[15] Der Kiureghian A., Sackman J.L., Hong K.J. – Interaction in interconnected electrical substation equipment subjected to earthquake ground motions – *PEER report 1999/01, University of California, Berkeley*, (1999).

[16] Der Kiureghian A. – The geometry of random vibrations and solutions by FORM and SORM – *Probabilistic Engineering Mechanics*, **15**, 81-90, (2000).

[17] Der Kiureghian A., Hong K.J., Sackman J.L. – Further studies on seismic interaction in interconnected electrical substation equipment – *PEER report 2000/01, University of California, Berkeley*, (2000).

[18] Der Kiureghian A., Fujimura K. – Computational nonlinear stochastic dynamics by tail linearization – *Proceedings ECCOMAS, Rethymno, Crete, Greece*, (2007).

[19] Der Kiureghian A., Razaeian S. – A stochastic model for earthquake ground motion with separable temporal and spectral nonstationarity – *Proceedings ICASP10, Tokyo, Japan*, 924-963, (2007).

[20] Di Paola M., Santoro R. – Non linear systems under Poisson White Noise handled by Path Integral Solution – *Journal of Vibration and Control*, **14**, 35-49, (2008).

[21] Donley M.G., Spanos P.D. – Dynamic Analysis of Non-Linear Structures by the Method of Statistical Quadratization – *Springer, New York*, (1990).

[22] Elishakoff I., Zhang R. – Comparison of new stochastic linearization criteria – *In: Bellomo N., Casciati F., editors. Nonlinear stochastic dynamics. Berlin: Springer-Verlag*, 201-212, (1992).

[23] Elishakoff I., Andriamasy L., Dolley M. – Application and extension of the stochastic linearization by Ahn and Di Paola – *Acta Mechanica*, (published online) (2008).

[24] Falsone G., Elishakoff I. – Modified stochastic linearization technique for colored noise excitation of Duffing oscillator – *International Journal of Non-Linear Mechanics*, **29**(1) 65-69 (1994).

[25] Fan F.G., Ahmadi G. – On loss of accuracy an non-uniqueness of solutions generated by equivalent linearization and cumulant-neglect methods – *Journal of Sound and Vibrations*, **137**(3) 385-401 (1990).

[26] Foliente G.C. – Stochastic dynamic response of wood structural systems – *PhD Thesis*, Virginia Polytechnic Institute and State University, Blacksburg VA, (1993).

[27] Foliente G.C. – Hysteresis modeling of wood joints and structural systems – *J. Struct. Engrg. ASCE*, **121**, 1013-1022, (1995).

[28] Fujimura K., Der Kiureghian A. – Tail-equivalent linearization method for nonlinear random vibration – *Prob. Engng. Mech.*, **22**, 63-76, (2007).

[29] Fujimura K. – Tail equivalent linearization method for nonlinear random vibration – *PhD dissertation, UC Berkeley*, (2006).

[30] Grigoriu M. – Simulation of non-stationary Gaussian processes by random trigonometric polynomials – *Journ. of Engrg. Mech. ASCE*, **119(2)**, 328-343, (1993).

[31] Hasofer A.M. – Distribution of the maximum of a Gaussian process by a Monte Carlo method – *Journal of Sounds and Vibrations*, **112**, 283-293, (1987).

[32] Haukaas T., Der Kiureghian A. – Finite element reliability and sensitivity methods for performance-based earthquake engineering – *PEER Report*, **2003-14**, Pacific Earthquake Engineering Research Center, UC Berkeley (2003).

[33] Haukaas T., Scott M.H. – Shape sesnitivities in the reliability analysis of nonlinear frame structures – *Computers & Structures*, **84**, 964-977 (2006).

[34] Hurtado J.E., Barbat A.H. – Equivalent linearization of the Bouc-Wen hysteretic model – *Engineering Structures*, **22**, 1121-1132 (2000).

[35] Koo H., Der Kiureghian A., Fujimura K. – Design-point excitation for nonlinear random vibrations – *Prob. Engrg. Mech.*, **20**, 136-147, (2005).

[36] Lacquaniti S., Ricciardi G. – A probabilistic linearization method for non-linear systems subjected to additive and multiplicative excitations – *International Journal of Non-Linear Mechanics ASCE*, **41**, 1192-1205, (2006).

[37] Li C-C. Der Kiureghian A. – Optimal discretization of random fields – *Journ. of Engrg. Mech. ASCE*, **119(6)**, 1136-1154, (1993).

[38] Lin Y.K., Yong Y. – Evolutionary Kanai-Tajimi Earthquake Models – *Journal of Engineering Mechanics*, **113**(8), 1119-1137 (1987).

[39] Lin Y.K., Cai G.Q. – Probabilistic structural dynamic-advanced theory and applications – *McGraw-Hill inc., New York (NY)*, (2004).

[40] Loéve M. – Probability Theory – *4New York: Springer*, (1977).

[41] Lutes L.D., Sarkani S. – Random Vibrations, analysis of structural and mechanical systems – *Elsevier*, (2004).

[42] Polidori D.C., Beck J.L. – Approximate solutions for non-linear random vibration problems – *Probabilistic Engineering Mechanics*, **11** 179-185 (1996).

[43] Priestly M.B. – Non-Linear and Non-Stationary Times Series Analysis – *Academic Press, London*, (1988).

[44] Riske H. – The Fokker-Planck equation. Methods of solution and applications. – *Berlin, Springer*, (1989).

[45] Roberts J.B., Spanos P.D. – Random vibrations and statistical linearization. – *John Wiley & sons, New York (NY)*, (1990).

[46] Roberts J.B. – Multiple solutions generated by statistical linearization and their physical significance – *International Journal of Non-Linear Mechanics*, **26**(6), 945-959 (1991).

[47] Shinozuka M. – Monte Carlo solution of structural dynamics – *Computers and Structures*, **2**, 855-874, (1972).

[48] Song J., Der Kiureghian A., Sackman J.L. – Seismic interaction in electrical substation equipment connected by non-linear rigid bus conductors – *Earthq. Engrg. and Struct. Dyn.*, **36**, 167-190, (2006).

[49] Song J., Der Kiureghian A. – Generalized Bouc-Wen model for highly asymmetric hysteresis – *Journ. Engrg. Mech. ASCE*, **132**(6), 610-618, (2006).

[50] Vanmarcke E.H. – Properties of spectral moments with applications to random vibrations – *Journal of the Engineering Mechanics Division, ASCE*, **98**, 425-446, (1972).

[51] Vanmarcke E.H. – On the distribution of the first-passage time for normal stationary random processes – *Journal of Applied Mechanics, ASME*, **42**, 215-220, (1975).

[52] Wen Y.K. – Equivalent linearization for hysteretic systems under random excitation – *Journal of Applied Mechanics, ASME*, **47(3)**, 150-154, (1980).

[53] Zhang Y., Der Kiureghian A. – Dynamic response sensitivity of inelastic structures – *Computer Methods in Applied Mechanics and Engineering*, **108**(1), 23-26, (1993).

[54] Zhang Z.G., Tsui S.C., Chan S.C., Lau W.Y., Aboy M. – A novel method for nonstationary power spectral density estimation of cardiovascular pressure signals based on a Kalman filter with variable number of measurements – *Medical and Biological Engineering and Computing*, **46**, 789-797, (2008).